



**RESEARCH & REVIEWS  
IN SCIENCE AND  
MATHEMATICS -  
Summer, 2019**



|                              |   |
|------------------------------|---|
| <b>Kitap Adı</b>             | : <b>Research &amp; Reviews in Science and Mathematics – Summer, 2019</b>                                     |
| <b>İmtiyaz Sahibi</b>        | : Gece Kitaplığı  |
| <b>Genel Yayın Yönetmeni</b> | : Doç. Dr. Atilla ATİK  |
| <b>Kapak&amp;İç Tasarım</b>  | : Sevda KIRDAR  |
| <b>Sosyal Medya</b>          | : Arzu ÇUHACIOĞLU   |
| <b>Yayına Hazırlama</b>      | : Gece Akademi  Dizgi Birimi |
| <b>Yayıncı Sertifika No</b>  | : 15476   |
| <b>Matbaa Sertifika No</b>   | : 34559   |
| <b>ISBN</b>                  | : 978-605-288-479-9   |

**Editor**

Prof. Dr. Hüsnüye AKA SAĞLIKER

The right to publish this book belongs to Gece Kitaplığı. Citation can not be shown without the source, reproduced in any way without permission. Gece Akademi is a subsidiary of Gece Kitaplığı.

Bu kitabın yayın hakkı Gece Kitaplığı'na aittir. Kaynak gösterilmeden alıntı yapılamaz, izin almadan hiçbir yolla çoğaltılamaz. Gece Akademi, Gece Kitaplığı'nın yan kuruluşudur.

**Birinci Basım/First Edition** © Haziran 2019/Ankara/TURKEY ©copyright



**Gece Publishing**

**ABD Adres/ USA Address:** 387 Park Avenue South, 5th Floor, New York, 10016, USA

**Telefon/Phone:** +1 347 355 10 70

**Gece Akademi**

**Türkiye Adres/Turkey Address:** Kocatepe Mah. Mithatpaşa Cad. 44/C Çankaya, Ankara, TR

**Telefon/Phone:** +90 312 431 34 84 - +90 555 888 24 26

**web:** [www.gecekitapligi.com](http://www.gecekitapligi.com) — [www.gecekitap.com](http://www.gecekitap.com)

**e-mail:** [geceakademi@gmail.com](mailto:geceakademi@gmail.com)

## CONTENTS

### CHAPTER 1

#### ANAEROBIC TREATMENT OF SYNTHETIC WASTEWATER CONTAINING DIFFERENT ANTIBIOTIC GROUPS IN UP-FLOW PACKED BED REACTOR AND INVESTIGATION OF MICROBIAL DIVERSITY

*Dilek MALAY, Cansu FİLİK İŞÇEN* ..... 5

### CHAPTER 2

#### EVALUATION OF RADIOLOGICAL RISK IN HERBAL TEAS CONSUMED IN RIZE, TURKEY

*Erkan KIRIŞ* ..... 25

### CHAPTER 3

#### THE PREPARATION AND CHARACTERIZATION OF SEMI-INTERPENETRATING POLYMER NETWORK HYDROGELS FOR CONTROLLED RELEASE OF 5-FLUOROURACIL

*Gülen Oytun AKALIN* ..... 37

### CHAPTER 4

#### THE VALUE OF THE SEED IN THE SYSTEMATIC OF THE FAMILY BRASSICACEAE

*Mehmet Cengiz KARAİSMAİLOĞLU* ..... 51

### CHAPTER 5

#### COMPARISON OF ANTIOXIDANT CAPACITY OF OXIDANT IN BEE POLLEN IN TERMS OF REGION AND STORAGE CONDITIONS

*Naci Ömer ALAYUNT* ..... 81

### CHAPTER 6

#### PRODUCTS OF FOUR HOMOGENEOUS COMPONENTS IN FREE LIE ALGEBRAS

*Nil MANSUROĞLU, Derya KARATAŞ* ..... 91



# **ANAEROBIC TREATMENT OF SYNTHETIC WASTEWATER CONTAINING DIFFERENT ANTIBIOTIC GROUPS IN UP-FLOW PACKED BED REACTOR AND INVESTIGATION OF MICROBIAL DIVERSITY**

Dilek MALAY<sup>1</sup>  
Cansu FİLİK İŞÇEN<sup>2</sup>



---

<sup>1</sup> Eskişehir Osmangazi University, Graduate School of Sciences, Eskişehir/Turkey.

<sup>2</sup> Prof. Dr., Eskişehir Osmangazi University, Faculty of Education, Department of Education, Department of Mathematical and Science Education, Eskişehir/Turkey.



## INTRODUCTION

Among all the pharmaceutical drugs that cause contamination of the environment, antibiotics occupy an important place due to their high consumption rates in both veterinary and human medicine. The presence of pharmaceutical compounds, namely antibiotics, in the ecosystem has been known for almost 30 years. Antibiotics wastewater has high COD and very low BOD and hence is difficult to treat biologically (Toloti and Mehrdadi, 2011).

Usually, antibiotics are detected in the higher  $\mu\text{g/L}$  range in hospital effluents, lower  $\mu\text{g/L}$  range in municipal wastewater and  $\text{ng/L}$  in surface, sea and groundwater. Moreover, it has been verified that sediments from agriculture-influenced rivers have higher antibiotic concentrations than the overlying water matrix or than other sediments from rivers located far from agricultural areas. This indicates the possibility of run-off contamination from farmland (Kümmerer, 2009).

In the last years, the presence and fate of antibiotics in environmental matrices have received a special attention by the scientific community. For these reasons, several degradation/removal processes have been studied to solve environmental contamination issues. The most important merits of anaerobic treatment are the ability to treat high strength wastes, low energy input, low sludge yield, low nutrient requirement, low operating cost, low space requirement and net benefit of energy generation in the form of biogas (Toloti and Mehrdadi, 2011).

In this study, it is investigated that synthetic waste waters prepared in vitro and containing cephalosporin group (cephamycin), aminoglikozid group (kanamycin) and polyene group (amphotericin B) of antibiotic active substances used in treatment of the infection diseases seen frequently in people and animal may be treated anaerobically, in a mixture in the up flow packed bed reactor reactors. Success of the anaerobic processes as a basic treatment to be applied to waste water depends on type of treated wastewater and correct selection of process parameters. In this context, the anaerobic parameters such as pH, alkalinity, COD (Chemical Oxygen Demand), volatile fatty acids and biogas composition are monitored in the treatment process to operate the anaerobic reactors efficiently. Next generation sequencing was used for determining microbial diversity.

## MATERIAL and METHOD

### Antibiotics

The antibiotics used in this study are cephamycin sodium (Zentiva), amphotericin b (Sigma), and kanamycin sulfate (Roth).

## Anaerobic Sludge

The anaerobic sludge used in the batch and laboratory scale up flow packed bed reactor studies is provided by the anaerobic treatment unit of the Eskişehir Central Waste Water Treatment Plant. The sludge is mixed thoroughly before use, and filtered through a membrane filter having a pore diameter of 1mm. Its important treatment properties such as pH, suspended solid and total solid are determined. Before the study, the anaerobic sludge is fed by a feeding solution containing starch.

### 1) Preparation of the Synthetic Wastewater

A mixture of cephamycin sodium, amphotericin b and kanamycin sulfate are used as a type of antibiotic in the synthetic wastewaters prepared for the upflow packed bed reactor studies. 100 mL basal medium, and a mixture of propionic acid, propionic acid-butyric acid-acetic acid as types of co-substrate are used in a 4500 mL solution. The antibiotic concentration increases from 10 mg/L to 100 mg/L.

### 2) The Upflow Packed-Bed Reactor (UPBR) Experiments

The used upflow packed-bed reactor is seen in Figure 1. These reactors are also called as stabilized bed filters. The system consists of two reactors having a liquid volume of 5 liters. The operation volume of the reactors is 4.3 liters. The feeding operation is ensured by a peristaltic pump at the different rates. The packing material used in the reactor is plastic. The liquid extracted from first reactor is transferred to the collecting vessel. Second reactor is also fed by a peristaltic pump at different rates. Gas generated in first and second reactors is collected in the vessels having a capacity of 5 liters. Gas collection is based on water replacement. Each reactor is heated by an electrical heating blanket.

### *Experimental study plan*

In the anaerobic treatment, the parameters such as hydraulic retention time, initial COD concentration and loading rate are examined in stepping of the process. COD, suspended solid and biogas measurements are conducted to control the reactors and to evaluate pH, alkalinity, volatile fatty acids and efficiency properties of the systems.

### 3) Ecotoxicological studies

When the treated water obtained at the end of anaerobic treatment process is discharged, it is investigated whether it has a toxic effect in the recipient medium. The ecotoxicological tests are conducted by using the Microtox analyzer (Microtox® Model 500 analyser). The Microtox test is conducted according to the standard method specified by the manufacturer. The tests are carried out within 2% NaCl vitalization solution and according to the operation principle of the device at 15° and in a luminescence of 490 nm. It is determined as a result of reduction in its radiation property in the presence of the toxic materials by using *Vibrio fischeri* culture as a marine

bacterium. The results are stated as a concentration ( $EC_{50}$ ), in which 50% of the radiation disappears in 5 and 15 minutes (Gottlieb et al., 2003).

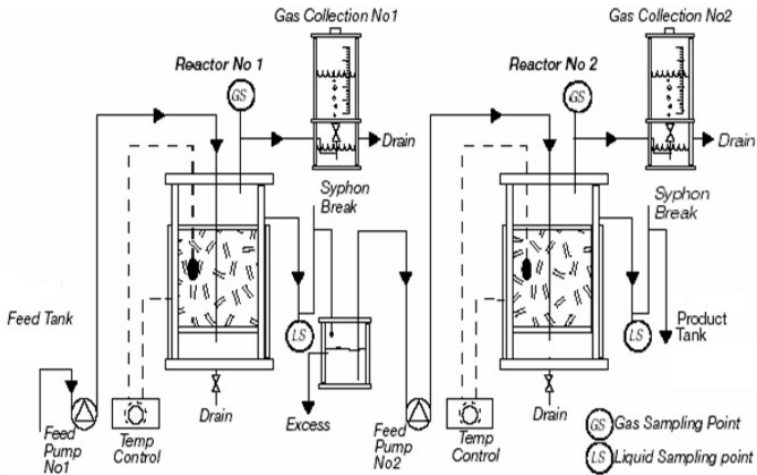


**Figure 1.** Design of UAPB reactor (Armfield W8)

#### 4) DNA Sequence Analysis with the New Generation Sequence (NGS)

A service procurement is carried out from Bioeksen company for the NGS analysis. To conduct a genomic DNA extraction and to reproduce 16S rRNA genes by PCR, three similar samples are taken from the inoculation sludge of the reactor, and stored at  $-20^{\circ}\text{C}$ . Invitrogen PureLink<sup>TM</sup> Genomic DNA Mini Kit (Life Technologies, A.B.D.) is used for genomic DNA isolation, and is made of 0.2 mL sludge sample in accordance with the protocol proposed by the extraction kit manufacturer. The used kit contains detergent, proteinase K and lysozyme for cell fractionation and contains silica columns for purification of DNAs.

The bacterial 16S rRNA zones of the isolated DNAs are reproduced by the Bact8f and Bact1541r primers (Lane, 1991) and the archaeal 16S rRNA zones of the DNAs are reproduced by the Arc46f (Ovreas et al., 1997) and Arc1384r (Lueders and Manfield, 2004) primers. PCR is realized in 30s and at  $95^{\circ}\text{C}$  (10 minutes in first cycle) in 30s and at  $53^{\circ}\text{C}$  and in 45s at  $72^{\circ}\text{C}$ . The reactions are realized in 1,5mM  $\text{MgCl}_2$ , 0,2mM dNTP mix, 1x Reaction Buffer, 0,1U Taq DNA Polymerase, 5ng/ $\mu\text{l}$  mold DNA and in 20 $\mu\text{L}$  volumes containing 0,5 $\mu\text{M}$  from each primer. The dimensional analysis of the PCR products is conducted with 1% (w/v) agarose gel, 1 $\times$  Tris-acetate- EDTA buffer solution (40 mM Tris, 20 mM acetic acid, 1 mM EDTA; pH 8.0) and 7V $\text{cm}^{-1}$  agarose gel electrophoresis. The PCR products are dyed by SybrGreen (Bioeksen, Turkey) and photographed manually under UV.

The PCR products are cleaned from other PCR components by using a Biospeedy PCR Product Purification Kit (Bioeksen Ar-Ge Ltd. Sti.) before NGS. The V3-V5 zones of the purified 16S rRNAs are arranged by NGS in sequences. An adaptor required by Illumina-Miseq platform and index sequences, by which each sample shall be marked, are integrated to Bact339-F (5'-CTCCTACGGGAGGCAGCAG-3') and Bact815-R(5'CTCCTACGGGAGGCAGCAG-3'), and Arch349-F (5'-GYGCASCAGKCGMGAAW-3') and Arch806-R (5'-GGACTACVSGGGTATCTAAT-3') primers for bacteria and archaea, and the DNA library necessary for new generation sequence. The obtained DNA libraries are purified and the quality amounts are measured by the fluorescence-based methods and then the sequence operation is realized by the Illumina-Miseq device. After the sequence operation, any information about sequence of around 10.000 fragments is obtained from the libraries prepared for each sample.

The readings obtained as a result of sequence are cleaned firstly from the adaptor sequences added to each fragment. Then, the sample pertaining to the reading is determined by using the index sequences and the readings are grouped by the samples. After the adaptor and index sequences are trimmed and removed, the readings pass through the necessary filtering steps according to the sequence length and quality data. Furthermore, the noise reduction is conducted to prevent the chimeric readings from affecting the analysis (Edgar et al., 2011; Haas et al., 2011). Thus, it is ensured that the high quality readings are obtained. Each taxonomic level and OTU (Operational Taxonomic Unit) classification are analyzed and the number of the readings assigned to the taxonomic levels by using the BLAST and GreenGenes database (DeSantis et al., 2006). In Table 1, the OTU classification is given according to the sequence similarities. The OTU classification is conducted by examining the groupings of the sequences by 97% similarities (Sun et al., 2011). Consequently, the ratios of the microorganisms contained in each sample are obtained for each taxonomic level and a microbial profile is obtained.

**Table 1.** OTU classification according to sequence similarities

| Reference sequence similarity rate (%) | Assigned level       |
|--|----------------------|
| > 97                                   | Species              |
| 97 - 95                                | Unclassified genus   |
| 95 - 90                                | Unclassified family  |
| 90 - 85                                | Unclassified order   |
| 85 - 80                                | Unclassified classis |
| 80 - 77                                | Unclassified divisio |
| < 77                                   | Unclassified         |

## RESULTS

### 5) The Upflow Packed-Bed Reactor (UPBR) Experiments

According to the results obtained from the Upflow Anaerobic Packed Bed Reactor (UAPB), different concentrations of the wastewater containing cephamycin, amphotericin b and kanamycin antibiotics in the continuous reactor are eliminated.

The Upflow Packed Bed Reactor (UPBR) studies last for 173 days. The anaerobic sludge already fed and activated by starch is used in the reactor. The treatment operation is started so that concentration of the synthetic wastewater shall be 10 mg/L, and it is continued by increasing the amount up to 10 mg/L. The hydraulic retention time is determined as 96 hours. However, the redox potential is measured during the study in the reactor is measured and the variations between -382 and -411mV are observed. The data obtained during the testing process is given in Table 2.

In Figures 2 and 3, the input and output COD (Chemical oxygen demand) values, organic loading ratios (OLR), input and output VFA concentrations, bicarbonate alkalinity values (BA), pH and wastewater concentration variations applied for 173 days are given.

According to the obtained results, the highest COD removal is determined, when 30 mg/L antibiotic concentration is applied, and when HRT, OLR, and COD are 96 hours, 0.618 g and L<sup>-1</sup> day<sup>-1</sup> respectively. But, COD removal varies between 95% and 98% during the study. Namely, a high elimination efficiency is obtained in high antibiotic concentration as well.

### Ecotoxicological Studies

In the continuous reactor studies, toxicities of the synthetic waters in different antibiotic concentrations are determined before and after the treatment study. In the study, it is determined that an amount of 100 mg/L tested as the highest antibiotic concentration is fairly toxic before the treatment operation. It is determined that the wastewater never shows a toxic property after the treatment operation. The results are shown in Table 3.

When 10% concentration of the synthetic waste water containing 100 mg/L antibiotic is subject to the test organism for 5 minutes, it corresponds to EC<sub>50</sub> value. EC<sub>50</sub> values state %11 wastewater concentration in 15 minutes. A concentration value of EC<sub>50</sub> value of the water obtained after treatment is not encountered in 5 and 15 minutes. This results from the fact that the water has an equivalent radiation as the control well not containing any toxic material. This is an indication that the treated water never contains any toxic material.

## Determination of Microbial Composition

### 6) NGS analysis results

The NGS results are given by stating number of sequences and calculating ration at the type and species level for bacteria and archaea in Table 4 and Table 5 respectively.

When the NGS results are examined, it determined that 347 different species are available in the bacteria domain in the anaerobic bacteria used in the study. Most available species are *Syntrophobacter spp.* with 19.5%, *op8 (candidate division)* with 19.3% and *Delftia lacustris* with 16.5%. When it is examined in terms of archaea domain, 26 different species are determined. Among methanogens, most available species *Methanosaeta concilii* with 87%.

**Table 2.** The Anaerobic Treatment Results of the The Upflow Packed-Bed Reactor

| Influent Parameters |   |        |      |     | Effluent Parameters |            |     |     |                            |            |     |                 |                |
|---------------------|---|--------|------|-----|---------------------|------------|-----|-----|----------------------------|------------|-----|-----------------|----------------|
| Day                 | Synthetic Wastewater Concentration (mg/L) | HRT(h) | COD  | pH  | OLR                 | Alkalinity | COD | pH  | Bio-gas (CH <sub>4</sub> ) | Alkalinity | VFA | COD removal (%) | VFA/Alkalinity |
| 1-16                | 10  | 96     | 2200 | 7,1 | 0,55                | 3000       | 92  | 8,4 | -                          | 1165       | 37  | 95,82           | 0,031          |
| 17-33               | 20  | 96     | 2250 | 7,1 | 0,563               | 3000       | 86  | 8,3 | -                          | 1233       | 42  | 96,18           | 0,034          |
| 34-50               | 30  | 96     | 2472 | 7,1 | 0,618               | 3000       | 44  | 8,9 | -                          | 1149       | 39  | 98,22           | 0,033          |
| 51-71               | 40  | 96     | 2540 | 7,1 | 0,635               | 3000       | 96  | 8,6 | -                          | 1212       | 35  | 96,22           | 0,029          |
| 72-92               | 50  | 96     | 2670 | 7,1 | 0,668               | 3000       | 52  | 8,9 | -                          | 1139       | 46  | 98,05           | 0,040          |
| 93-105              | 60  | 96     | 2740 | 7,1 | 0,685               | 3000       | 82  | 8,9 | 0,181                      | 1049       | 52  | 97,00           | 0,049          |
| 106-122             | 70  | 96     | 2824 | 7,0 | 0,706               | 3000       | 99  | 8,9 | 0,362                      | 1045       | 40  | 96,50           | 0,048          |
| 123-139             | 80  | 96     | 2900 | 7,0 | 0,725               | 3000       | 101 | 8,9 | 0,454                      | 1011       | 48  | 96,52           | 0,047          |
| 140-156             | 90  | 96     | 2976 | 6,7 | 0,744               | 3000       | 141 | 8,9 | 0,636                      | 978        | 40  | 95,26           | 0,040          |
| 157-173             | 100                                       | 96     | 3110 | 6,8 | 0,778               | 3000       | 137 | 8,2 | 0,727                      | 952        | 37  | 95,59           | 0,039          |

Note: HRT (h); COD (mg l<sup>-1</sup>); OLR (g COD l<sup>-1</sup> d<sup>-1</sup>); Alkalinity (mg CaCO<sub>3</sub> l<sup>-1</sup>); VFA (mg l<sup>-1</sup>); Gas Production l CH<sub>4</sub> l<sup>-1</sup> d<sup>-1</sup>

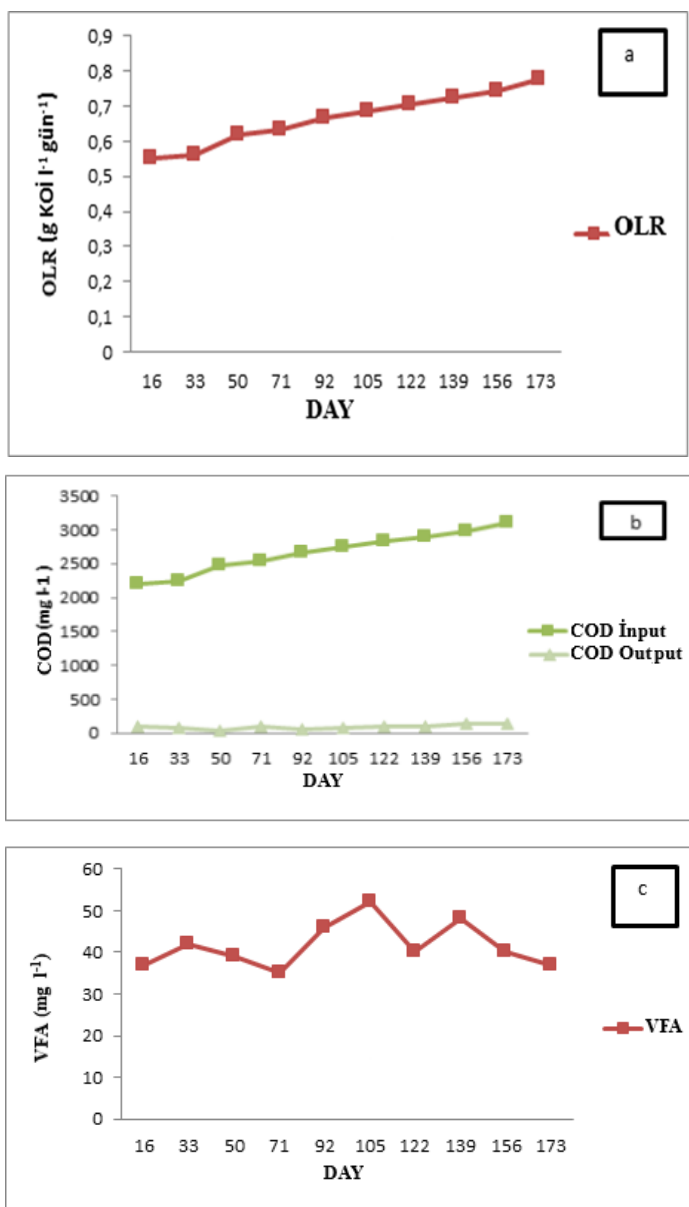


**Figure 2.** The variations during the treatment process in the upflow anaerobic packed-bed reactor: a) OLR b) input and output COD and c) VFA

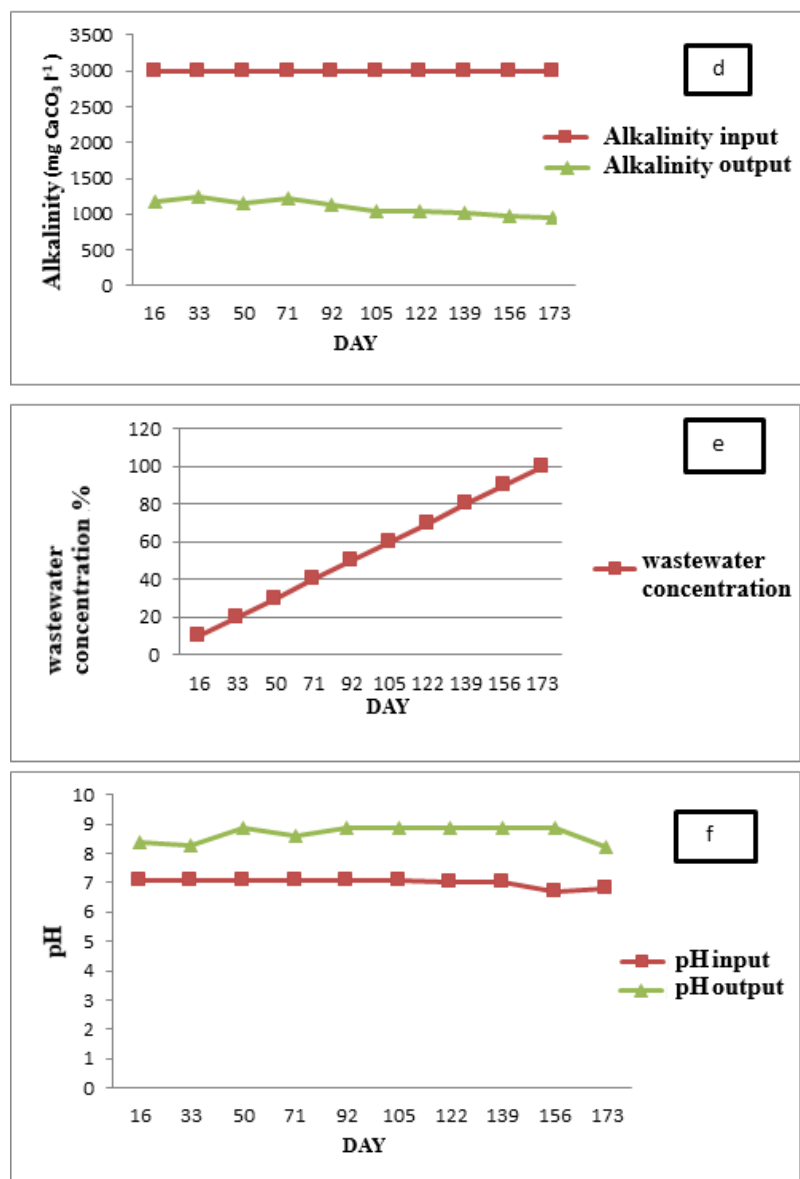


**Figure 3.** The variations during the treatment process in the upstream anaerobic packed-bed reactor: d) Alkalinity (input and output); e) wastewater concentration; and f) pH (input and output).

**Table 3.** Toxicity results

|                                      | <b>5 min results<br/>(% concentration)</b> | <b>15 min results<br/>(% concentration)</b> |
|--------------------------------------|--|---|
| Influent wastewater (100 mg/L)       | 10   | 11  |
| Effluent (After anaerobic treatment) | Nontoxic                                   | Nontoxic                                    |

**Table 4.** The results of the NGS analysis for bacteria.

| <b>Species</b>                    | <b>Number of Sequences</b> | <b>%</b> |
|-----------------------------------|----------------------------|----------|
| <i>Syntrophobacter spp.</i>       | 8496                       | 19,563   |
| <i>op8 (candidate division)</i>   | 8414                       | 19,374   |
| <i>Delftia lacustris</i>          | 7186                       | 16,546   |
| <i>Rhodopseudomonas palustris</i> | 2350                       | 5,411    |
| <i>Kosmotoga spp.</i>             | 1721                       | 3,963    |
| <i>Syntrophobacter</i>            | 860                        | 1,980    |
| <i>Syntrophobacteraceae</i>       | 841                        | 1,936    |
| <i>Desulfovibrio aminophilus</i>  | 571                        | 1,315    |
| <i>Azospirillum oryzae</i>        | 552                        | 1,271    |
| <i>Comamonadaceae</i>             | 473                        | 1,089    |
| <i>Ochrobactrum tritici</i>       | 438                        | 1,009    |
| <i>Rhodocyclaceae</i>             | 419                        | 0,965    |
| <i>Longilinea spp.</i>            | 392                        | 0,903    |
| <i>Syntrophaceae</i>              | 389                        | 0,896    |
| <i>Variovorax spp.</i>            | 383                        | 0,882    |
| <i>Ottowia spp.</i>               | 349                        | 0,804    |
| <i>Rhizobium giardinii</i>        | 349                        | 0,804    |

Table 5. The results of the NGS analysis for archaea.

| Species                           | Number of Sequences | %      |
|-----------------------------------|---------------------|--------|
| <i>Methanosaeta concilii</i>      | 140389              | 87,211 |
| <i>Methanosaeta spp.</i>          | 7295                | 4,532  |
| <i>Methanosaeta</i>               | 3736                | 2,321  |
| <i>Methanospirillum hungatei</i>  | 3540                | 2,199  |
| <i>Methanosphaerula palustris</i> | 2925                | 1,817  |
| <i>Methanosarcina barkeri</i>     | 957                 | 0,594  |
| <i>Methanospirillum spp.</i>      | 377                 | 0,234  |
| <i>Family unspecified</i>         | 364                 | 0,226  |
| <i>Methanosaetaceae</i>           | 346                 | 0,215  |
| <i>Methanomicrobiales</i>         | 270                 | 0,168  |
| <i>Methanosphaerula</i>           | 214                 | 0,133  |
| <i>Methanomicrobia</i>            | 179                 | 0,111  |
| <i>Methanosarcinaceae</i>         | 138                 | 0,086  |
| <i>Methanoculleus spp.</i>        | 100                 | 0,062  |

## DISCUSSION

In this study, it is aimed to reveal the treatment capacity of the wastewaters, which may form possibly as a result of environmental dispersion of the antibiotics as a group mostly used in the drug industry in the anaerobic systems, to offer any alternative treatment methods to the facilities generating these waste waters, to determine the microorganisms playing active role in the treatment operation and to create a specific inoculum for waste water. In the scope of the study, firstly the treatment

potentials of the synthetic waste waters prepared with different groups *in vitro* are determined in the batch anaerobic reactor. The optimum data obtained from the batch studies, and the antibiotic groups, which provide the best elimination are first steps to pass to the continuous anaerobic system. In the studies conducted in the batch reactor, the efficiency of COD elimination is considered primarily by a biological method in the anaerobic UPBR reactor. However, microbial variety is determined by NGS in the sludge samples taken under highest treatment efficiency conditions. Thus, variety of the microorganisms that are active under best conditions may be determined.

### **7) The Upflow Packed-Bed Reactor (UPBR) Experiments**

Operation of the continuous reactor is started under most suitable conditions determined in the batch reactor tests conducted to ensure that the anaerobic treatment may be efficient and cost-effective. In the reactor, the parameters specified in Table 2 and especially COD removal during 173 days are monitored.

It is endeavored to reach the conditions having the highest treatment efficiency by changing COD and OLR as input parameters during this process. It is ensured that the anaerobic sludge in the upflow anaerobic packed bed anaerobic reactor is fed by the feeding solution containing starch, and thus the anaerobic consortium becomes active. Upon activation, the waste water concentration is increased to 100 mg/L in an increment of 10 mg/L at each step beginning from the antibiotic concentration. HAS is stabilized as 96 hours during the study. In 173 day study, the organic loading is 0.55 to 0.77g COD L<sup>-1</sup> daily, and COD elimination varies between 95.26% and 98.22%. When the literature is reviewed, any studies on the anaerobic treatment of different antibiotic groups are seen. In the study of (Celebi et al. 2008), the anaerobic treatment capacity of 50 mg/L amoxicillin, oxytetracycline, tylosin and erythromycin is examined individually in the Anaerobic Multiple-Stage Bed reactor (AMSBR) system. It is found that the elimination efficiency for amoxicillin is 76% in the reactors containing oxytetracycline, tylosin, erythromycin and amoxicillin. It is determined that maximum COD removal efficiencies are 87%, 83%, 86% and 83% respectively at the end of 30<sup>th</sup> day. In a different research, the treatment capacities of tylosin and erythromycin antibiotics in the Anaerobic Multiple-Stage Bed reactor (AMSBR) system and then in the Aerobic Continuous Stirring Tank Reactor (CSTR) system are investigated. As a result of the study, it is found that COD elimination efficiencies of tylosin and erythromycin fed into the reactor in the increased concentrations (50, 100, 150, 200 and 250 mg/L) are 70% to 100% and 80% to 95% for erythromycin and tylosin respectively in the Anaerobic Multiple-Stage Bed reactor (AMSBR) system. In the consecutive anaerobic/aerobic reactor system, approximately 95% COD and 100% antibiotic elimination efficiencies are obtained in all tylosin and erythromycin concentrations (Celebi and Sponza, 2009).

In the study conducted by Zhiqiang (Chen et al. 2010), the anaerobic treatment of the synthetic drug waste waters such as 6 – APA, amoxicillin,

etc. are investigated at a high loading rate of 12.57 to 21.02 Kg m<sup>-3</sup> and at a pH value of 5.57 to 8.26. In the upstream sludge bed reactor, 52.2% and 26.3% COR eliminations are obtained for 6 - APA and amoxicillin respectively.

pH, alkalinity and volatile fatty acid variations, which enable us to get information about stability of the anaerobic treatment, are monitored during the study. When pH values are examined, it is seen that pH varies between 8.2 and 8.9 in all OLR concentrations applied in the reactor. This increase in the output pH is attributable to presence of OH groups in the structure of amphotericin b and cephamycin antibiotics used by us. As a result of decomposition, these groups break free and may increase pH a little bit. It is endeavored to stabilize this increase by means of bicarbonate buffer. Therefore, 3g L<sup>-1</sup> NaHCO<sub>3</sub> is added into the synthetic waste water having a low alkalinity. The buffering procedure keeps the pH range, in which methanogens are developed in best way in the reactor. High pH values and buffering capacity guarantee that the reactor is not acidified.

If the VFA/Alkalinity ratios used in monitoring the process stability are less than 0.4, this shows that the reactor is stable. If the VFA/Alkalinity ratios are between 0.4 and 0.8, this shows that the reactor is partially stable. If the VFA/Alkalinity ratios are bigger than 0.8, this shows that the reactor is unstable (Behling et al., 1997). If the VFA/Alkalinity ratio of the outlet water increases, this indicates that the bacteria generating acid in the reactor becomes more active. In our study, total volatile fatty acid concentration varies between 37 and 52 mg L<sup>-1</sup> for acetic acid in the anaerobic reactor (Table 2). The UYA/Alkalinity value varies between 0.029 and 0.049 during the anaerobic treatment process. These values show that the reactor is stable throughout the testing process.

Toxicity is an important parameter as well as organic material elimination in discharge of the outlet water obtained after biological treatment of the waste waters of different industrial facilities into the recipient media. In this study, the input toxicity of the synthetic wastewater containing three treated different antibiotic groups, and its output toxicity are investigated with regards to organic material elimination (Table 3). In the study, it is determined that the initial toxicity, EC<sub>50</sub>, of the synthetic waste water tested as the highest concentration (100mg/L) is equal averagely to 10±0.2 and 11±0.2mg/L. It is determined that toxicity of this wastewater, which shall show a toxic effect, when it is delivered into the recipient medium, never remains after the anaerobic treatment. (Yuan ji et al. 2013) determine toxicity values of the drug wastewaters containing antibiotics in any microbial groups efficient in the anaerobic treatment. EC<sub>50</sub> values are found as 3.99, 5.11, 4.32 and 5.63g L<sup>-1</sup> for amoxicillin, kanamycin, lincomycin and ciprofloxacin antibiotics respectively in 15 minutes.

## Determination and monitoring of the microbial consortium in the anaerobic reactor

In the studies conducted to determine the microbial consortium in the anaerobic treatment process of the industrial wastewaters, due to enculturation challenges of the microorganisms, use of the molecular based techniques such as cloning, HRM, FISH, Real Time PCR, T-RFLP, DGGE, NGS, etc. is preferred and the successful results are obtained (Casserly and Erijman, 2003; Sanz and Köchling, 2007; Talbot et al., 2008). In this study, The NGS analysis is used for determination of the microbial consortium playing a role in the anaerobic treatment process of the synthetic wastewater containing antibiotics.

When the NGS results are examined, presence of 347 different species of the bacteria domain is determined in the anaerobic sludge used in the study. When their presence percentages are observed, *Syntrophobacter spp.* (19.5%) is most available species. *Syntrophobacter* oxidizes propionate and produces acetate, CO<sub>2</sub> and H<sub>2</sub> (Madigan and Martinko, 2010). The above given final products *Syntrophobacter*, as a syntrophic bacterium, constitute the significant substrates used in the anaerobic mechanism of the methanogens. Another bacterium identified in the reactor is *op8 (candidate division)* (19.37%). OP8 is a bacterium, which is not encultured yet, and is identified first time in the Yellowstone Obsidian pool (Hugenholtz et al., 1998; López-García et al., 2002). Then, it is determined that this bacterium is encountered in the non-thermophilic aquatic environments and in the anoxic waters of the Cariaco river basin (Dojka et al., 1998; Madrid et al., 2001). There is not any certain information about their physiologies yet (Dhillon et al., 2003). Another species found in the reactor are *Delftia lacustris* (16.5%). *Delftia lacustris* is isolated from the mesotrophic water in Denmark. Various monosaccharides, disaccharides, amino acids and organic materials are used (Niels et al., 2009). Another bacterium is *Rhodopseudomonas palustris*, a purple non-sulfur bacterium. Various aromatic compounds (phenolic, aromatic acids, aromatic aldehyde and hydro acids) are used growth of *Rhodopseudomonas palustris* under the anaerobic conditions (Harwood and Gibson, 1988).

When it is examined with regards to archaea domain, 26 different species are determined. With 87% presence ratio, *Methanosaeta concilii* is most dominant type in the reactor. It is also reported previously that *Methanosaeta* is more superior numerically than other methanogens in the anaerobic reactor (Angenent et al., 2004b). The major cause of this numerical superiority is that the semi-saturation coefficient (K<sub>s</sub>) of *Methanosaeta* on acetate is lower than *Methanosarcina* (Stams et al., 2003). In the bioreactors having a high carbon elimination efficiency, COD and thus acetate concentration are very low. Due to its low acetate concentration, *Methanosaeta* reaches maximum growth rate in a highly shorter time than other archaea species. It is determined that granulation of *Methanosaeta* is increased and this causes a stable reactor performance (MacLeod et al., 1990). It is known that, of archaea generating methane defined up to now,

substrate of only *Methanosaeta* and *Methanosarcina* species may be used as acetate (Zinder, 1993). In our study, *Methanosarcina barkeri* (0.594) is found even at a low ration in the reactor. In the study conducted by Shreeshivadasan (Chelliapan et al. 2011), the microbial community efficient in the anaerobic treatment of the waste waters in the drug industry is investigated. It is determined that the bacteria species dominant in all organic loadings *Desulfovibrio* (8 to 36%), and the archaea species in the lower organic loadings are *Methanosaeta* and the species dominant in the high organic loadings are *Methanosarcina*.

Consequently, the anaerobic treatment efficiencies of the antibiotics found in first ranks in the drug use in the batch and upflow packed bed reactors, and the consortium efficient in treatment are determined in this study. Of course, it is essential primarily to control the drug manufacture and consumption to prevent pollution of the environment by the drug residues. The necessary measurements to be taken include optimization in the drug manufacture, a reduction in a variety of materials, restriction or prohibition of any non-fragmentized materials, reduction of waste amounts, optimum storage, etc. Furthermore, the awareness trainings are given to people for purpose of reducing the drug use. Thus the drug amount released to the environment may be reduced. Upon these possible measures to be taken in researches and consumers, the waste water treatment must also be improved and operated by the more advanced treatment system than the existing systems.

In the study, it is determined that treatment the synthetic wastewaters containing antibiotics may be implemented only by the anaerobic methods without requiring the consecutive anaerobic/aerobic methods, and meet the discharge methods. Of course, the upflow packed bed reactor studies obtained from different antibiotic groups are efficient for us to reach this result. Furthermore, it is noted the wastewater may differ in the microbial consortium members playing a role in the treatment operation depending on chemical components of the wastewater. In the study conducted by Comoglu (2016) on wastewater in the drug industry, it is determined *op8* (candidate division), among bacteria species, and *Methanobacterium formicicum* species, among archaea, are dominant. In this study conducted by us on antibiotic groups, it is determined that *Syntrophobacter spp*, among bacteria species, and *Methanosaeta spp*, among archaea, are more dominant. Based on these results, it may be said that use of inoculums specific for wastewater may provide a high treatment efficiency and time saving in the anaerobic treatment of the waste waters in different industries. Use of inoculums specific for wastewater shall enable to reduce the hydraulic retention time of the reactor. This shall provide power and time saving.

According to the findings obtained as a result of the study, the practice may be started by the sludge, in which *Syntrophobacter spp*, among bacteria species, and *Methanosaeta spp*, among archaea, are dominant, to start the bioreactors to be operated in treatment of the waste waters containing any antibiotic residues in the waste water treatment applications. Upon

commissioning of the reactor, the stability of the reactor may be monitored by measuring the relative amounts of these microorganisms in the sludge.

### **ACKNOWLEDGEMENTS**

This study was supported by Eskişehir Osmangazi University Scientific Research Projects Committee (Project No: 2014-3859).

## REFERENCES

1. Akbarpour Toloti, A. and Mehrdadi, N. (2011). Wastewater treatment from Antibiotics Plant (UASB Reactor) *Int. J. Environ. Res.*, 5(1):241-246.
2. Angenent, L.T., Sung, S., Raskin, L., (2004b). Formation of granules and *Methanosaeta fibres* in an anaerobic migrating blanket reactor (AMBR). *Environmental Microbiology* 6, 315-322.
3. Behling, E., Diaz, A., Colina, G., Herrera, M., Gutierrez, E., Chacin, E., Fernandez, N., Forster, C., (1997). Domestic wastewater treatment using a UASB reactor. *Bioresource Technology* 61, 239-245.
4. Casserly, C., Erijman, L., (2003). Molecular monitoring of microbial diversity in an UASB reactor. *International Biodeterioration & Biodegradation* 52, 7-12.
5. Chelliapan S., Wilby T., Yuzir A., Sallis P.J., (2011) Influence of Organic Loading On The Performance And Microbial Community Structure of an Anaerobic Stage Reactor Treading Pharmaceutical Wastewater, *Desalination*. 271, 257-264.
6. Chen, Z., Wang, H., Chen, Z., Ren, N., Wang A., Shi Y. Li, X, (2010) ,Performance and model of a full-scale up-flow anaerobic sludge blanker (UASB) to treat the pharmaceutical wastewater containing 6-APA and amoxicillin, *Journal of Hazardous Materials* 185, 905-913.
7. Çelebi H., Sponza D., (2008), Antibiyotiklerin Anaerobik Ayrışabilirlikleri, *Biyoloji Bilimleri Araştırma Dergisi*, 1(2), 01-08
8. Çelebi H., Sponza D., (2009). Tilosin ve eritromisin anaerobik/aerobik arıdışık sistemde artırlabilirliği ve toksisite giderimi, *itüdergisi/e su kirlenmesi kontrolü* 19 (1-2), 39-49.
9. Çomoğlu A., B., Iscen Filik C., İlhan S. (2016) The anaerobic treatment of pharmaceutical industry wastewater in an anaerobic batch and upflow packed-bed reactor, *Desalination and Water Treatment* 57, 6278-6289.
10. DeSantis TZ, Hugenholtz P, Larsen N, Rojas M, Brodie EL, Keller K, Huber T, Dalevi D, Hu P, Andersen GL. (2006) Greengenes, a chimera-checked 16S rRNA gene database and workbench compatible with ARB. *Appl. Environ. Microbiol.* 72(7), 5069-72.
11. Dhillon, A., Teske, A., Dillon, J., Stahl, D.A., Sogin, M.L., (2003). Molecular characterization of sulfate-reducing bacteria in the Guaymas Basin. *Applied and Environmental Microbiology* 69, 2765-2772.
12. Dojka, M.A., Hugenholtz, P., Haack, S.K., Pace, N.R., (1998). Microbial diversity in a hydrocarbon-and chlorinated-solvent-contaminated aquifer undergoing intrinsic bioremediation. *Applied and Environmental Microbiology* 64, 3869-3877.
13. Edgar RC, Haas BJ, Clemente JC, Quince C, Knight R. (2011). UCHIME improves sensitivity and speed of chimera detection. *Bioinformatics* 27, 2194-2200.
14. Gottlieb, A., Shaw, C., Smith, A., Wheatley, A., Forsythe, S., (2003). The toxicity of textile reactive azo dyes after hydrolysis and decolourisation. *Journal of Biotechnology* 101, 49-56.
15. Haas BJ, Gevers D, Earl AM, Feldgarden M, Ward DV, Giannoukos G, Ciulla D, Tabbaa D, Highlander SK, Sodergren E, Methé B, DeSantis TZ; Human Microbiome Consortium, Petrosino JF, Knight R, Birren BW. (2011). Chimeric 16S rRNA sequence formation and detection in Sanger and 454-pyrosequenced PCR amplicons. *Genome Res.* 21(3). 494-504.
16. Harwood C S, Gibson J. (1988). Anaerobic and aerobic metabolism of diverse aromatic compounds by the photosynthetic bacterium *Rhodospseudomonas palustris*. *Appl. Environ. Microbiol.* 54(3), 712-7.

17. Hugenholtz, P., Pituille, C., Hershberger, K.L., Pace, N.R., (1998). Novel division level bacterial diversity in a Yellowstone hot spring. *Journal of Bacteriology* 180, 366-376.
18. Kümmerer K. (2009). Antibiotics in the aquatic environment A review part 1, *Chemosphere* 75(4) 417-434.
19. Lane, D.J., (1991). 16S/23S rRNA sequencing. In: Stackebrandt, E., Goodfellow, M. (Eds.), *Nucleic acid techniques in Bacterial systematics*. Wiley, Chichester, England, pp. 205-248
20. López-García, P., Gaill, F., Moreira, D., (2002). Wide bacterial diversity associated with tubes of the vent worm *Riftia pachyptila*. *Environmental Microbiology* 4, 204-215.
21. Lueders, M. Manefield, M.W. Friedrich, (2004). Enhanced sensitivity of DNA- and rRNA-based stable isotope probing by fractionation and quantitative analysis of isopycnic centrifugation gradients, *Environ. Microbiol.* 6, 73-78
22. MacLeod, F., Guiot, S., Costerton, J., (1990). Layered structure of bacterial aggregates produced in an upflow anaerobic sludge bed and filter reactor. *Applied and Environmental Microbiology* 56, 1598-1607.
23. Madigan, M.T., Martinko, J.M., (2010). *Mikroorganizmaların Biyolojisi* (Çev. C. Çökmüş) Palme Yayıncılık, 992 s.
24. Madrid, V.M., Taylor, G.T., Scranton, M.I., Chistoserdov, A.Y., (2001). Phylogenetic diversity of bacterial and archaeal communities in the anoxic zone of the Cariaco Basin. *Applied and Environmental Microbiology* 67, 1663-1674.
25. N. O. G. Jorgensen, K. K. Brandt, O. Nybroe and M. Hansen, (2009). *Delftia lacustris* sp. nov., a peptidoglycandegrading bacterium from fresh water, and emended description of *Delftia tsuruhatensis* as a peptidoglycan-degrading bacterium *International Journal of Systematic and Evolutionary Microbiology* 59, 2195-2199.
26. Ovreas, L., Forney, L., Daae, F.L., Torsvik, V., (1997). Distribution of bacterioplankton in meromictic Lake Saelelanet, as determined by denaturant gradient gel electrophoresis of PCR-amplified gene fragments coding for 16S rRNA. *Appl. Environ. Microbiol.* 63, 3367-3373.
27. Sanz, J.L., Köchling, T., (2007). Molecular biology techniques used in wastewater treatment: an overview. *Process Biochemistry* 42, 119-133.
28. Stams, A., Elferink, S.O., Westermann, P., 2003. Metabolic interactions between methanogenic consortia and anaerobic respiring bacteria, *Biomethanation I*. Springer, pp. 31-56.
29. Sun Y, Cai Y, Huse SM, Knight R, Farmerie WG, Mai V. (2011) A large-scale benchmark study of existing algorithms for taxonomy- independent microbial community analysis. *Brief Bioinform* 13,107-121.
30. Talbot, G., Topp, E., Palin, M., Masse, D., 2008. Evaluation of molecular methods used for establishing the interactions and functions of microorganisms in anaerobic bioreactors. *Water Research* 42, 513-537.
31. Yuan ji J. ,Xing Y.J., Ma Z.T., Zhang M., Zheng P. (2013) Acute Toxicity of Pharmaceutical Wastewater Containing Antibiotics To Anaerobic Digestion Treatment. *Chemosphere* 91, 1094-1098.
32. Zinder, S.H., (1993). *Physiological ecology of methanogens, Methanogenesis*. Springer, pp. 128-206.

# EVALUATION OF RADIOLOGICAL RISK IN HERBAL TEAS CONSUMED IN RIZE, TURKEY

Erkan KIRIŞ<sup>1</sup>



---

<sup>1</sup> Dr. Öğr. Üyesi Recep Tayyip Erdoğan University, Faculty of Arts and Sciences,  
Department of Physics, 53100 Rize, Turkey.



## INTRODUCTION

Humans are constantly exposed to the radiation emitted by natural and artificial radionuclides throughout their lives. Natural radiation is generally composed from cosmic rays and terrestrial radiation sources. The main radionuclides forming terrestrial natural radiation sources are  $^{238}\text{U}$ ,  $^{232}\text{Th}$  and  $^{40}\text{K}$ . The concentrations of these natural radionuclides vary from region to region due to factors such as geographical and geological structure, climate and various agricultural practices (Gündoğdu, 2019). Artificial radionuclides such as  $^{137}\text{Cs}$  may be released into the environment because of human activities including energy production, nuclear weapon testing, and nuclear accidents (Poursharif et al., 2015).

Radioactive particles are transferred to the plants in two basic ways. These are direct and indirect deposition. Direct deposition is the accumulation of radionuclides in the atmosphere above the soil. Indirect deposition is the absorption of radionuclides in the soil with the roots of plants (Sussa et al., 2013). Humans have been using herbal teas for a long time as a complementary treatment in different diseases and still have a significant role in traditional medicine in many countries. In addition, herbal teas are used by humans as refreshing drinks and as aromatic plants in their diet (Mitrovic et al., 2014). The most commonly used plant parts for this purpose are the leaves, flowers, fruit, seeds, stems, wood, bark, roots and rhizomes (WHO, 2007).

If herbal teas used by humans in daily life contain high concentrations of natural and artificial radionuclides, herbal teas can cause health problems. Therefore, the studies on determination the levels of radioactivity in herbal teas and evaluation the risks of these levels to human health are required. This work was aimed at determination of the activity concentrations of  $^{226}\text{Ra}$ ,  $^{232}\text{Th}$ ,  $^{40}\text{K}$  and  $^{137}\text{Cs}$  using High-Purity Germanium (HPGe) detector in eleven different herbal teas consumed in the Rize province. In addition, the annual effective dose and cancer risk values of  $^{226}\text{Ra}$ ,  $^{232}\text{Th}$ ,  $^{40}\text{K}$  and  $^{137}\text{Cs}$  due to the consumption of herbal teas were calculated.

## MATERIALS AND METHODS

### Sample collection and preparation

Eleven different samples of herbal teas were obtained from the markets selling medicinal plants in the center of Rize province in November 2018. The most frequently consumed herbal tea samples in Rize were selected. Scientific name, common name and part used of herbal teas used in this study are given in Table 1.

**Table 1.** Names and parts used of some herbal teas investigated in this study.

| Scientific name                 | Common name | Part used    |
|---------------------------------|-------------|--------------|
| <i>Matricaria chamomilla L.</i> | Chamomile   | Flower       |
| <i>Mentha Piperita L.</i>       | Peppermint  | Leaf         |
| <i>Thymus vulgaris L.</i>       | Thyme       | Leaf         |
| <i>Rosa canina L.</i>           | Dog Rose    | Fruit        |
| <i>Tilia cordata Mill.</i>      | Linden      | Leaf, Flower |
| <i>Salvia Officinalis L.</i>    | Sage        | Leaf         |
| <i>Urtica dioica L.</i>         | Nettle      | Leaf         |
| <i>Achillea millefolium L.</i>  | Yarrow      | Flower       |
| <i>Camellia sinensis L.</i>     | Green Tea   | Leaf         |
| <i>Glycyrrhiza glabra L.</i>    | Licorice    | Root         |
| <i>Melissa officinalis L.</i>   | Lemon Balm  | Leaf         |

The samples were stored in plastic food grade containers at room temperature. Then, the samples were dried in a stove at a temperature of 80 °C for 48 h to remove moisture (Harb, 2015). The dried samples were powdered in a mixer grinder. Then, the samples were passed through a sieve to obtain uniform particle size. Finally, the samples were homogenized and transferred to cylindrical polyethylene containers of 100 mL volume and sealed for a period of 4 weeks in order to allow secular radioactive equilibrium between radium and thorium and their decay products (Celik et al., 2008).

### Radionuclide activity measurement

The activities of radionuclides were measured using HPGe detector (Ortec, GEM55P4-95 model) having a relative efficiency of 55% and a resolution of 1.9 keV at the 1332 keV gamma of  $^{60}\text{Co}$ . The detector was shielded with a cylindrical lead (10 cm thick) to decrease the gamma ray background due to cosmic rays and radiation in the environment in which the measurement is performed. The gamma peak analysis was carried out using Maestro-32 software provided from Ortec. The measurement time was selected to be 100,000 s for all samples.

In order to determine the activity values of the radionuclides, the gamma-ray energies of  $^{214}\text{Pb}$  (351.9 keV) and  $^{214}\text{Bi}$  (609.3 keV) were used for  $^{226}\text{Ra}$ ,

the gamma-ray energies of  $^{228}\text{Ac}$  (911.1 keV) and  $^{208}\text{Tl}$  (583.1 keV) were used to for  $^{232}\text{Th}$ , gamma line of 1460.8 keV was used for  $^{40}\text{K}$  and gamma line of 661.6 keV were used for  $^{137}\text{Cs}$ . The activity concentrations of the radionuclides were given as  $\text{Bq kg}^{-1}$  in dry weight for the herbal tea samples.

Below equation was used to determine the activity concentrations (A) of  $^{226}\text{Ra}$ ,  $^{232}\text{Th}$ ,  $^{40}\text{K}$  and  $^{137}\text{Cs}$  in the measured samples (Cevik et al. 2010):

$$A = \frac{N_{\text{net}}}{\varepsilon \cdot P_{\gamma} \cdot t \cdot m} \quad (\text{Bq kg}^{-1}) \quad (1)$$

in which  $N_{\text{net}}$  represent the net count (background subtracted) of the related gamma lines,  $\varepsilon$  is the absolute gamma peak detection efficiency,  $P_{\gamma}$  is the intensity of the gamma line in a radionuclide,  $t$  is the measurement time in second, and  $m$  is the mass of herbal tea sample in kg.

The following formula was used to calculate the MDA - minimum detectable activity - of the current system of measurement (Currie, 1968):

$$\text{MDA} = \frac{1.645\sqrt{B}}{\varepsilon \cdot P_{\gamma} \cdot t \cdot m} \quad (\text{Bq kg}^{-1}) \quad (2)$$

where  $B$  is the background count for the related gamma line in a radionuclide. The MDA values for the related radionuclides in herbal tea samples was calculated as  $0.38 \text{ Bq kg}^{-1}$  for  $^{226}\text{Ra}$ ,  $0.35 \text{ Bq kg}^{-1}$  for  $^{232}\text{Th}$ ,  $2.6 \text{ Bq kg}^{-1}$  for  $^{40}\text{K}$  and  $0.03 \text{ Bq kg}^{-1}$  for  $^{137}\text{Cs}$ . The certified activity values of  $^{226}\text{Ra}$ ,  $^{232}\text{Th}$ ,  $^{40}\text{K}$  and  $^{137}\text{Cs}$  for reference material (IAEA-447) were given as 25.04, 37.3, 550 and 371.11  $\text{Bq kg}^{-1}$ , respectively. The activity values of  $^{226}\text{Ra}$ ,  $^{232}\text{Th}$ ,  $^{40}\text{K}$  and  $^{137}\text{Cs}$  for the measurement system were determined to be 23.96, 35.7, 521 and 362.55  $\text{Bq kg}^{-1}$ , respectively.

### Radiological hazard parameters in herbal teas

The annual effective dose due to ingestion of  $^{226}\text{Ra}$ ,  $^{232}\text{Th}$ ,  $^{40}\text{K}$  and  $^{137}\text{Cs}$  in the herbal teas has been calculated by the following equation (Harb, 2015):

$$\text{AED} = A \times I \times \text{DCF} \quad (3)$$

where, AED is the annual effective dose ( $\text{Sv y}^{-1}$ ),  $A$  is the mean activity value of radionuclides ( $\text{Bq kg}^{-1}$ ), and  $I$  is the annual consumption of herbal tea ( $\text{kg y}^{-1}$ ), annually ingested quantity for herbal tea was  $1 \text{ kg y}^{-1}$  per person for adults (Parmaksız and Ağuş, 2014). DCF is the ingestion dose conversion factor for each radionuclide ( $2.8 \times 10^{-7} \text{ Sv Bq}^{-1}$  for  $^{226}\text{Ra}$ ,  $2.3 \times 10^{-7} \text{ Sv Bq}^{-1}$  for  $^{232}\text{Th}$ ,  $6.2 \times 10^{-9} \text{ Sv Bq}^{-1}$  for  $^{40}\text{K}$  and  $1.3 \times 10^{-8} \text{ Sv Bq}^{-1}$  for  $^{137}\text{Cs}$ ) (IAEA, 2011).

Fatal cancer risk was estimated from effective dose obtained using the International Commission on Radiological Protection cancer risk assessment methodology (ICRP, 2007) as stated in the following equation:

$$\text{CR} = \text{AED} \times \text{DL} \times \text{RF} \quad (4)$$

where, DL is life expectancy (70 years) and RF is risk factor ( $\text{Sv}^{-1}$ ). For stochastic effects, International Commission on Radiological Protection uses a value of 0.05 for public as risk factor (ICRP, 1991).

## RESULTS AND DISCUSSION

The mean activity values of  $^{226}\text{Ra}$ ,  $^{232}\text{Th}$ ,  $^{40}\text{K}$  and  $^{137}\text{Cs}$  determined in the herbal teas consumed in Rize are presented in Table 2. As shown in Table 2, the activity values of  $^{226}\text{Ra}$  in the herbal teas varied from 0.40 to 5.79  $\text{Bq kg}^{-1}$  with a mean value of 2.20  $\text{Bq kg}^{-1}$ . For the activity values of  $^{232}\text{Th}$  in the herbal teas, it ranged from 0.71 to 3.55  $\text{Bq kg}^{-1}$  with a mean value of 1.46  $\text{Bq kg}^{-1}$ . The highest value of  $^{226}\text{Ra}$  and  $^{232}\text{Th}$  was recorded in chamomile. The activity values of  $^{40}\text{K}$  in the herbal teas ranged from 153.4 to 1024.9  $\text{Bq kg}^{-1}$  with a mean value of 425.7  $\text{Bq kg}^{-1}$ . The highest value of  $^{40}\text{K}$  was observed in nettle. The activity value of  $^{137}\text{Cs}$  was determined only in linden, and it was 7.51  $\text{Bq kg}^{-1}$ . Also, all the activity values of  $^{226}\text{Ra}$  and  $^{232}\text{Th}$  in the herbal teas are lower than the world mean value (33 and 45  $\text{Bq kg}^{-1}$ , respectively) (UNSCEAR, 2000). The  $^{40}\text{K}$  activity value for chamomile, peppermint and nettle was determined to be higher than the world mean value (420  $\text{Bq kg}^{-1}$ ) (UNSCEAR, 2000).

In addition, the concentration levels of  $^{226}\text{Ra}$ ,  $^{232}\text{Th}$ ,  $^{40}\text{K}$  and  $^{137}\text{Cs}$  for herbal tea samples in present study were compared with the activity values determined in previous studies in the literature. The highest level of  $^{226}\text{Ra}$ ,  $^{232}\text{Th}$ ,  $^{40}\text{K}$  and  $^{137}\text{Cs}$  obtained in present study was determined to be lower than the highest value of  $^{226}\text{Ra}$ ,  $^{232}\text{Th}$ ,  $^{40}\text{K}$  and  $^{137}\text{Cs}$  reported for herbal teas in Serbian (8.2, 18.3, 1243.7 and 82.5  $\text{Bq kg}^{-1}$ , respectively) (Jevremovic et al., 2011) and Egypt (115.08, 40.32, 2090 and 12.62  $\text{Bq kg}^{-1}$ , respectively) (Ahmed et al., 2010). The highest level of  $^{226}\text{Ra}$  and  $^{40}\text{K}$  in present study was determined to be lower than the highest value of  $^{226}\text{Ra}$  and  $^{40}\text{K}$  (15.1 and 1311.5  $\text{Bq kg}^{-1}$ ) reported for medicinal herbs in Turkey, but the same comparison was not observed for the  $^{232}\text{Th}$  and  $^{137}\text{Cs}$  level (3.5 and  $<1.8 \text{ Bq kg}^{-1}$ ) (Parmaksız and Ağuş, 2014).

**Table 2.** Activity concentrations (Bq kg<sup>-1</sup>, dw) of radionuclides such as <sup>226</sup>Ra, <sup>232</sup>Th, <sup>40</sup>K and <sup>137</sup>Cs in herbal teas.

| Sample     | <sup>226</sup> Ra | <sup>232</sup> Th | <sup>40</sup> K | <sup>137</sup> Cs |
|------------|-------------------|-------------------|-----------------|-------------------|
| Chamomile  | 5.79±0.28         | 3.55±0.16         | 554.0±26.8      | <MDA              |
| Peppermint | 1.64±0.07         | 1.01±0.04         | 481.1±22.9      | <MDA              |
| Thyme      | 0.48±0.02         | 0.77±0.03         | 339.1±15.2      | <MDA              |
| Dog Rose   | <MDA              | <MDA              | 337.4±14.6      | <MDA              |
| Linden     | <MDA              | 0.84±0.04         | 312.7±13.4      | 7.51±0.33         |
| Sage       | 0.40±0.02         | 1.22±0.05         | 388.5±18.6      | <MDA              |
| Nettle     | 2.69±0.12         | 1.27±0.05         | 1024.9±52.7     | <MDA              |
| Yarrow     | <MDA              | 1.09±0.04         | 349.0±15.5      | <MDA              |
| Green Tea  | <MDA              | 2.70±0.12         | 317.1±13.7      | <MDA              |
| Licorice   | <MDA              | <MDA              | 153.4±5.9       | <MDA              |
| Lemon Balm | <MDA              | 0.71±0.03         | 269.8±10.7      | <MDA              |
| Average    | 2.20              | 1.46              | 425.7           | 7.51              |

The annual effective doses due to ingestion of <sup>226</sup>Ra, <sup>232</sup>Th, <sup>40</sup>K and <sup>137</sup>Cs in the herbal teas are given in Table 3. The annual effective dose value of <sup>226</sup>Ra, <sup>232</sup>Th and <sup>40</sup>K varied from 0.11 to 1.62, 0.16 to 0.82 and 0.95 to 6.35  $\mu\text{Sv y}^{-1}$ , respectively. The annual effective dose value of <sup>137</sup>Cs was 0.10  $\mu\text{Sv y}^{-1}$ , and only calculated for linden. All the effective dose values calculated for the herbal teas consumed in Rize are much lower than the world mean of 70  $\mu\text{Sv y}^{-1}$  proposed by United Nation Scientific Committee on Energy and Atomic Research (UNSCEAR, 2000) and also lower than the mean radiation dose of 0.3 mSv  $\text{y}^{-1}$  received per person worldwide (WHO, 2007).

**Table 3.** Annual effective dose values of radionuclides such as  $^{226}\text{Ra}$ ,  $^{232}\text{Th}$ ,  $^{40}\text{K}$  and  $^{137}\text{Cs}$  in herbal teas.

| Sample     | AED ( $\mu\text{Sv y}^{-1}$ ) |                   |                 |                   |
|------------|-------------------------------|-------------------|-----------------|-------------------|
|            | $^{226}\text{Ra}$             | $^{232}\text{Th}$ | $^{40}\text{K}$ | $^{137}\text{Cs}$ |
| Chamomile  | 1.62                          | 0.82              | 3.43            | –                 |
| Peppermint | 0.46                          | 0.23              | 2.98            | –                 |
| Thyme      | 0.13                          | 0.18              | 2.10            | –                 |
| Dog Rose   | –                             | –                 | 2.09            | –                 |
| Linden     | –                             | 0.19              | 1.94            | 0.10              |
| Sage       | 0.11                          | 0.28              | 2.41            | –                 |
| Nettle     | 0.75                          | 0.29              | 6.35            | –                 |
| Yarrow     | –                             | 0.25              | 2.16            | –                 |
| Green Tea  | –                             | 0.62              | 1.97            | –                 |
| Licorice   | –                             | –                 | 0.95            | –                 |
| Lemon Balm | –                             | 0.16              | –               | –                 |

The cancer risk values of  $^{226}\text{Ra}$ ,  $^{232}\text{Th}$ ,  $^{40}\text{K}$  and  $^{137}\text{Cs}$  due to the consumption of the herbal teas can be observed in Table 4. The cancer risk value of  $^{226}\text{Ra}$ ,  $^{232}\text{Th}$  and  $^{40}\text{K}$  ranged from  $0.39 \times 10^{-6}$  to  $5.67 \times 10^{-6}$ ,  $0.57 \times 10^{-6}$  to  $2.86 \times 10^{-6}$  and  $3.33 \times 10^{-6}$  to  $22.24 \times 10^{-6}$ , respectively. The cancer risk value of  $^{137}\text{Cs}$  is  $0.34 \times 10^{-6}$ , and only calculated for linden. All the cancer risk values calculated are much lower than world's mean value of cancer risk ( $0.29 \times 10^{-3}$ ) (UNSCEAR, 2000).

**Table 4.** Cancer risk values of radionuclides such as  $^{226}\text{Ra}$ ,  $^{232}\text{Th}$ ,  $^{40}\text{K}$  and  $^{137}\text{Cs}$  in herbal teas.

| Sample     | CR ( $\times 10^{-6}$ ) |                   |                 |                   |
|------------|-------------------------|-------------------|-----------------|-------------------|
|            | $^{226}\text{Ra}$       | $^{232}\text{Th}$ | $^{40}\text{K}$ | $^{137}\text{Cs}$ |
| Chamomile  | 5.67                    | 2.86              | 12.02           | -                 |
| Peppermint | 1.61                    | 0.81              | 10.44           | -                 |
| Thyme      | 0.47                    | 0.62              | 7.36            | -                 |
| Dog Rose   | -                       | -                 | 7.32            | -                 |
| Linden     | -                       | 0.68              | 6.79            | 0.34              |
| Sage       | 0.39                    | 0.98              | 8.43            | -                 |
| Nettle     | 2.64                    | 1.02              | 22.24           | -                 |
| Yarrow     | -                       | 0.88              | 7.57            | -                 |
| Green Tea  | -                       | 2.17              | 6.88            | -                 |
| Licorice   | -                       | -                 | 3.33            | -                 |
| Lemon Balm | -                       | 0.57              | -               | -                 |

## CONCLUSIONS

The activity concentrations of natural radionuclides such as  $^{226}\text{Ra}$ ,  $^{232}\text{Th}$ ,  $^{40}\text{K}$  and artificial radionuclide  $^{137}\text{Cs}$  in eleven different herbal tea samples consumed in Rize were determined. All the activity concentration values of  $^{226}\text{Ra}$  and  $^{232}\text{Th}$  in the herbal teas are lower than the world mean value proposed by UNSCEAR (2000), except for the activity value of  $^{40}\text{K}$  determined for chamomile, peppermint and nettle. The activity levels of  $^{226}\text{Ra}$ ,  $^{232}\text{Th}$ ,  $^{40}\text{K}$  and  $^{137}\text{Cs}$  were compared with previous studies in literature. The annual effective doses because of ingestion of  $^{226}\text{Ra}$ ,  $^{232}\text{Th}$ ,  $^{40}\text{K}$  and  $^{137}\text{Cs}$  calculated to be much lower than the world mean value proposed by UNSCEAR (2000). In addition, cancer risks from ingestion of  $^{226}\text{Ra}$ ,  $^{232}\text{Th}$ ,  $^{40}\text{K}$  and  $^{137}\text{Cs}$  due to the consumption of herbal teas were calculated to be much lower than the world mean value proposed by UNSCEAR (2000). According to the results obtained in present study, the herbal teas consumed in Rize are considered safe for human health in terms of the radiological hazard.

## REFERENCES

1. A. Parmaksız, Y. Ağuş, "Activity concentrations of  $^{226}\text{Ra}$ ,  $^{232}\text{Th}$ ,  $^{40}\text{K}$  and  $^{137}\text{Cs}$  radionuclides in Turkish medicinal herbs, their ingestion doses and cancer risks", *Radiat. Eff. Defect. S.*, 169(11): 980–988, 2014.
2. B. Gündoğdu, "Türkiye'de yetiştirilen farklı gıda ürünlerindeki radyoaktivite seviyelerinin gama spektroskopi sistemi ile ölçülmesi", İstanbul Üniversitesi Fen Bilimleri Enstitüsü Yüksek Lisans Tezi, İstanbul.
3. B.M. Mitrovic, S.N. Grdovic, G.S. Vitorovic, D.P. Vitorovic, G.K. Pantelic, G.A. Grubic, " $^{137}\text{Cs}$  and  $^{40}\text{K}$  in some traditional herbal teas collected in the mountain regions of Serbia", *Isot. Environ. Health. S.*, 50(4):538–545, 2014.
4. F. Ahmed, M.M. Daif, N.M. El-Masry, M. Abo-Elmagd, "External and internal radiation exposure of herbal plants used in Egypt", *Radiat. Eff. Defect. S.*, 165(1):65–71, 2010.
5. F.V. Sussa, S.R. Damatto, M.M. Alencar, B.P. Mazzilli, P.S.C. Silva, "Natural radioactivity determination in samples of *Peperomia pellucida* commonly used as a medicinal herb", *J. Environ. Radioact.* 116:148–151, 2013.
6. IAEA (International Atomic Energy Agency), "Radiation Protection and Safety of Radiation Sources: International Basic Safety Standards", IAEA Safety standards series no. GSR Part 3 (Interim), STI/PUB/1531, 190–219, 2011.
7. ICRP (International Commission on Radiological Protection), "1990 Recommendations of the International Commission on Radiological Protection", Oxford:Pergamon Press. ICRP publication 60, *Annals of the ICRP* 21(1–3):1–201, 1991.
8. ICRP (International Commission on Radiological Protection), "The 2007 Recommendations of the International Commission on Radiological Protection", Oxford:Pergamon Press. ICRP Publication 103. *Annals of the ICRP* 37(2–4):1–332, 2007.
9. M. Jevremovic, N. Lazarevic, S. Pavlovic, M. Orlic, "Radionuclide concentrations in samples of medicinal herbs and effective dose from ingestion of  $^{137}\text{Cs}$  and natural radionuclides in herbal tea products from Serbian market", *Isot. Environ. Health. S.*, 47(1):87–92, 2011.
10. L.A. Currie, "Limits for qualitative detection and quantitative determination", *Anal. Chem.* 40:586–593, 1968.
11. N. Celik, U. Cevik, A. Celik, B. Kucukomeroglu, "Determination of indoor radon and soil radioactivity levels in Giresun, Turkey", *J. Environ. Radioact.*, 99:1349–1354, 2008.
12. N. Damla, U. Cevik, A.I. Koby, A. Celik, R. Van Grieken, Y. Koby, "Characterization of gas concrete materials used in buildings of Turkey" *J. Hazard. Mater.*, 168:681–687, 2009.
13. S.R.M. Harb, "Natural radioactivity concentrations in some medicinal plants and annual committed effective dose from their consumption" *Radiat. Prot. Environ.* 38(1&2):35–38, 2015.
14. UNSCEAR (United Nations Scientific Committee on the Effects of Atomic Radiation), "Sources and Effects of Ionizing Radiation", United Nations, New York, 2000.

15. WHO (World Health Organization), "Guidelines for assessing quality of herbal medicines with reference to contaminants and residues", Geneva:World Health Organization; 2007.
16. Z. Poursharif, A. Ebrahiminia, M. Asadinezhad, A. Nickfarjam, A. Haeri, K. Khoshgard, "Determination of radionuclide concentrations in tea samples cultivated in Guilan Province, Iran" Iranian Journal of Medical Physics, 12(4):271-277, 2015.



# THE PREPARATION AND CHARACTERIZATION OF SEMI-INTERPENETRATING POLYMER NETWORK HYDROGELS FOR CONTROLLED RELEASE OF 5-FLUOROURACIL

Gülen Oytun AKALIN <sup>1</sup>



---

<sup>1</sup> Dr., Aksaray Üniversitesi, Bilimsel ve Teknolojik Uygulama ve Araştırma Merkezi, Aksaray



## Introduction

5-Fluorouracil (5-FU) is one of the mostly used anticancer drugs because DNA synthesis can be inhibited by its active form. It effects positively [1]. It is used actively in the treatment of the gastrointestinal tract pancreas, colon, head, rectal and breast cancers. Its common usage method is in the constitute of injections into vein as an intravenous or an infusion but, this application led to severe dermatological, cardiac, gastrointestinal, hematological effects. The toxic effects may be reduced by using oral rate-controlled formulation. In this formulation, the biological half-life of the drug is short due to nonhomogeneous absorption and rapid metabolism incomplete [2,3]. The most effective method of drug 5-FU delivery systems is controlled release systems. It is ensured that the active substance remains in effect for a long time with a single application. In controlled release systems, natural or synthetic polymers use for controllable support materials. In general, natural polymers were preferred over synthetic polymers due to their excellent properties such as non-toxicity and biodegradability. The copolymers are used for the design of the 5-FU delivery systems.

Hydrogels are water-insoluble, three-dimensional network homopolymers or copolymers that are crosslinked and capable of containing more than 20% of their volume in water [4]. Hydrogels generally consist of hydrophilic polymer molecules. At least one component of the hydrogels formed from the copolymers must have a hydrophilic property. Hydrogels have found many applications due to their water content, rubbery structures similar to natural tissues and low surface tensions [5]. The controlled drug delivery systems are one of these applications.

Interpenetrating polymer network (IPN) are formed by the physically bonding of two crosslinked synthetic or natural polymers. In semi-IPN-type hydrogels, one of the polymers has a cross-link while the other is linear [6,7]. In such hydrogels, guest polymer chains may be connected covalently or uncovalently within the host network. Hydrogels that affect the pH of the environment in certain proportions are important for the release of drugs in various body regions. These properties are achieved by the combination of many different polymers to form hydrogel.

Gelatin is a natural polymer which is extracted by acid or alkaline treatment of collagen. It is widely used for support material for drug delivery systems [8,9].

In this work, it was aimed to synthesize semi-IPN type hydrogels containing gelatin, acrylic acid (AA) and citraconic acid (CA) by free radical polymerization and to determine swelling behaviors of hydrogels. Ammonium persulphate /sodium metabisulphite  $[(\text{NH}_4)_2\text{S}_2\text{O}_8/\text{Na}_2\text{S}_2\text{O}_5]$  were chosen as an initiator and ethylene glycol dimethacrylate as a crosslinker. The controlled 5-FU release experiments were also performed by using UV-spectrometer. The release kinetics parameters and mechanism of 5-FU from hydrogel were also determined.

## Experimental

### Materials

Gelatin, CA, AA, ethylene glycol dimethacrylate, 5-FU and phosphate-buffered saline (PBS) tablets were obtained from Sigma-Aldrich (Steinem, Germany). Initiators  $[(\text{NH}_4)_2\text{S}_2\text{O}_8/\text{Na}_2\text{S}_2\text{O}_5]$  was purchased from Merck.

### Preparation of hydrogels

AA and CA monomer solutions was mixed with vortex and taken into 10 ml tube. Gelatin (1.0%, 5ml) solution and ethylene glycol dimethacrylate (0.2 ml) and the initiators were mixed into the monomer solution. The fresh hydrogel rods were obtained after 24 h. They were divided into two pieces. The obtained discs were washed with water. The first drying of discs was done in air, the second was made oven in a vacuum oven at 40°C [10]. Discs were stored for further use. The components used to prepare hydrogels are given in Table 1.

**Table 1.** The components used to prepare hydrogels

| Hydrogel | AA (mol/L) | CA (mol/L) |
|----------|------------|------------|
| GEL-1    | 3.0        | 0.5        |
| GEL-2    | 3.0        | 1.0        |
| GEL-3    | 3.0        | 1.5        |
| GEL-4    | 3.0        | 2.0        |

### Swelling Behaviors

Swelling tests were gravimetrically performed with time, temperature and pH. Dried samples were weighed firstly ( $W_1$ ) and then they were put into PBS solutions at pH 7.4, 37.0°C for swelling. Swollen samples took from the medium at certain time, were filtered with paper and weighed. The measuring was continued until constant weight was attained. The swelling percentage of hydrogels were calculated from Equation 1[11].:

$$\text{Swelling\%} = \frac{(W_2 - W_1)}{W_1} \times 100 \quad (1)$$

Where  $W_1$  is the dry mass of the sample,  $W_2$  is the swollen mass of sample in every 24 h.

The temperature test was done by swelling dry samples in PBS solution (pH 7.4) at different temperatures (20.0-60.0°C). pH test was done by

swelling dry samples in PBS solution (37.0°C) at different pH values (from 2.0 to 12.0) [12].

### Scanning electron microscopy (SEM)

Swollen hydrogels were frozen at - 80°C for 24 h and then transferred into Labconco FreeZone 4.5 Freeze Dryer. Samples were coated with gold using a Polaron SC 502 Sputter Coater. The morphology analysis was done with a JEOL, JSM 6060 LV SEM.

### Release of 5-FU from hydrogels

5-FU drug was loaded in crosslinked polymer networks during the copolymerization/crosslinking procedure. Drug-loaded samples were placed into PBS solution. Aliquots of 100 µL were taken from the solution at regular times and the amount of release was measured with UV spectrophotometer (Unicam UV-2100 spectrophotometer) at a wavelength of 266 nm [13,14].

The cumulative release (%) was measured with the following Equation 2:

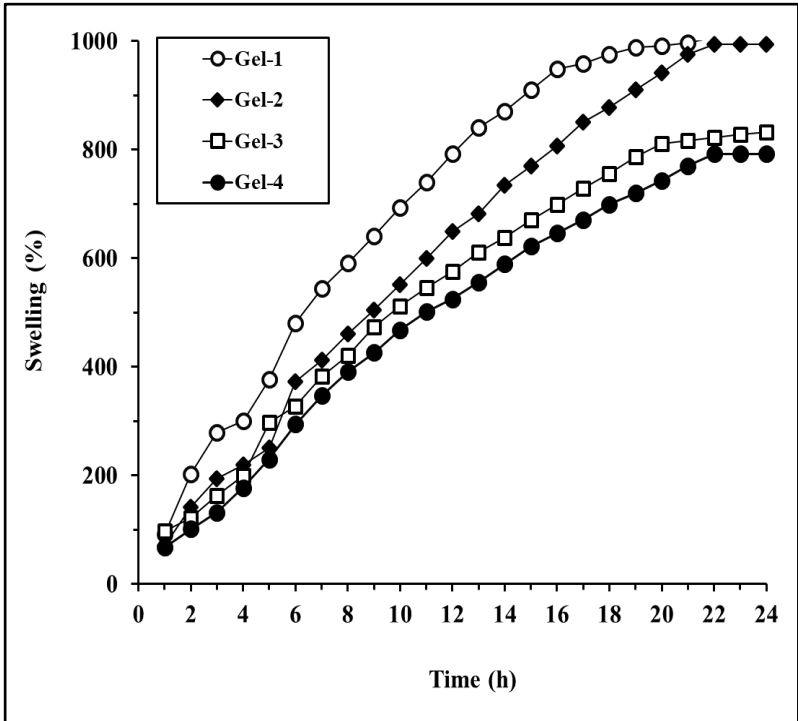
$$\text{Cumulative Release\%} = \frac{W_t}{W_{total}} \times 100 \quad (2)$$

where  $W_t$  is the amount of the released drug at any time and  $W_{total}$  is the initial total drug amount in samples.

## Results and Discussions

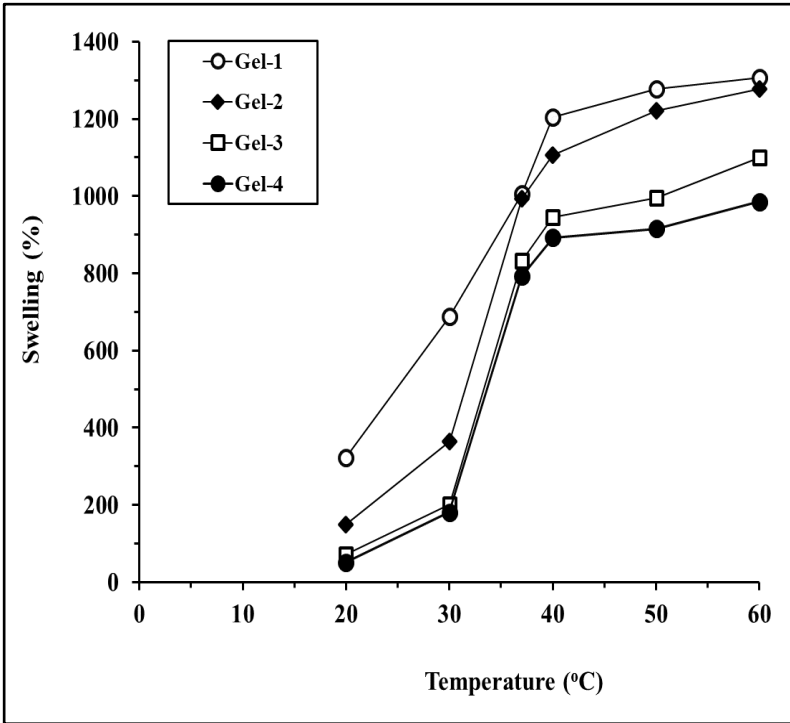
### Swelling test

Figure 1 shows the swelling behavior of hydrogels with time. First, swelling increased with time and then remained stable at 24 h. Swelling values decreased from 1006 to 792% with an increase the content of CA monomer. By increasing the molar concentration, the hydrophobicity of structure was increased, which finally caused decrease in swelling values. Several studies have been reported that swelling depends on the composition or monomer ratio, crosslinker density, crosslinker type and polymerization pathway [15,16].



**Figure 1.** The variation of swelling behavior with time

Figure 2 exhibits the variation of swelling values with the temperature. Samples were swollen more less at low temperatures than at high temperatures. The increase of swelling with temperature can be explained by the breaking of hydrogen bonds in the structure and increase of thermal mobility [17,18].



**Figure 2.** The variation of swelling behavior with temperature

Figure 3 shows the variation of swelling values with pH. Low values were observed at pH 2.0 against other pH values. The highest values were observed at pH 7.0. It can be said that the complete dissociation of AA and CA acid groups cause maximum swelling at this pH value. Their dissociation constants were  $pK_a$  4.25 and  $pK_{a1}$  6.17. The values with respect to pH variations may be due to the difference between these values [19,20].

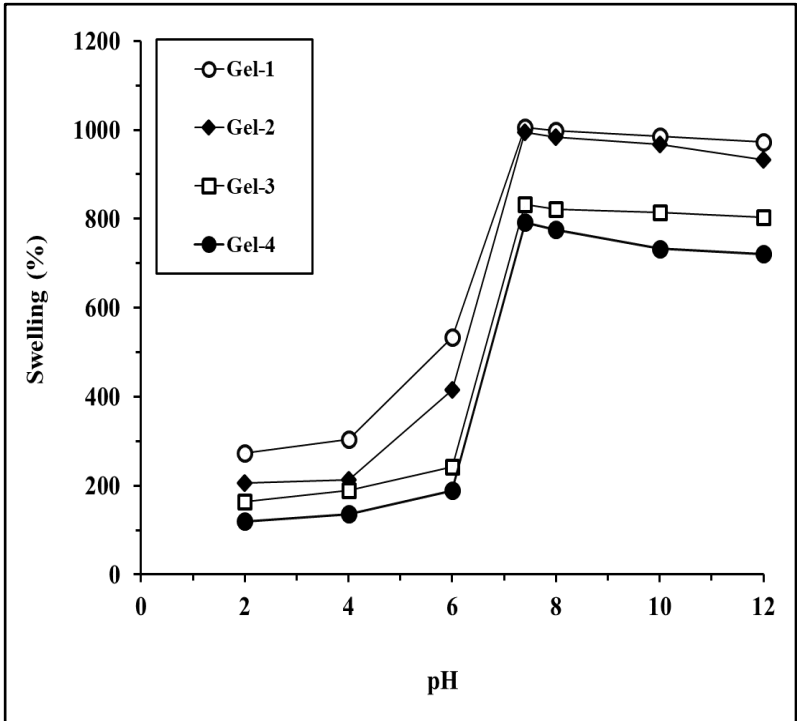
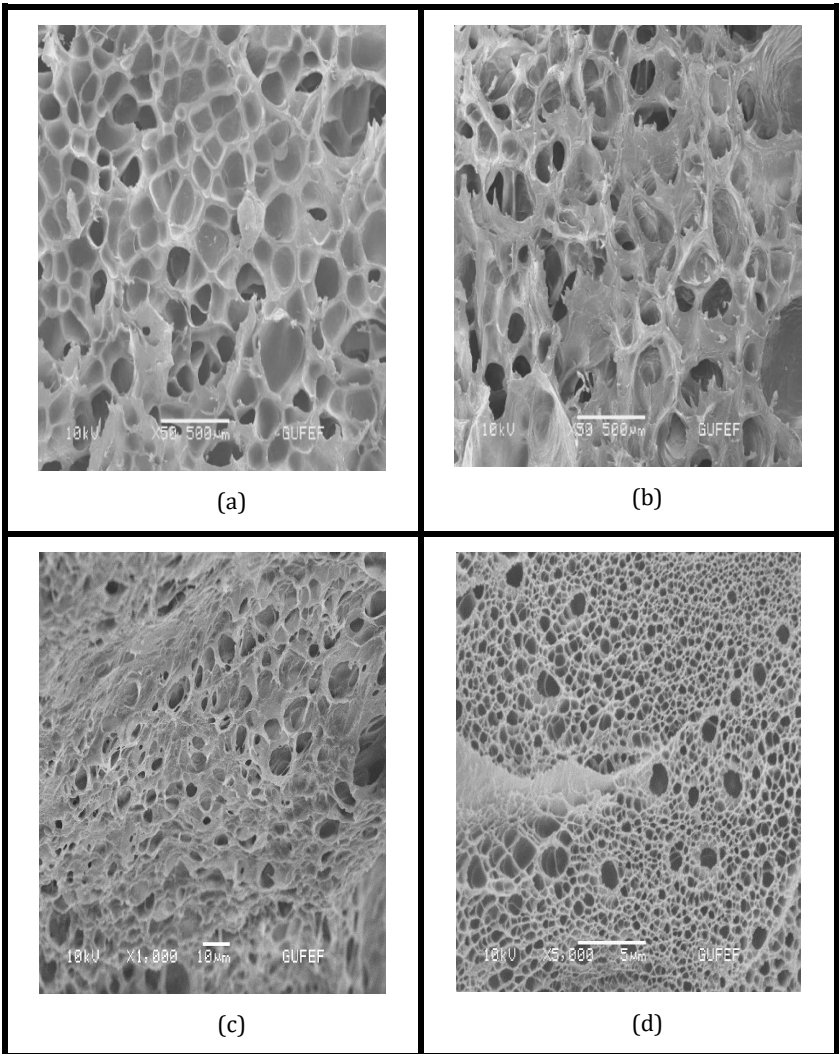


Figure 3. The variation of swelling behavior with pH

### SEM analysis

Morphological observations of samples are presented in Figure 4. GEL-1 sample had larger porous. This porosity permits easy penetration of water into structure. While pore sizes reduced strongly, the pore numbers arised with increasing the content of CA.



**Figure 4.** The SEM images of (a) swollen GEL-1 hydrogel, (b) swollen GEL-2 hydrogel, (c) swollen GEL-3 hydrogel, (d) swollen GEL-4

The porosity properties of hydrogels are given in Table 2. Average pore sizes varied from  $0.75 \pm 0.04 \mu\text{m}$  to  $183.42 \pm 15.44 \mu\text{m}$ . The values were accordant with the swelling degrees. While the most swollen GEL-1 sample had large pore, the least swollen GEL-4 sample had small size.

**Table 2.** The morphological properties of samples

| Hydrogel | Average Pore Size<br>( $\mu\text{m}$ ) | Average Pore Density<br>(number of pore/ $\text{cm}^2$ ) |
|----------|--|--|
| GEL-1    | 183.42 $\pm$ 15.44                     | 1.23 $\times$ 10 <sup>2</sup> $\pm$ 0.05                 |
| GEL-2    | 137.21 $\pm$ 10.22                     | 1.52 $\times$ 10 <sup>2</sup> $\pm$ 0.06                 |
| GEL-3    | 6.93 $\pm$ 1.23                        | 4.21 $\times$ 10 <sup>3</sup> $\pm$ 0.03                 |
| GEL-4    | 0.75 $\pm$ 0.04                        | 6.01 $\times$ 10 <sup>5</sup> $\pm$ 0.04                 |

### 5-FU drug release

The cumulative release results are presented in Figure 5. Drug release from hydrogels increased with time and the equilibrium values was obtained at nearly 8 h. The releasing are in good agreement with the swelling test. The most rapid release was observed for GEL-1 because of its larger pore sizes. The release values decreased with increasing CA concentration.

The Equation 3 represents the drug release process of swollen hydrogel.

$$F = M_t / M_\infty = kt^n \quad (3)$$

where  $M_t$  and  $M_\infty$  are the content of the 5-FU released at time  $t$  and the maximum amount of the 5-FU release, respectively;  $k$  is the constant value of gel;  $F$  is the fractional value and  $n$  is an exponent.  $n$  value identifies the type of diffusion.

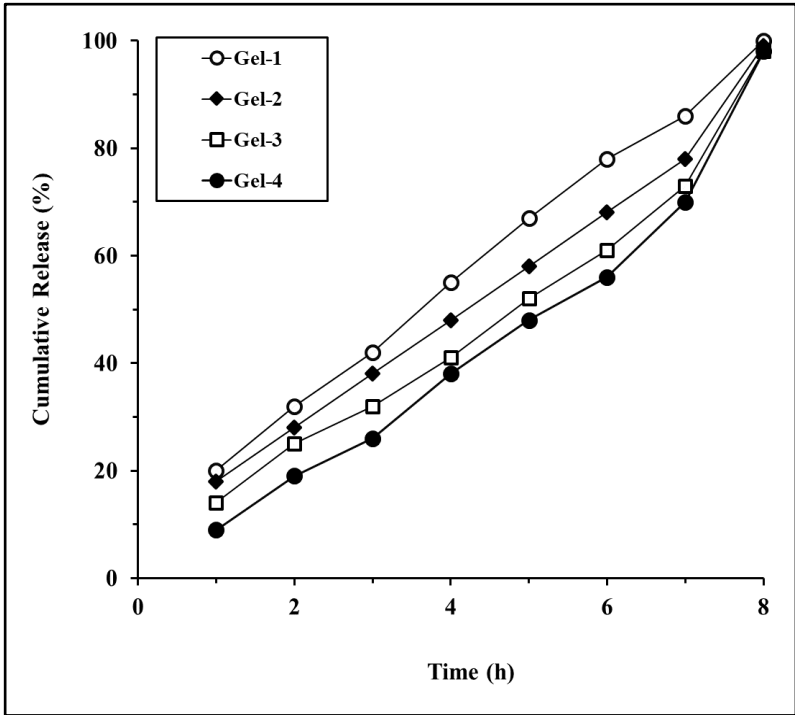


**Figure 5.** The cumulative release of 5- FU from hydrogels

$n = 0.45-0.50$  corresponds to Fickian diffusion, whereas  $0.50 < n < 1.0$  implies non-Fickian diffusion.  $n \geq 1.0$  indicates super case II transport. Results of release exponent and release factor for hydrogels were determined from the graphs driven in via Equation 3 and are listed in Table 3. As  $n$  value of all hydrogels was calculated near 1.0, this situation explains that the rapid increment osmotic pressure and an increase the diffusion rate exponentially over time [21].

**Table 3.** Release parameters of hydrogels

| Hydrogel | $n$  | $k \times 10^{-3}$ |
|----------|------|--------------------|
| GEL-1    | 1.11 | 1.13               |
| GEL-2    | 1.08 | 1.33               |
| GEL-3    | 1.04 | 1.25               |
| GEL-4    | 0.99 | 1.22               |

## Conclusions

In this study, semi-interpenetrating polymer network (semi-IPN) hydrogels containing acrylic acid (AA), citraconic acid (CA) and gelatin were synthesized by free-radical polymerization for the controlled release of 5-FU. The swelling behavior of hydrogels was researched against time, temperature and pH. The swelling values were decreased with increasing concentration of CA. In Scanning Electron Microscope (SEM) observations, average pore sizes reduced with increasing the concentration of CA. The controlled release of 5-Fluorouracil (5-FU) was also investigated. The kinetic release mechanisms were found to be super case II transport for all hydrogels.

## References

1. Babu, V. R., Sairam, M., Hosamani, K. M., Aminabhavi, T. M. (2006). Development of 5-Fluorouracil Loaded Poly (Acrylamide-co-methylmethacrylate) Novel Core-Shell Microspheres: In Vitro Release Studies. *International Journal of Pharmaceutics*, 325(1-2), 55-62.
2. Fournier, E., Passirani, C., Vonarbourg, A., Lemaire L., Colin, N., Sagodira, S., Menei, P., Benoit, J. P. (2003). Therapeutic Efficacy Study of Novel 5-FU-Loaded PMM 2.1.2-Based Microspheres on C6 Glioma. *International Journal of Pharmaceutics*, 268 (1-2), 31-35.
3. Gudasi, K. B., Vadavi, R. S., Shelke, N. B., Sairam, M., Aminabhavi, T. M. (2006). Synthesis and Characterization of Novel Polyorganophosphazanes Substituted with 4-Methoxybenzylamine and 4-Methoxyphenethylamine for In Vitro Release of Indomethacin and 5-Fluorouracil. *Reactive and Functional Polymers*, 66 (10), 1149-1157.
4. Zhang, J., Peppas, N.A., (2000). Synthesis and characterization of pH- and temperature-sensitive poly(methacrylic acid)/poly(N-isopropylamide) interpenetrating polymeric Networks. *Macromolecules*, 33: 102-107.
5. Alvarez-Lorenzo, C., Concheiro, A., Dubovik, A.S., Grinberg, N.V., Burova, T.V., Grinberg, V.Y., (2005). Temperature-sensitive chitosan-poly(Nisopropylacrylamide) interpenetrated networks with enhanced loading capacity and controlled release properties. *J. Control. Release*, 102, 629-641.
6. Wu, S.X., Hoffman, S.A., Yager, P. (1992). Synthesis and characterization of thermally reversible macroporous poly(N-isopropyl acrylamide) hydrogels. *J. Polym. Sci. Part A, Pol. Chem.*, 30,2121-2129.
7. Zhang, X.Z., Yang, Y.Y., Chung, T.S., Ma, K.X. (2001). Preparation and characterization of response macroporous poly(N-isopropyl acrylamide) hydrogels. *Langmuir*, 17, 6094-6099.
8. Singh, S., Rama Rao, K. V., Venugopal, K., and Manikandan, R. (2002). Alteration in Dissolution Characteristics of Gelatin-Containing Formulations. *Pharmaceutical Technology*, 36-58.
9. Cortesia, R., Esposito, E., Ostia, M., Squarzonza, G., Menegattia, E., Spencer Davis, S. and Nastruzzia, C. (1999). Dextran cross-linked gelatin microspheres as a drug delivery system. *European Journal of Pharmaceutics and Biopharmaceutics*, 47(2), 153-160.
10. Seon Jeong, K., Sang Jun, P., and Sun, I.K. (2003). Swelling behavior of Interpenetrating polymer network hydrogels composed of poly(vinyl alcohol) and chitosan. *Department of Biomedical Engineering*, Hanyang University, Seoul South Korea, 89(1), 133-605.
11. Chen, K.S., Ku, Y.A., Lin, H.R., Yan, T.R., Sheu, D.C., Chen, T.M., Lin, (2005). Preparation and characterization of sensitive poly(N-vinyl-2-pyrrolidone/itaconic acid) copolymer hydrogels. *Mater. Chem. Phys.*, 91, 484-489.
12. Gudeman, L.F., Peppas, N.A. (1995). Preparation and characterization of pH-sensitive, interpenetrating networks of poly(vinyl alcohol) and poly(acrylic acid). *J. Appl. Polym. Sci.*, 55, 919-928.

13. Zambito, Y., Baggiani, A., Carelli, V., Serafini, M.F., Colo, G.D., "Matrices for site-specific controlled-delivery of 5-fluorouracil to descending colon", *Journal of Controlled Release*, 102: 669-677 (2005).
14. Hussain, M., Beale, G., Hughes, M., Akhtar, S. (2002). Co-delivery of an antisense oligonucleotide and 5-fluorouracil using sustained release poly(lactide-co-glycolide) microsphere formulations for potential combination therapy in cancer. *International Journal of Pharmaceutics*, 234, 129-138 .
15. Jin, L., Bai, R. (2002). Mechanisms of lead adsorption chitosan/PVA hydrogel beads. *Langmuir*, 18, 9765-9770.
16. Saraydın, D., Ünver-saraydın, S., Karadağ, E., Koptagel, E., Güven, O. (2004). In vivo biocompatibility of radiation crosslinked acrylamide copolymers. *Nucl. Instrum. Meth. Physics Research B*, 217, 281-292.
17. Bajpai, S.K., Sonkusley, J. (2002). Hydrogels for oral drug delivery of peptides: synthesis and characterization. *J. Appl. Polym. Sci.*, 83, 1717-1799.
18. Rodriguez, D.E., Garcia, J.R., Vargos, E.R. (2006). Synthesis and swelling characteristics of semi-interpenetrating polymer network hydrogels composed of poly(acrylamide) and poly( $\gamma$ -glutamic acid). *Mater. Lett.*, 60, 1390-1393.
19. Jin, X., Hsieh, Y. (2005). pH-responsive swelling behavior of poly(vinyl alcohol)/poly(acrylic acid) bi-component fibrous hydrogel membranes. *Polymer*, 46, 5149-5160.
20. Gudeman, L.F., Peppas, N.A. (1995). pH-sensitive membranes from poly(vinyl alcohol)/poly(acrylic acid) interpenetrating Networks. *J. Membrane Sci.*, 107, 239-248.
21. Warren, S.J., Kellaway, I.W. (1998). The synthesis and in vitro characterization of the mucoadhesion and swelling of poly(acrylic acid) hydrogels. *Pharm. Dev. Technol.*, 3(2), 199-208.

# THE VALUE OF THE SEED IN THE SYSTEMATIC OF THE FAMILY BRASSICACEAE

Mehmet Cengiz KARAİSMAİLOĞLU<sup>1</sup>



---

<sup>1</sup> Dr., Department of Biology, Faculty of Arts and Sciences, Siirt University, Siirt, Turkey.



Brassicaceae (Cruciferae) family includes about 365 genera and 3250 species in worldwide, it is acknowledged as a huge family including economic significance (Simpson, 2006; Tekin et al., 2013; Karaismailoğlu, 2016 and 2017). For this family, Turkey is one of the most diverse places with 61 genera and 653 species (Al Shehbaz et al., 2006). This family is simply identified, nevertheless, no widely accepted classification structure is not current yet (Khosravi et al., 2009; Karaismailoğlu, 2016; Karaismailoğlu and Erol, 2019).

It is not likely to clarify the evolutionary relationships among most of the taxa within the family Brassicaceae by merely examining morphological characteristics due to widespread convergence (Franzke et al., 2011). Therefore, it is necessary to study other characters of the taxa as well, to solve the taxonomic problems concerning closely related taxa.

Also, the taxonomic usability of seed characters has been ignored. Because, the seeds of Brassicaceae family members are difficult to separate with the naked eye or lens (Bernard, 2000). However, the seed coat structure is considered as an important character in systematics investigations of the family. It is frequently utilized to explain classification difficulties regarding closely related taxa (Zeng et al., 2004; Kaya et al., 2011; Karaismailoğlu, 2017 and 2018). Additionally, several investigators have approved on the taxonomic implication of macro and micro structures of the seeds in separating the taxa within the family Brassicaceae (Mulligan and Bailey, 1976; Brisson and Peterson, 1977; El-Naggar, 1996; Khalik et al., 2002; Tantawy et al., 2004; Kaya et al., 2011; Bona, 2013; Karaismailoğlu, 2016 and 2019; Özüdoğru et al., 2016; Karaismailoğlu and Erol, 2018).

Also, reviewing the anatomical structures of the seed coat may offer answer to the taxonomical problems concerning Brassicaceae. Most of the performed studies on the seed coat of Brassicaceae concern with the species of economic significance (Barton, 1967) and they are deal with diagnosis of taxa. Various works utilized structures as a reliable approach for evaluating phenetic correlations and elucidating taxonomic problems in the Brassicaceae family (Murley, 1951; Vaughan and Whitehouse, 1971; Bouman, 1975; Barthlott, 1981; Buth and Ara, 1987; Moazzeni et al., 2007; Karaismailoğlu, 2018).

So far, the morphological and anatomical features of a very limited number of taxa within Brassicaceae have been studied. It is the reason micromorphological and anatomical have been examined on the limited number seeds to be found in interpretations in terms of systematic and phylogenetic relationships.

## **1. Morphological and anatomical features of seed of family Brassicaceae**

In this work, it has studied the seed morphological and anatomical characteristics of 40 taxa within Brassicaceae family from Turkey (Table 1). The characters of the observed taxa have morphologically shown in Figures 1

and 2. Also, anatomical cross-sections taken from the seeds have presented in Figure 3. The detailed seed structures of the examined taxa have been submitted:

**Table 1.** The studied taxa and their origins.

| No | Taxa   | Location                              | Voucher             |
|----|--|---------------------------------------|---------------------|
| 1  | <i>Alliaria petiolata</i> Cavara et Grande                 | Uşak, Banaz                           | Karaismailoğlu 291  |
| 2  | <i>Arabidopsis thaliana</i> (L.) Heyn.                     | Bursa, Uludağ                         | Karaismailoğlu 297  |
| 3  | <i>Brassica nigra</i> (L.) Koch                            | Erzurum, Aşkale                       | Karaismailoğlu 340b |
| 4  | <i>Camelina rumelica</i> Velen.                            | Çorum, İskilip                        | Karaismailoğlu 147  |
| 5  | <i>Calepina irregularis</i> (Asso) Thell.                  | Kırklareli, Demirköy                  | Karaismailoğlu 107  |
| 6  | * <i>Conringia grandiflora</i> Boiss. et Heldr.            | Antalya, Konyaaltı                    | Karaismailoğlu 328  |
| 7  | <i>Conringia orientalis</i> (L.) Dumort.                   | Kütahya, Gediz                        | Karaismailoğlu 283  |
| 8  | <i>Conringia perfoliata</i> (C.A. Meyer) Busch             | Kütahya, Gediz<br>İstanbul,           | Karaismailoğlu 284  |
| 9  | <i>Diploaxis tenuifolia</i> (L.) DC.                       | Büyükçekmece                          | Karaismailoğlu 344  |
| 10 | <i>Eruca vesicaria</i> (L.) Cav.                           | Mersin, Mut                           | Karaismailoğlu 10   |
| 11 | <i>Erysimum crassipes</i> Fisch. et Mey.                   | Osmaniye, Urun                        | Karaismailoğlu 180b |
| 12 | <i>Erysimum cuspidatum</i> (Bieb.) DC.                     | Kütahya, Gediz                        | Karaismailoğlu 282  |
| 13 | <i>Erysimum leucanthemum</i> Fedtsch.                      | Konya, Cihanbeyli                     | Karaismailoğlu 317  |
| 14 | <i>Erysimum goniocaulon</i> Boiss.                         | Osmaniye, Zorkun                      | Karaismailoğlu 224b |
| 15 | * <i>Hesperis bicuspidata</i> (Willd.) Poir.               | Bitlis, Alançı                        | Karaismailoğlu 2b   |
| 16 | <i>Hesperis persica</i> Boiss.                             | Trabzon, Çaykara                      | Karaismailoğlu 70a  |
| 17 | <i>Iberis acutiloba</i> Bertol.                            | Osmaniye, Düziçi                      | Karaismailoğlu 130  |
| 18 | <i>Iberis sempervirens</i> L.                              | Bolu, Abant                           | Karaismailoğlu 249  |
| 19 | <i>Iberis spruneri</i> Jord.                               | Bursa, Uludağ<br>İstanbul,            | Karaismailoğlu 304  |
| 20 | * <i>Isatis arenaria</i> Azn.                              | Büyükçekmece                          | Karaismailoğlu 306  |
| 21 | <i>Isatis cappadocica</i> Desv. subsp. <i>cappadocica</i>  | Bursa, Uludağ                         | Karaismailoğlu 301  |
| 22 | <i>Isatis erzurimica</i> Davis                             | Bayburt, Kop                          | Karaismailoğlu 338  |
| 23 | <i>Isatis glauca</i> Aucher ex Boiss. subsp. <i>glauca</i> | Erzurum, Aşkale                       | Karaismailoğlu 340a |
| 24 | <i>Malcolmia africana</i> (L.) R. Br.                      | Amasya, Taşova                        | Karaismailoğlu 335  |
| 25 | <i>Malcolmia chia</i> (L.) DC.                             | Mersin, Mut                           | Karaismailoğlu 12   |
| 26 | <i>Malcolmia flexuosa</i> Sibth. et Sm.                    | Antalya, Çiğdemler                    | Karaismailoğlu 322a |
| 27 | <i>Matthiola incana</i> (L.) W.T. Aiton                    | Ağrı, Hamur                           | Karaismailoğlu 161  |
| 28 | <i>Matthiola montana</i> Boiss.                            | Trabzon, Çaykara                      | Karaismailoğlu 70b  |
| 29 | <i>Matthiola longipetala</i> DC. subsp. <i>longipetala</i> | Antalya, Çiğdemler                    | Karaismailoğlu 322b |
| 30 | <i>Peltaria alliacea</i> Jacq.                             | Mersin, Mut                           | Karaismailoğlu 6    |
| 31 | <i>Sinapis arvensis</i> L.                                 | Samsun, Kavak                         | Karaismailoğlu 140b |
| 32 | <i>Sisymbrium altissimum</i> L.                            | Kütahya, Gediz                        | Karaismailoğlu 281  |
| 33 | <i>Sisymbrium officinale</i> (L.) Scop.                    | Balıkesir, Bandırma                   | Karaismailoğlu 314  |
| 34 | <i>Sisymbrium orientale</i> L.                             | Kütahya, Gediz                        | Karaismailoğlu 280  |
| 35 | <i>Tchihatchewia isatidea</i> Boiss.                       | Niğde, Aladağ                         | Karaismailoğlu 329  |
| 36 | <i>Thlaspi alliaceum</i> L.                                | Samsun, Engiz                         | Karaismailoğlu 138  |
| 37 | <i>Thlaspi kurdicum</i> Hedge                              | Van, Güzeldere pass<br>Kahramanmaraş, | Karaismailoğlu 185  |
| 38 | <i>Thlaspi oxyceras</i> (Boiss.) Hedge                     | Andırın                               | Karaismailoğlu 207  |
| 39 | <i>Turritis glabra</i> L.                                  | Hatay, Dörtiyol                       | Karaismailoğlu 239b |
| 40 | <i>Turritis laxa</i> Hayek                                 | Hatay, Dörtiyol                       | Karaismailoğlu 239a |

\*=endemic taxon

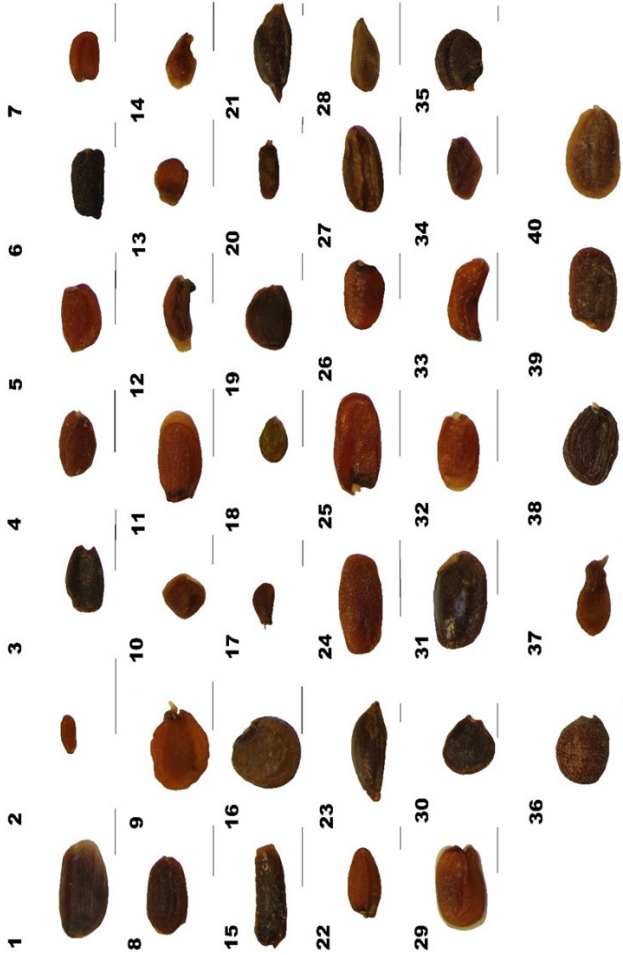


**Figure 1.** The seeds of the examined taxa: **1:** *Alliaria petiolata*, **2:** *Arabidopsis thaliana*, **3:** *Brassica nigra*, **4:** *Camelina rumellica*, **5:** *Calepina irregularis*, **6:** *Conringia grandiflora*, **7:** *C. orientalis*, **8:** *C. perfoliata*, **9:** *Diplotaxis tenuifolia*, **10:** *Eruca vesicaria*, **11:** *Erysimum crassipes*, **12:** *E. cuspidatum*, **13:** *E. leucanthemum*, **14:** *E. goniocalon*, **15:** *Hesperis bicuspidata*, **16:** *H. persica*, **17:** *Iberis acutiloba*, **18:** *I. sempervirens*, **19:** *I. spruneri*, **20:** *Isatis arenaria*, **21:** *I. cappadocica* subsp. *cappadocica*, **22:** *I. erzurumica*, **23:** *I. glauca* subsp. *glauca*, **24:** *Malcolmia africana*, **25:** *M. chia*, **26:** *M. flexuosa*, **27:** *Matthiola incana*, **28:** *M. montana*, **29:** *M. longipetala*, **30:** *Peltaria alliacea*, **31:** *Sinapis arvensis*, **32:** *Sisymbrium altissimum*, **33:** *S. officinale*, **34:** *S. orientale*, **35:** *Tchihatchewia isatidea*, **36:** *Thlaspi alliaceum*, **37:** *T. kurdicum*, **38:** *T. oxyceras*, **39:** *Turritis glabra*, **40:** *T. laxa* (Scale bars=1 mm)

### 1.1. *Alliaria petiolata*

The seeds of this taxon are ellipticus in shape, dark brown in colour (Figure 1). Their surfaces are slightly striped. Seed sizes are  $2.15 \pm 0.15$  mm in length,  $1.32 \pm 0.12$  mm in width, and they do not have raphe. The surface ornamentation of seeds is rugose, their anticlinal and periclinal cell walls and epidermal cell structures are unclear (Figure 2).

In cross sections, the seeds of this taxon consist of four layers, including (1) the outer epidermis and (2) inner epidermis (the outer integument), (3) the inner integument (sclerotic or palisade layer), and (4) parenchyma. The epidermis layer is either parenchymatic or scleranchymatic type and consist of two layers including the outer and inner epidermis. In outer integument, outer epidermis occurs from large flat cells with 1-layer while inner epidermis consists of elongated rectangular cells with 1-layer. Thickness of outer integument is  $105.27 \pm 5.12$   $\mu\text{m}$ . Inner integument, which is a compressed tissue under the outer integument, consists of crushed cells with 1-2 layer, and its thickness  $27.98 \pm 3.27$   $\mu\text{m}$ . Parenchyma layer occurs from flat cells with 1-layer, and its thickness is  $29.46 \pm 2.27$   $\mu\text{m}$ . The endosperm cells are large radial, decreased intercellular gaps and their cell walls are thinned (Figure 3).

### 1.2. *Arabidopsis thaliana*

The seeds are ovatus-anguste in shape, brown in colour. Their surfaces are smooth. Seed sizes are  $0.38 \pm 0.12$  mm in length,  $0.12 \pm 0.04$  mm in width, and they are not of raphe (Figure 1). The surface ornamentation of seeds is reticulate, their anticlinal and periclinal cell walls are raised and concave. Furthermore, their epidermal cell structures are in polygonal form (Figure 2).

The epidermis layer is parenchymatic type and consist of one layer. It occurs from cubic cells with 1 layer. Thickness of integument is  $38.14 \pm 1.56$   $\mu\text{m}$ . Parenchyma layer occurs from flat cells with 2 layers, and its thickness is  $48.62 \pm 1.86$   $\mu\text{m}$  (Figure 3).

### 1.3. *Brassica nigra*

The seeds are ovatus in shape, black in colour. Their surfaces are smooth. Seed sizes are  $0.86 \pm 0.10$  mm in length,  $0.51 \pm 0.06$  mm in width, and they are not of raphe (Figure 1). The surface ornamentation of seeds is reticulate, their anticlinal and periclinal cell walls are raised and concave. Also, their epidermal cell structures are in polygonal form (Figure 2).

In cross sections, the seeds of this taxon consist of four layers, including (1) the outer epidermis and (2) inner epidermis (the outer integument), (3) the inner integument, and (4) parenchyma. The epidermis layer is either parenchymatic type and consist of two layers including the outer and inner epidermis. In outer integument, outer epidermis occurs from flat cells with 1 layer, as inner epidermis consists of elongated rectangular cells with 1-3 layers. Thickness of outer integument is  $60.07 \pm 5.18$   $\mu\text{m}$ . Inner integument

consists of rectangular cells with 1 layer, and its thickness  $20.17 \pm 2.12 \mu\text{m}$ . Parenchyma layer occurs from flat cells with 1-layer, and its thickness is  $28.71 \pm 1.23 \mu\text{m}$  (Figure 3).

#### **1.4. *Camelina rumelica***

The seeds are ellipticus in shape, brown in colour. Their surfaces are smooth. Seed sizes are  $1.06 \pm 0.12 \text{ mm}$  in length,  $0.68 \pm 0.04 \text{ mm}$  in width, and they are not of raphe (Figure 1). The surface ornamentation of seeds is reticulate, their anticlinal and periclinal cell walls are raised and concave. Furthermore, their epidermal cell structures are in polygonal form (Figure 2).

The epidermis layer is either parenchymatic or scleranchymatic type and consist of two layers including the outer and inner epidermis. In integument, outer epidermis occurs from cubic cells with 1 layer while inner epidermis consists of flat cells with 2 layers. Thickness of integument is  $58.77 \pm 4.12 \mu\text{m}$ . Parenchyma layer occurs from flat cells with 1 layer, and its thickness is  $40.58 \pm 1.25 \mu\text{m}$  (Figure 3).

#### **1.5. *Calepina irregularis***

The seeds are ovatus late in shape, brown in colour. Their surfaces are smooth. Seed sizes are  $0.84 \pm 0.16 \text{ mm}$  in length,  $0.49 \pm 0.06 \text{ mm}$  in width, and they are not of raphe (Figure 1). The surface ornamentation of seeds is scalariform, their anticlinal and periclinal cell walls are raised and concave. Furthermore, their epidermal cell structures are in rectangular form (Figure 2).

The epidermis layer is parenchymatic type and consist of one layer. It occurs from flat cells with 1-2 layers. Thickness of integument is  $33.27 \pm 1.16 \mu\text{m}$ . Parenchyma layer occurs from flat cells with 1 layer, and its thickness is  $37.26 \pm 2.14 \mu\text{m}$  (Figure 3).

#### **1.6. *Conringia grandiflora***

The seeds are rectangularis late in shape, black in colour. Their surfaces are rugose. Seed sizes are  $2.12 \pm 0.12 \text{ mm}$  in length,  $1.37 \pm 0.10 \text{ mm}$  in width, and they are not of raphe (Figure 1). The surface ornamentation of seeds is ruminant, their anticlinal, periclinal cell walls and epidermal cell structures are unclear (Figure 2).

The epidermis layer is parenchymatic type and consist of one layer. It occurs from flat cells with 5-6 layers. Thickness of integument is  $140.65 \pm 7.18 \mu\text{m}$ . Parenchyma layer occurs from flat cells with 1 layer, and its thickness is  $38.41 \pm 4.42 \mu\text{m}$  (Figure 3).

#### **1.7. *Conringia orientalis***

The seeds are ellipticus-rectangularis in shape, brown in colour. Their surfaces are smooth. Seed sizes are  $1.62 \pm 0.10 \text{ mm}$  in length,  $1.23 \pm 0.06 \text{ mm}$  in

width, and they do not have raphe (Figure 1). The surface ornamentation of seeds is reticulate-areolate, their anticlinal and periclinal cell walls are sunken and concave. Also, their epidermal cell structures are in polygonal form (Figure 2).

In cross sections, the seeds of this taxon consist of four layers, including (1) the outer epidermis and (2) inner epidermis (the outer integument), (3) the inner integument, and (4) parenchyma. The epidermis layer is either parenchymatic type and consist of two layers including the outer and inner epidermis. In outer integument, outer epidermis occurs from flat cells with 1 layer, as inner epidermis consists of cubic cells with 1 layer. Thickness of outer integument is  $41.56 \pm 3.77 \mu\text{m}$ . Inner integument consists of flat cells with 1 layer, and its thickness  $22.44 \pm 2.44 \mu\text{m}$ . Parenchyma layer occurs from flat cells with 1-layer, and its thickness is  $23.15 \pm 2.08 \mu\text{m}$  (Figure 3).

### 1.8. *Conringia perfoliata*

The seeds are ellipticus in shape, dark brown in colour. Their surfaces are reticulate. Seed sizes are  $1.45 \pm 0.21 \text{ mm}$  in length,  $0.75 \pm 0.12 \text{ mm}$  in width, and they do not have raphe (Figure 1). The surface ornamentation of seeds is foveate-lineate, their anticlinal and periclinal cell walls are raised and concave. Also, their epidermal cell structures are in polygonal form (Figure 2).

In cross sections, the seeds of this taxon consist of four layers, including (1) the outer epidermis and (2) inner epidermis (the outer integument), (3) the inner integument, and (4) parenchyma. The epidermis layer is either parenchymatic type and consist of two layers including the outer and inner epidermis. In outer integument, outer epidermis occurs from rectangular cells with 1 layer, as inner epidermis consists of flat cells with 1 layer. Thickness of outer integument is  $55.69 \pm 4.36 \mu\text{m}$ . Inner integument consists of flat cells with 1 layer, and its thickness  $25.19 \pm 2.68 \mu\text{m}$ . Parenchyma layer occurs from flat cells with 1-layer, and its thickness is  $41.17 \pm 2.95 \mu\text{m}$  (Figure 3).

### 1.9. *Diploaxis tenifolia*

The seeds are ovatus in shape, brown in colour. Their surfaces are smooth. Seed sizes are  $1.54 \pm 0.15 \text{ mm}$  in length,  $1.09 \pm 0.12 \text{ mm}$  in width, and they are not of raphe (Figure 1). The surface ornamentation of seeds is foveate, their anticlinal and periclinal cell walls are raised and concave. Furthermore, their epidermal cell structures are in alveolar form (Figure 2).

The epidermis layer is either parenchymatic or scleranchymatic type and consist of two layers including the outer and inner epidermis. In integument, outer epidermis occurs from rectangular cells with 1 layer while inner epidermis consists of crushed cells with 1 layer. Thickness of integument is  $78.51 \pm 4.12 \mu\text{m}$ . Parenchyma layer occurs from rectangular cells with 1 layer, and its thickness is  $19.15 \pm 1.25 \mu\text{m}$  (Figure 3).

### 1.10. *Eruca vesicaria*

The seeds are ellipticus-transverse late in shape, dark brown in colour. Their surfaces are smooth. Seed sizes are  $1.32 \pm 0.12$  mm in length,  $1.51 \pm 0.16$  mm in width, and they do not have raphe (Figure 1). The surface ornamentation of seeds is alveolate, their anticlinal and periclinal cell walls are raised and concave. Also, their epidermal cell structures are in alveolar form (Figure 2).

In cross sections, the seeds of this taxon consist of four layers, including (1) the outer epidermis and (2) inner epidermis (the outer integument), (3) the inner integument, and (4) parenchyma. The epidermis layer is either parenchymatic type and consist of two layers including the outer and inner epidermis. In outer integument, outer and inner epidermises occur from elongated rectangular cells with 1 layer. Thickness of outer integument is  $137.54 \pm 6.54$   $\mu\text{m}$ . Inner integument consists of crushed cells with 1 layer, and its thickness  $20.18 \pm 1.34$   $\mu\text{m}$ . Parenchyma layer occurs from flat cells with 1-layer, and its thickness is  $35.46 \pm 3.84$   $\mu\text{m}$  (Figure 3).

### 1.11. *Erysimum crassipes*

The seeds are ellipticus-rectangularis in shape, brown in colour. Their surfaces are smooth. Seed sizes are  $1.14 \pm 0.18$  mm in length,  $0.67 \pm 0.12$  mm in width, and they are not of raphe (Figure 1). The surface ornamentation of seeds is reticulate-foveate, their anticlinal and periclinal cell walls are raised and concave. Furthermore, their epidermal cell structures are in polygonal and alveolar forms (Figure 2).

The epidermis layer is either parenchymatic or scleranchymatic type and consist of two layers including the outer and inner epidermis. In integument, outer epidermis occurs from elongated rectangular cells with 1 layer while inner epidermis consists of crushed cells with 1 layer. Thickness of integument is  $61.65 \pm 4.56$   $\mu\text{m}$ . Parenchyma layer occurs from flat cells with 1 layer, and its thickness is  $24.67 \pm 3.25$   $\mu\text{m}$  (Figure 3).

### 1.12. *Erysimum cuspidatum*

The seeds are ovatus-anguste in shape, dark brown in colour. Their surfaces are smooth. Seed sizes are  $1.37 \pm 0.15$  mm in length,  $0.42 \pm 0.04$  mm in width, and they have a raphe (Figure 1). The surface ornamentation of seeds is alveolate, their anticlinal and periclinal cell walls are sunken and convex. Also, their epidermal cell structures are in alveolar form (Figure 2).

In cross sections, the seeds of this taxon consist of four layers, including (1) the outer epidermis and (2) inner epidermis (the outer integument), (3) the inner integument, and (4) parenchyma. The epidermis layer is either parenchymatic type and consist of two layers including the outer and inner epidermis. In outer integument, outer epidermis occurs from cubic cells with 1 layer, as inner epidermis consists of rectangular cells with 1 layer. Thickness of outer integument is  $55.62 \pm 3.95$   $\mu\text{m}$ . Inner integument consists

of crushed cells with 1 layer, and its thickness  $17.37 \pm 2.51 \mu\text{m}$ . Parenchyma layer occurs from flat cells with 1-layer, and its thickness is  $18.64 \pm 2.34 \mu\text{m}$  (Figure 3).

### 1.13. *Erysimum leucanthemum*

The seeds are ovatus in shape, brown in colour. Their surfaces are smooth. Seed sizes are  $0.56 \pm 0.12 \text{ mm}$  in length,  $0.29 \pm 0.06 \text{ mm}$  in width, and they are not of raphe (Figure 1). The surface ornamentation of seeds is reticulate, their anticlinal and periclinal cell walls are raised and concave. Furthermore, their epidermal cell structures are in polygonal form (Figure 2).

The epidermis layer is either parenchymatic or scleranchymatic type and consist of two layers including the outer and inner epidermis. In integument, outer epidermis occurs from large flat cells with 1 layer while inner epidermis consists of crushed cells with 2-3 layers. Thickness of integument is  $79.56 \pm 4.88 \mu\text{m}$ . Parenchyma layer occurs from flat cells with 1 layer, and its thickness is  $21.15 \pm 2.73 \mu\text{m}$  (Figure 3).

### 1.14. *Erysimum goniocaulon*

The seeds are ovatus in shape, brown in colour. Their surfaces are smooth. Seed sizes are  $1.13 \pm 0.15 \text{ mm}$  in length,  $0.61 \pm 0.04 \text{ mm}$  in width, and they are not of raphe (Figure 1). The surface ornamentation of seeds is reticulate-areolate, their anticlinal and periclinal cell walls are sunken and convex. Furthermore, their epidermal cell structures are in polygonal form (Figure 2).

The epidermis layer is either parenchymatic or scleranchymatic type and consist of two layers including the outer and inner epidermis. In integument, outer epidermis occurs from cubic cells with 1 layer while inner epidermis consists of flat cells with 1 layer. Thickness of integument is  $43.51 \pm 3.71 \mu\text{m}$ . Parenchyma layer occurs from rectangular cells with 1 layer, and its thickness is  $14.08 \pm 1.46 \mu\text{m}$  (Figure 3).

### 1.15. *Hesperis bicuspidata*

The seeds are rectangularis in shape, black in colour. Their surfaces are rugose. Seed sizes are  $1.40 \pm 0.18 \text{ mm}$  in length,  $0.51 \pm 0.12 \text{ mm}$  in width, and they do not have raphe (Figure 1). The surface ornamentation of seeds is reticulate-foveate, their anticlinal and periclinal cell walls are raised and concave. Furthermore, their epidermal cell structures are in polygonal form (Figure 2).

The epidermis layer is either parenchymatic or scleranchymatic type and consist of two layers including the outer and inner epidermis. In integument, outer epidermis occurs from cubic cells with 1 layer while inner epidermis consists of elongated rectangular cells with 1 layer. Thickness of integument is  $88.45 \pm 3.48 \mu\text{m}$ . Parenchyma layer occurs from flat cells with 1 layer, and its thickness is  $41.26 \pm 2.85 \mu\text{m}$  (Figure 3).

### 1.16. *Hesperis persica*

The seeds are ellipticus-late in shape, dark brown in colour. Their surfaces are reticulate. Seed sizes are  $1.05\pm 0.14$  mm in length,  $1.01\pm 0.10$  mm in width, and they do not have raphe (Figure 1). The surface ornamentation of seeds is reticulate, their anticlinal and periclinal cell walls are raised and concave. Furthermore, their epidermal cell structures are in polygonal form (Figure 2).

The epidermis layer is parenchymatic type and consist of one layer. It occurs from rectangular cells with 1-2 layers. Thickness of integument is  $28.46\pm 2.44$   $\mu\text{m}$ . Parenchyma layer occurs from flat cells with 1 layer, and its thickness is  $18.43\pm 2.19$   $\mu\text{m}$  (Figure 3).

### 1.17. *Iberis acutiloba*

The seeds are ovatus in shape, dark brown in colour. Their surfaces are reticulate. Seed sizes are  $1.62\pm 0.18$  mm in length,  $1.20\pm 0.12$  mm in width, and they do not have raphe (Figure 1). The surface ornamentation of seeds is reticulate, their anticlinal and periclinal cell walls are raised and concave. Furthermore, their epidermal cell structures are in polygonal form (Figure 2).

The epidermis layer is either parenchymatic or scleranchymatic type and consist of two layers including the outer and inner epidermis. In integument, outer epidermis occurs from large flat cells with 1 layer while inner epidermis consists of flat cells with 2-3 layers. Thickness of integument is  $92.62\pm 3.11$   $\mu\text{m}$ . Parenchyma layer occurs from flat cells with 1 layer, and its thickness is  $38.63\pm 4.18$   $\mu\text{m}$  (Figure 3).

### 1.18. *Iberis sempervirens*

The seeds are ovatus in shape, brown in colour. Their surfaces are reticulate. Seed sizes are  $0.71\pm 0.12$  mm in length,  $0.52\pm 0.04$  mm in width, and they do not have raphe (Figure 1). The surface ornamentation of seeds is reticulate, their anticlinal and periclinal cell walls are raised and concave. Furthermore, their epidermal cell structures are in polygonal form (Figure 2).

The epidermis layer is either parenchymatic or scleranchymatic type and consist of two layers including the outer and inner epidermis. In integument, outer epidermis occurs from papilla flat cells with 1 layer while inner epidermis consists of flat cells with 1 layer. Thickness of integument is  $48.54\pm 6.88$   $\mu\text{m}$ . Parenchyma layer occurs from flat cells with 1 layer, and its thickness is  $16.54\pm 0.77$   $\mu\text{m}$  (Figure 3).

### 1.19. *Iberis spruneri*

The seeds are ovatus in shape, black in colour. Their surfaces are reticulate. Seed sizes are  $2.44\pm 0.21$  mm in length,  $1.76\pm 0.18$  mm in width, and they do not have raphe (Figure 1). The surface ornamentation of seeds is

reticulate, their anticlinal and periclinal cell walls are raised and concave. Furthermore, their epidermal cell structures are in polygonal form (Figure 2).

The epidermis layer is either parenchymatic or scleranchymatic type and consist of two layers including the outer and inner epidermis. In integument, outer epidermis occurs from cubic cells with 1 layer while inner epidermis consists of flat cells with 1 layer. Thickness of integument is  $96.52 \pm 5.42 \mu\text{m}$ . Parenchyma layer occurs from flat cells with 1 layer, and its thickness is  $38.47 \pm 2.33 \mu\text{m}$  (Figure 3).

### 1.20. *Isatis arenaria*

The seeds are ellipticus-anguste in shape, black in colour. Their surfaces are rugose. Seed sizes are  $3.12 \pm 0.18 \text{ mm}$  in length,  $1.03 \pm 0.10 \text{ mm}$  in width, and they do not have raphe (Figure 1). The surface ornamentation of seeds is reticulate, their anticlinal and periclinal cell walls are raised and concave. Furthermore, their epidermal cell structures are in polygonal form (Figure 2).

The epidermis layer is either parenchymatic or scleranchymatic type and consist of two layers including the outer and inner epidermis. In integument, outer epidermis occurs from flat cells with 1 layer while inner epidermis consists of rectangular cells with 1 layer. Thickness of integument is  $61.48 \pm 3.17 \mu\text{m}$ . Parenchyma layer occurs from flat cells with 1 layer, and its thickness is  $39.44 \pm 3.72 \mu\text{m}$  (Figure 3).

### 1.21. *Isatis cappadocica* subsp. *cappadocica*

The seeds are ovatus-anguste in shape, black in colour. Their surfaces are reticulate. Seed sizes are  $4.53 \pm 0.27 \text{ mm}$  in length,  $2.69 \pm 0.15 \text{ mm}$  in width, and they do not have raphe (Figure 1). The surface ornamentation of seeds is reticulate, their anticlinal and periclinal cell walls are raised and concave. Furthermore, their epidermal cell structures are in polygonal form (Figure 2).

The epidermis layer is either parenchymatic or scleranchymatic type and consist of two layers including the outer and inner epidermis. In integument, outer and inner epidermises occur from flat cells with 1 layer. Thickness of integument is  $71.21 \pm 4.80 \mu\text{m}$ . Parenchyma layer occurs from flat cells with 1 layer, and its thickness is  $27.56 \pm 3.14 \mu\text{m}$  (Figure 3).

### 1.22. *Isatis erzurimica*

The seeds are ovatus in shape, brown in colour. Their surfaces are smooth. Seed sizes are  $2.76 \pm 0.21 \text{ mm}$  in length,  $1.51 \pm 0.12 \text{ mm}$  in width, and they do not have raphe (Figure 1). The surface ornamentation of seeds is reticulate-foveate, their anticlinal and periclinal cell walls are raised and concave. Furthermore, their epidermal cell structures are in polygonal form (Figure 2).

The epidermis layer is parenchymatic type and consist of one layer. It occurs from rectangular cells with 1 layer. Thickness of integument is

32.43±3.21 µm. Parenchyma layer occurs from flat cells with 1 layer, and its thickness is 29.35±2.63 µm (Figure 3).

### 1.23. *Isatis glauca* subsp. *glauca*

The seeds are ovatus in shape, black in colour. Their surfaces are smooth. Seed sizes are 3.42±0.27 mm in length, 1.74±0.21 mm in width, and they do not have raphe (Figure 1). The surface ornamentation of seeds is reticulate-foveate, their anticlinal and periclinal cell walls are raised and concave. Furthermore, their epidermal cell structures are in polygonal form (Figure 2).

The epidermis layer is parenchymatic type and consist of one layer. It occurs from flat cells with 2-3 layers. Thickness of integument is 65.78±4.68 µm. Parenchyma layer occurs from rectangular cells with 1 layer, and its thickness is 35.94±4.11 µm (Figure 3).

### 1.24. *Malcolmia africana*

The seeds are rectangularis in shape, dark brown in colour. Their surfaces are reticulate. Seed sizes are 1.09±0.12 mm in length, 0.56±0.08 mm in width, and they do not have raphe (Figure 1). The surface ornamentation of seeds is reticulate-foveate, their anticlinal and periclinal cell walls are raised and concave. Furthermore, their epidermal cell structures are in polygonal form (Figure 2).

The epidermis layer is parenchymatic type and consist of one layer. It occurs from flat cells with 1 layer. Thickness of integument is 19.51±2.19 µm. Parenchyma layer occurs from flat cells with 1 layer, and its thickness is 27.14±3.41 µm (Figure 3).

### 1.25. *Malcolmia chia*

The seeds are rectangularis in shape, dark brown in colour. Their surfaces are reticulate. Seed sizes are 1.23±0.18 mm in length, 0.74±0.15 mm in width, and they do not have raphe (Figure 1). The surface ornamentation of seeds is alveolate, their anticlinal and periclinal cell walls are sunken and convex. Furthermore, their epidermal cell structures are in alveolar form (Figure 2).

The epidermis layer is either parenchymatic or scleranchymatic type and consist of two layers including the outer and inner epidermis. In integument, outer and inner epidermises occur from cubic cells with 1 layer. Thickness of integument is 79.88±3.77 µm. Parenchyma layer occurs from flat cells with 1 layer, and its thickness is 29.36±2.91 µm (Figure 3).

### 1.26. *Malcolmia flexuosa*

The seeds are ovatus in shape, brown in colour. Their surfaces are smooth. Seed sizes are 1.34±0.15 mm in length, 0.83±0.12mm in width, and they do not have raphe (Figure 1). The surface ornamentation of seeds is

alveolate, their anticlinal and periclinal cell walls are sunken and convex. Also, their epidermal cell structures are in alveolar form (Figure 2).

In cross sections, the seeds of this taxon consist of four layers, including (1) the outer epidermis and (2) inner epidermis (the outer integument), (3) the inner integument, and (4) parenchyma. The epidermis layer is either parenchymatic type and consist of two layers including the outer and inner epidermis. In outer integument, outer epidermis occurs from flat cells with 1 layer, as inner epidermis consists of cubic cells with 1 layer. Thickness of outer integument is  $62.34 \pm 2.81 \mu\text{m}$ . Inner integument consists of rectangular cells with 1 layer, and its thickness  $30.77 \pm 1.19 \mu\text{m}$ . Parenchyma layer occurs from flat cells with 1-layer, and its thickness is  $25.21 \pm 1.98 \mu\text{m}$  (Figure 3).

### **1.27. *Matthiola incana***

The seeds are ellipticus in shape, dark brown in colour. Their surfaces are smooth. Seed sizes are  $1.01 \pm 0.12 \text{ mm}$  in length,  $0.60 \pm 0.14 \text{ mm}$  in width, and they do not have raphe (Figure 1). The surface ornamentation of seeds is reticulate-alveolate, their anticlinal and periclinal cell walls are sunken and convex. Furthermore, their epidermal cell structures are in polygonal and alveolar forms (Figure 2).

The epidermis layer is either parenchymatic or scleranchymatic type and consist of two layers including the outer and inner epidermis. In integument, outer epidermis occurs from papilla flat cells with 1 layer while inner epidermis consists of flat cells with 1 layer. Thickness of integument is  $35.79 \pm 1.63 \mu\text{m}$ . Parenchyma layer occurs from flat cells with 1 layer, and its thickness is  $20.58 \pm 0.79 \mu\text{m}$  (Figure 3).

### **1.28. *Matthiola montana***

The seeds are ovatus in shape, pale green in colour. Their surfaces are smooth. Seed sizes are  $1.13 \pm 0.16 \text{ mm}$  in length,  $0.62 \pm 0.08 \text{ mm}$  in width, and they do not have raphe (Figure 1). The surface ornamentation of seeds is reticulate-verrucate, their anticlinal and periclinal cell walls are sunken and convex. Furthermore, their epidermal cell structures are in polygonal form (Figure 2).

The epidermis layer is either parenchymatic or scleranchymatic type and consist of two layers including the outer and inner epidermis. In integument, outer epidermis occurs from papilla flat cells with 1 layer while inner epidermis consists of flat cells with 1 layer. Thickness of integument is  $39.42 \pm 6.75 \mu\text{m}$ . Parenchyma layer occurs from flat cells with 1 layer, and its thickness is  $18.93 \pm 2.84 \mu\text{m}$  (Figure 3).

### **1.29. *Matthiola longipetala* subsp. *longipetala***

The seeds are rectangularis in shape, brown in colour. Their surfaces are smooth. Seed sizes are  $2.04 \pm 0.18 \text{ mm}$  in length,  $1.46 \pm 0.12 \text{ mm}$  in width, and they have a well-developed raphe (Figure 1). The surface ornamentation of

seeds is reticulate-foveate, their anticlinal and periclinal cell walls are raised and concave. Also, their epidermal cell structures are in polygonal form (Figure 2).

In cross sections, the seeds of this taxon consist of four layers, including (1) the outer epidermis and (2) inner epidermis (the outer integument), (3) the inner integument, and (4) parenchyma. The epidermis layer is either parenchymatic type and consist of two layers including the outer and inner epidermis. In outer integument, outer epidermis occurs from flat cells with 1 layer, as inner epidermis consists of cubic cells with 1 layer. Thickness of outer integument is  $55.61 \pm 3.44 \mu\text{m}$ . Inner integument consists of crushed cells with 1 layer, and its thickness  $20.18 \pm 1.22 \mu\text{m}$ . Parenchyma layer occurs from flat cells with 1-layer, and its thickness is  $32.46 \pm 1.58 \mu\text{m}$  (Figure 3).

### 1.30. *Peltaria alliacea*

The seeds are ovatus-transverse late in shape, black in colour. Their surfaces are reticulate. Seed sizes are  $2.02 \pm 0.21 \text{ mm}$  in length,  $2.19 \pm 0.15 \text{ mm}$  in width, and they do not have raphe (Figure 1). The surface ornamentation of seeds is rugose, their anticlinal, periclinal cell walls and epidermal cell structures are unclear (Figure 2).

The epidermis layer is either parenchymatic or scleranchymatic type and consist of two layers including the outer and inner epidermis. In integument, outer and inner epidermises occur from large flat cells with 1 layer. Thickness of integument is  $71.28 \pm 3.49 \mu\text{m}$ . Parenchyma layer occurs from flat cells with 1 layer, and its thickness is  $12.51 \pm 2.53 \mu\text{m}$  (Figure 3).

### 1.31. *Sinapis arvensis*

The seeds are ellipticus in shape, black in colour. Their surfaces are smooth. Seed sizes are  $1.75 \pm 0.21 \text{ mm}$  in length,  $1.16 \pm 0.10 \text{ mm}$  in width, and they do not have raphe (Figure 1). The surface ornamentation of seeds is ruminate, their anticlinal, periclinal cell walls and epidermal cell structures are unclear (Figure 2).

The epidermis layer is either parenchymatic or scleranchymatic type and consist of two layers including the outer and inner epidermis. In integument, outer epidermis occurs from large flat cells with 1 layer while inner epidermis consists of elongated rectangular cells with 1 layer. Thickness of integument is  $114.34 \pm 4.56 \mu\text{m}$ . Parenchyma layer occurs from flat cells with 1 layer, and its thickness is  $42.33 \pm 3.15 \mu\text{m}$  (Figure 3).

### 1.32. *Sisymbrium altissimum*

The seeds are ellipticus in shape, brown in colour. Their surfaces are reticulate. Seed sizes are  $0.98 \pm 0.08 \text{ mm}$  in length,  $0.56 \pm 0.04 \text{ mm}$  in width, and they do not have raphe (Figure 1). The surface ornamentation of seeds is reticulate-foveate, their anticlinal and periclinal cell walls are raised and

concave. Also, their epidermal cell structures are in polygonal form (Figure 2).

In cross sections, the seeds of this taxon consist of four layers, including (1) the outer epidermis and (2) inner epidermis (the outer integument), (3) the inner integument, and (4) parenchyma. The epidermis layer is either parenchymatic type and consist of two layers including the outer and inner epidermis. In outer integument, outer epidermis occurs from large flat cells with 1-2 layers, as inner epidermis consists of large flat cells with 1 layer. Thickness of outer integument is  $69.42 \pm 3.77 \mu\text{m}$ . Inner integument consists of flat cells with 5-6 layers, and its thickness  $81.24 \pm 3.22 \mu\text{m}$ . Parenchyma layer occurs from flat cells with 1-layer, and its thickness is  $37.84 \pm 2.62 \mu\text{m}$  (Figure 3).

### 1.33. *Sisymbrium officinale*

The seeds are ovatus in shape, brown in colour. Their surfaces are reticulate. Seed sizes are  $1.07 \pm 0.12 \text{ mm}$  in length,  $0.59 \pm 0.10 \text{ mm}$  in width, and they do not have raphe (Figure 1). The surface ornamentation of seeds is scalariform, their anticlinal and periclinal cell walls are raised and concave. Furthermore, their epidermal cell structures are in rectangular form (Figure 2).

The epidermis layer is parenchymatic type and consist of one layer. It occurs from elongated rectangular cells with 1 layer. Thickness of integument is  $43.59 \pm 2.61 \mu\text{m}$ . Parenchyma layer occurs from rectangular cells with 1 layer, and its thickness is  $33.09 \pm 2.53 \mu\text{m}$  (Figure 3).

### 1.34. *Sisymbrium orientale*

The seeds are ovatus in shape, dark brown in colour. Their surfaces are rugose. Seed sizes are  $0.71 \pm 0.08 \text{ mm}$  in length,  $0.46 \pm 0.08 \text{ mm}$  in width, and they do not have raphe (Figure 1). The surface ornamentation of seeds is scalariform, their anticlinal and periclinal cell walls are raised and concave. Furthermore, their epidermal cell structures are in rectangular form (Figure 2).

The epidermis layer is either parenchymatic or scleranchymatic type and consist of two layers including the outer and inner epidermis. In integument, outer epidermis occurs from crushed cells with 2 layers while inner epidermis consists of cubic cells with 1 layer. Thickness of integument is  $81.44 \pm 3.77 \mu\text{m}$ . Parenchyma layer occurs from cubic cells with 1 layer, and its thickness is  $28.75 \pm 1.65 \mu\text{m}$  (Figure 3).

### 1.35. *Tchihatchewia isatidea*

The seeds are ovatus in shape, dark brown in colour. Their surfaces are reticulate. Seed sizes are  $3.08 \pm 0.27 \text{ mm}$  in length,  $2.27 \pm 0.16 \text{ mm}$  in width, and they do not have raphe (Figure 1). The surface ornamentation of seeds is

reticulate, their anticlinal and periclinal cell walls are raised and concave. Furthermore, their epidermal cell structures are in polygonal form (Figure 2).

The epidermis layer is either parenchymatic or scleranchymatic type and consist of two layers including the outer and inner epidermis. In integument, outer epidermis occurs from crushed cells with 2-3 layers while inner epidermis consists of cubic cells with 1 layer. Thickness of integument is  $124.85 \pm 6.18 \mu\text{m}$ . Parenchyma layer occurs from flat cells with 1 layer, and its thickness is  $18.64 \pm 2.88 \mu\text{m}$  (Figure 3).

### 1.36. *Thlaspi alliaceum*

The seeds are ellipticus in shape, dark brown in colour. Their surfaces are reticulate. Seed sizes are  $1.44 \pm 0.18 \text{ mm}$  in length,  $1.25 \pm 0.15 \text{ mm}$  in width, and they do not have raphe (Figure 1). The surface ornamentation of seeds is reticulate-foveate, their anticlinal and periclinal cell walls are raised and concave. Also, their epidermal cell structures are in polygonal form (Figure 2).

In cross sections, the seeds of this taxon consist of four layers, including (1) the outer epidermis and (2) inner epidermis (the outer integument), (3) the inner integument, and (4) parenchyma. The epidermis layer is either parenchymatic type and consist of two layers including the outer and inner epidermis. In outer integument, outer epidermis occurs from large flat cells with 1 layer, as inner epidermis consists of large rectangular cells with 1 layer. Thickness of outer integument is  $100.88 \pm 5.43 \mu\text{m}$ . Inner integument consists of flat cells with 1 layer, and its thickness  $49.62 \pm 5.11 \mu\text{m}$ . Parenchyma layer occurs from flat cells with 1-layer, and its thickness is  $24.53 \pm 1.98 \mu\text{m}$  (Figure 3).

### 1.37. *Thlaspi kurdicum*

The seeds are ovatus in shape, dark brown in colour. Their surfaces are smooth. Seed sizes are  $0.83 \pm 0.12 \text{ mm}$  in length,  $0.39 \pm 0.06 \text{ mm}$  in width, and they do not have raphe (Figure 1). The surface ornamentation of seeds is scalariform, their anticlinal and periclinal cell walls are raised and concave. Also, their epidermal cell structures are in rectangular form (Figure 2).

In cross sections, the seeds of this taxon consist of four layers, including (1) the outer epidermis and (2) inner epidermis (the outer integument), (3) the inner integument, and (4) parenchyma. The epidermis layer is either parenchymatic type and consist of two layers including the outer and inner epidermis. In outer integument, outer epidermis occurs from crushed cells with 1 layer, as inner epidermis consists of elongated rectangular cells with 1 layer. Thickness of outer integument is  $72.46 \pm 4.50 \mu\text{m}$ . Inner integument consists of flat cells with 1 layer, and its thickness  $58.73 \pm 6.54 \mu\text{m}$ . Parenchyma layer occurs from flat cells with 1-layer, and its thickness is  $23.58 \pm 2.05 \mu\text{m}$  (Figure 3).

### 1.38. *Thlaspi oxyceras*

The seeds are ellipticus in shape, dark brown in colour. Their surfaces are striped. Seed sizes are  $1.30 \pm 0.12$  mm in length,  $1.05 \pm 0.10$  mm in width, and they do not have raphe (Figure 1). The surface ornamentation of seeds is reticulate, their anticlinal and periclinal cell walls are raised and concave. Also, their epidermal cell structures are in polygonal form (Figure 2).

In cross sections, the seeds of this taxon consist of four layers, including (1) the outer epidermis and (2) inner epidermis (the outer integument), (3) the inner integument, and (4) parenchyma. The epidermis layer is either parenchymatic type and consist of two layers including the outer and inner epidermis. In outer integument, outer epidermis occurs from large flat cells with 1 layer, as inner epidermis consists of elongated rectangular cells with 1 layer. Thickness of outer integument is  $79.88 \pm 5.29$   $\mu\text{m}$ . Inner integument consists of flat cells with 1 layer, and its thickness  $35.41 \pm 5.48$   $\mu\text{m}$ . Parenchyma layer occurs from flat cells with 1-layer, and its thickness is  $29.37 \pm 2.31$   $\mu\text{m}$  (Figure 3).

### 1.39. *Turritis glabra*

The seeds are ellipticus in shape, dark brown in colour. Their surfaces are rugose. Seed sizes are  $1.45 \pm 0.21$  mm in length,  $1.02 \pm 0.10$  mm in width, and they do not have raphe (Figure 1). The surface ornamentation of seeds is alveolate, their anticlinal and periclinal cell walls are raised and concave. Furthermore, their epidermal cell structures are in alveolar form (Figure 2).

The epidermis layer is either parenchymatic or scleranchymatic type and consist of two layers including the outer and inner epidermis. In integument, outer epidermis occurs from papilla flat cells with 1 layer while inner epidermis consists of flat cells with 1 layer. Thickness of integument is  $41.06 \pm 2.32$   $\mu\text{m}$ . Parenchyma layer occurs from flat cells with 1 layer, and its thickness is  $20.16 \pm 0.97$   $\mu\text{m}$  (Figure 3).

### 1.40. *Turritis laxa*

The seeds are ovatus in shape, brown in colour. Their surfaces are slightly striped. Seed sizes are  $1.71 \pm 0.15$  mm in length,  $1.09 \pm 0.08$  mm in width, and they do not have raphe (Figure 1). The surface ornamentation of seeds is reticulate, their anticlinal and periclinal cell walls are raised and concave. Furthermore, their epidermal cell structures are in polygonal form (Figure 2).

The epidermis layer is parenchymatic type and consist of one layer. It occurs flat cells with 2 layers. Thickness of integument is  $25.67 \pm 1.38$   $\mu\text{m}$ . Parenchyma layer occurs from flat cells with 1 layer, and its thickness is  $22.33 \pm 2.43$   $\mu\text{m}$  (Figure 3).

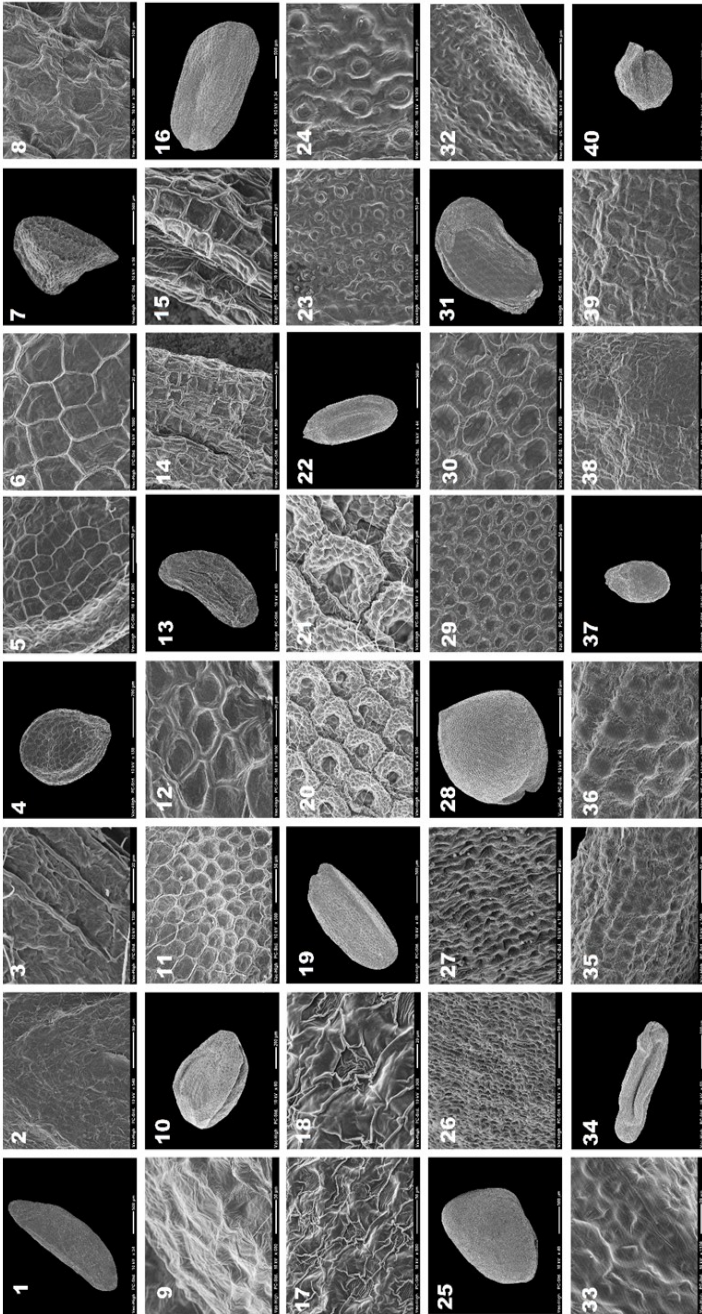
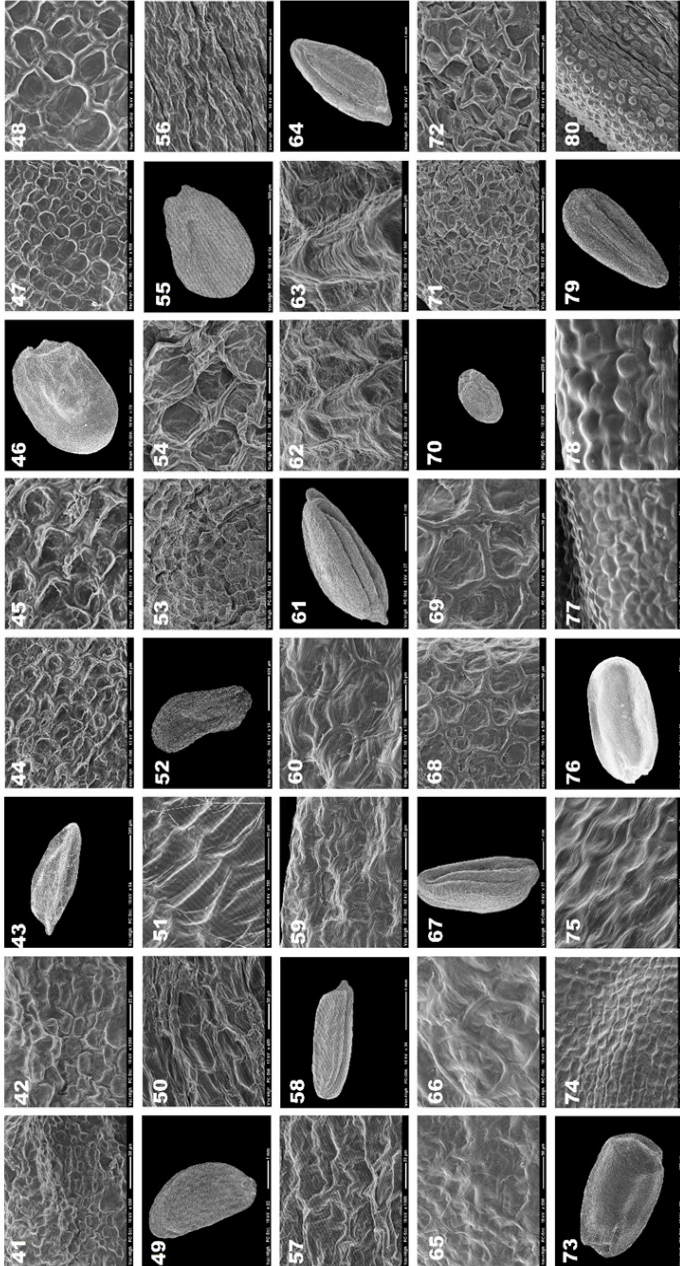
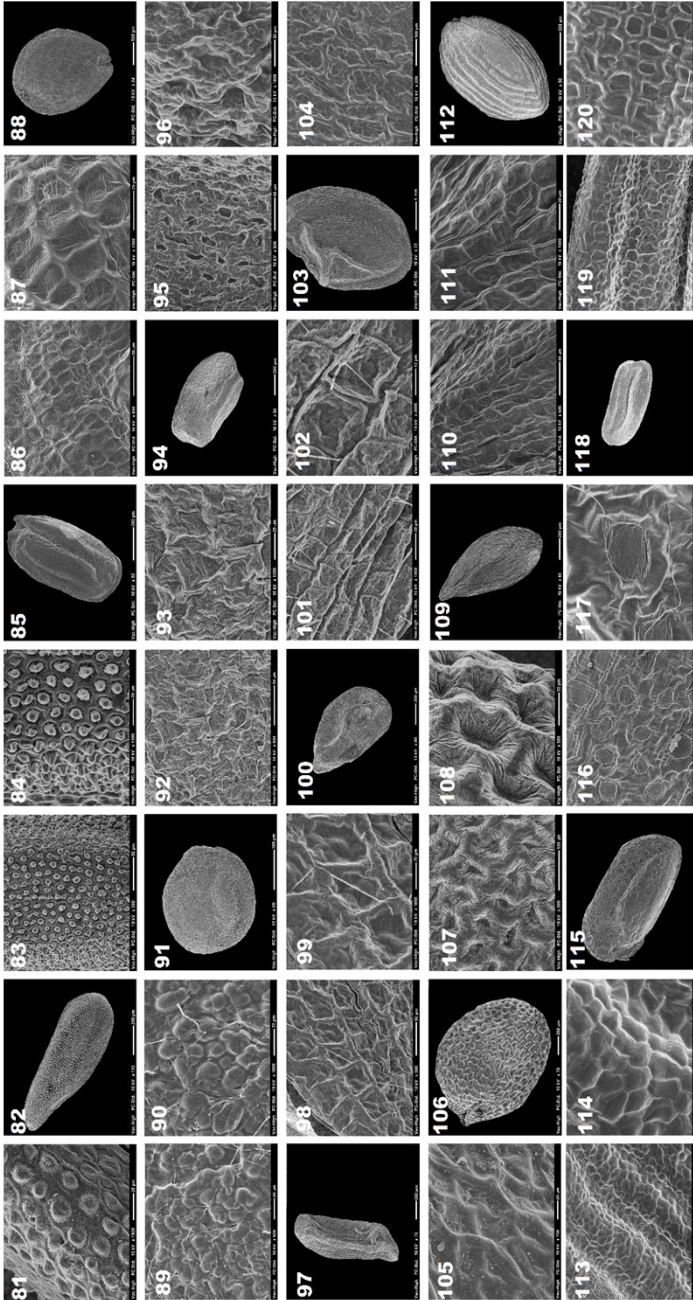


Figure 2. The SEM pictures of the seeds of the examined taxa; 1-3: *Alliaria petiolata*, 4-6: *Arabidopsis thaliana*, 7-9: *Brassica nigra*, 10-12: *Camelina rumelica*, 13-15: *Calepina irregularis*, 16-18: *Conringia grandiflora*, 19-21: *C. orientalis*, 22-24: *C. perfoliata*, 25-27: *Diplotaxis tenuifolia*, 28-30: *Eruca vesicaria*, 31-33: *Erysimum crassipes*, 34-36: *E. cuspidatum*, 37-39: *E. leucanthemum*, 40: *E. gontiocaulon*.



**Figure 2.** The SEM pictures of the seeds of the examined taxa: **41-42:** *Erysimum gonticaulon*, **43-45:** *Hesperis bicuspidata*, **46-48:** *H. persica*, **49-51:** *Iberis acutiloba*, **52-54:** *I. sempervirens*, **55-57:** *I. spruneri*, **58-60:** *Isatis arenaria*, **61-63:** *I. cappadocica* subsp. *cappadocica*, **64-66:** *I. erzurumica*, **67-69:** *I. glauca* subsp. *glauca*, **70-72:** *Matcolmia africana*, **73-75:** *M. chita*, **76-78:** *M. flexuosa*, **79-80:** *Matthiola incana*.



**Figure 2.** The SEM pictures of the seeds of the examined taxa: **81:** *Matthiola incana*, **82-84:** *M. montana*, **85-87:** *M. longipetala*, **88-90:** *Peltaria alliacea*, **91-93:** *Sinapis arvensis*, **94-96:** *Sisymbrium altissimum*, **97-99:** *S. officinale*, **100-102:** *S. orientale*, **103-105:** *Tchihatshewia isotidea*, **106-108:** *Thlaspi alliaceum*, **109-111:** *T. kurdicum*, **112-114:** *T. oxyceras*, **115-117:** *Turritis glabra*, **118-120:** *T. laxa*.

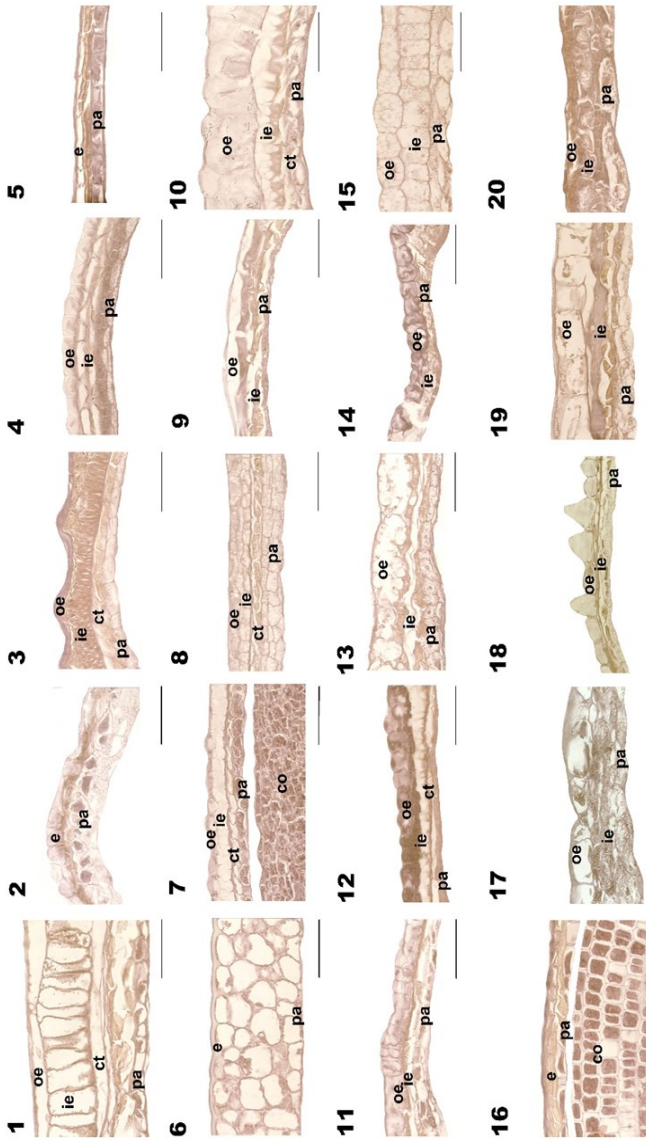


**Figure 3.** The anatomical structures of the seed testa of the examined taxa: **1:** *Alliaria petiolata*, **2:** *Arabidopsis thaliana*, **3:** *Brassica nigra*, **4:** *Camelina rumellica*, **5:** *Caleopina irregularis*, **6:** *Conringia grandiflora*, **7:** *C. orientalis*, **8:** *C. perfoliata*, **9:** *Diploraxis tenuifolia*, **10:** *Eruca vesicaria*, **11:** *Erysimum crassipes*, **12:** *E. cuspidatum*, **13:** *E. leucanthemum*, **14:** *E. goniocaulon*, **15:** *Hesperis bicuspidata*, **16:** *H. persica*, **17:** *Iberis acutiloba*, **18:** *I. sempervirens*, **19:** *I. spruneri*, **20:** *Isatis arenaria* (e: epidermis, oe: outer epidermis, ie: inner epidermis, ct: compressed tissue, co: cotyledon, pa: parenchyma), scale bars: 100  $\mu$ m).

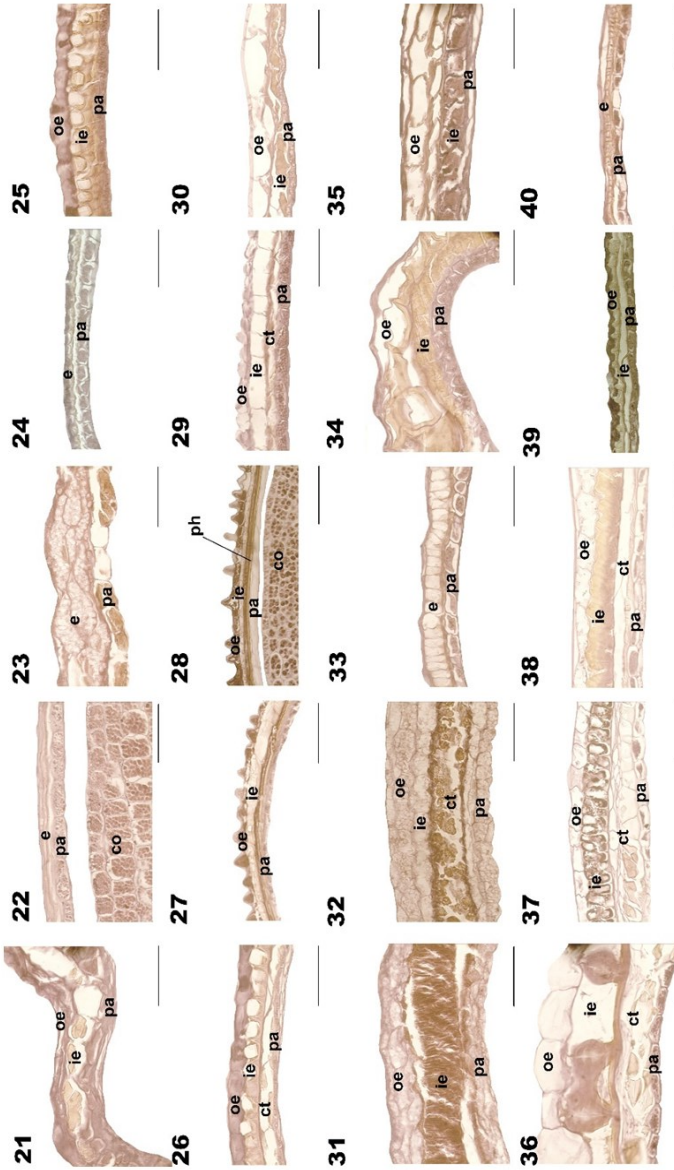


**Figure 3.** The anatomical structures of the seed testa of the examined taxa: **21:** *I. cappadocica* subsp. *cappadocica*, **22:** *I. erzurumica*, **23:** *I. glauca* subsp. *glauca*, **24:** *Malcolmia africana*, **25:** *M. chia*, **26:** *M. flexuosa*, **27:** *Matthiola incana*, **28:** *M. montana*, **29:** *M. longipetala*, **30:** *Peltaria alliaceae*, **31:** *Sinapis arvensis*, **32:** *Sisymbrium altissimum*, **33:** *S. officinale*, **34:** *S. orientale*, **35:** *Tchihatchewia isattidea*, **36:** *Thlaspi alliaceum*, **37:** *T. kurdicum*, **38:** *T. oxyceras*, **39:** *Turritis glabra*, **40:** *T. laxa* (e: epidermis, oet: outer epidermis, ie: inner epidermis, ct: compressed tissue, pa: parenchyma, ph: phytomelan, scale bars: 100 µm).

## 2. Comparison of the obtained information and literature

The present investigation covers seed morphological and anatomical features of seeds of 40 taxa belonging to 20 genera in Brassicaceae family and their phylogeny aspects. Morphological features in various genera within family have been widely investigated; however, comprehensive parallel evolution of traits confuse the definition of natural groups. Here, a preliminary work was performed to test the additional characteristics (seed morphology and anatomy) for their practicality in generic delimitation and infrageneric classification.

The morphological features of the seeds can offer precise evidence in terms of the evolutionary relationships of flowering plants (Corner, 1976; Karaismailoğlu, 2015). The surface, color, and size features of the seeds are useful characteristics in separating of the taxa in Brassicaceae family (Barthlott, 1981; Koul et al., 2000). Also, the work including 30 species belonging to 22 genera from Brassicaceae family of Tantawy et al. (2000) have revealed relationships between at present taxonomy within family and seed morphological features and pointed out that the macromorphological characters may be used to explain problems in the systematics of the taxa.

In this study, the figures of seeds among the studied taxa indicated a wide variation. Most of the seeds range from ovatus to ellipticus. Apart from these, it was rarely observed circularis and rectangularis. Seeds figures was found helpful to discriminate the closely related genera, these outcomes suitable with the results of Khalik and Measen (2002). The figure of seeds showed differences among the subspecies or species of *Conringia*, *Erysimum*, *Hesperis*, *Iberis*, *Matthiola*, *Isatis*, *Sisymbrium*, *Thlaspi* and *Turritis* (Figure 1). Seed size vary greatly among the studied taxa, the largest seeds in *Isatis cappadocica* subsp. *cappadocica* and the smallest seeds in *Arabidopsis thaliana*. The seed size was found helpful in the separation of taxa at the genus level. The limitation of tested characteristics is the color, which is almost all cases offer a small variation for the delimitation of genera or subgenera classification within Brassicaceae. The shape of epidermal cells can good a diagnostic and systematic character. The epidermal cells are well-developed in the majority of the studied taxa. In some taxa as *Alliaria petiolata*, *Conringia grandiflora*, *Peltaria alliacea* and *Sinapis arvensis*, the epidermal cells are ill-developed. The taxonomic usability of these characteristics has been ignored so far. And the detailed evaluation opportunities have found among the taxa studied by this study for the first time. At the same time, the morphological and anatomical applications led to new insights into generic and subgeneric interrelations within the Brassicaceae family. The obtained macromorphological outcomes of this work are suitable with the prior investigations conducted with exomorphic characters of seeds of Brassicaceae family (Tantawy et al., 2002; Khalik and Measen, 2002; Pınar et al., 2009; Kasem et al., 2011; Kaya et al., 2011; Bona, 2013; Karaismailoğlu, 2016 and 2019; Karaismailoğlu and Erol, 2018).

Comparative works of the micromorphological features on the surfaces of the seeds are very significant in terms of systematic relations (Bernard, 2000). Also, it has stated efficiency of scanning electron microscopy in answering taxonomic problems (Heywood, 1971). Various authors stated that seed micro-features are valuable characteristics to practices in separating of the taxa within Brassicaceae family (Barthlott, 1981; Koul et al., 2000; Tantawy et al., 2002; Kaya et al., 2011; Bona, 2013; Karaismailoğlu, 2016 and 2019; Karaismailoğlu and Erol, 2018).

SEM study indicated 11 types of the seed surface ornamentation, viz. reticulate, scalariform, reticulate-foveate, alveolate, reticulate-alveolate, ruminate, reticulate-areolate, foveate-lineate, foveate and reticulate-verrucate. The reticulate type is the basic type in majority of the investigated taxa (13 taxa). In addition, ruminate and lineate are the least common types among the studied taxa.

This study has shown compatibility with previous works on the seed surfaces of various genera in Brassicaceae. In some earlier studies were seen 15 surface types in 35 species of *Brassica*, 12 surface types in 25 species of *Diplotaxis*, 4 surface types in 5 species of *Sinapis*, 5 surface types in 25 species of *Erucastrum*, 9 surface types in *Thlaspi* and 2 surface types in 3 species of *Raphanus* (Koul et al., 2000; Kaya et al., 2011; Karaismailoğlu, 2018).

Many previous works were indicated that the most common seed surface types in Brassicaceae family were reticulate and reticulate-areolate as seen in this work. Besides, the tuberculate surface was found in some taxa of *Lepidium*, *Erysimum*, *Alyssum*, *Thlaspi* and *Camelina* genera (Murley, 1951; Bona, 2013). Ocellate type was recorded in *Carricthera* (Koul et al., 2000), *Hesperis* (Pınar et al., 2009), and *Thlaspi* (Karaismailoğlu and Erol, 2018). The ruminate surface type was seen in *Lepidium* and *Thlaspi* genera (Bona, 2013; Karaismailoğlu, 2018).

Earlier works have displayed that the structures of anticlinal and periclinal cell walls are useful identification characters in various levels within the family (Barthlott, 1981 and 1984; Khalik and Maesen, 2002; Tantawy et al., 2004; Bona, 2012; Karaismailoğlu, 2016; Karaismailoğlu and Erol, 2018). The mentioned structures are also beneficial in the separation of taxa within the genus in this study. The type of the anticlinal cell wall is raised, sunken, or unclear, and the type of the periclinal cell wall is concave, convex, or unclear. The examined taxa have showed variations in terms of the epidermal cell structure. Epidermal cells are in polygonal, rectangular, alveolar, oval, irregular, crushed or unclear forms. Polygonal cells are present in the majority of the studied taxa. Although the continuity of the seed surface characteristics might be observed within studied taxa, anticlinal and periclinal cell walls and epidermal cell structures should be interpreted with caution, which were not informative for taxa delimitation. Generally, SEM examinations has displayed that the comprehensive investigation of seed characters of the examined taxa are of valuable data in separating of taxa from each other.

Revisions of anatomical structures of seed coat in family Brassicaceae have overcome many taxonomic difficulties (Berggren, 1962; Vaughan et al., 1971; Koul et al., 2000; Zeng et al., 2004; Karcz et al., 2005; Ghaempanah et al., 2013; Karaismailoğlu, 2018; Karaismailoğlu and Erol, 2018). The anatomical characteristics of seed testa of taxa belonging to various genera in the family Brassicaceae have studied by Vaughan et al. (1976), Mulligan and Bailey (1976), Meyer (1973, 1979 and 1991), Iwanowska et al. (1994), Moazzeni et al. (2007) and Karaismailoğlu (2018). Nonetheless, few works have studied default evolutionary relations among taxa within family based on seed testa characters. In general, the seed coat occurs from two layers in Brassicaceae; the inner and outer integuments, which consist of (1) outer epidermis and (2) inner epidermis (outer integument), (3) inner integument (compressed tissue), and (4) parenchymatic layer (Ghaempanah et al., 2013; Karaismailoğlu, 2018).

In this work, anatomical structures of seed coats of the examined have been studied in detail for the first time, and it is discussed whether helpful in solving taxonomic problems. The seed coat occurs from distinguished layers like outer testa (outer and inner epidermis), inner testa, and parenchyma layer.

Vaughan and Whitehouse (1971) found 15 types of epidermis cells in their study, which included anatomical structures of seed coats of 200 taxa belonging to 90 genera within Brassicaceae. In this study, it is seen that the outer epidermis of the outer testa differ among the examined taxa. This layer can occur from flat, crushed, cubic, rectangular, oval, or polygonal cells with 1-6 layered. Flat cells are mostly seen, however; oval cells are infrequent in the examined taxa. In spite of the declared convergence of fruits and flowers in Brassicaceae family, the outer testa of the seed coat of the examined taxa have demonstrated to be more valuable characters than the old-style ones utilized in classification of the examined genera. Similar observations are expressed in some anatomical studies in family such as Meyer (1973, 1979, 1991, 2001 and 2006), Ghaempanah et al. (2013), Karaismailoğlu (2018).

The structure of the inner testa of the studied taxa has examined for the first time in this investigation. The type of the inner testa (compressed tissue under the epidermis layers) has demonstrated significant differences among taxa. The inner testa are in flat, crushed, or rectangular forms. This layer is absent in most of the examined taxa. However, inner testa can be effective, and provides in separating closely related taxa within genera. The structure and thickness of the parenchyma of the examined taxa has also investigated for the first time in this study, and they have showed variations among the taxa. The parenchymal layer occurs with flat, cubic or rectangular forms. The most common cell type is flat, whereas cubic and rectangular cells are less common types.

In conclusion, the morphological and anatomical characters of seeds of 40 taxa of Brassicaceae family have offered important contributions to the systematics of taxa belonging to genera.

**Acknowledgements**

The author thanks the professors in Istanbul University, Division of Botany for providing the facilities of some equipments.

## References

1. Algan, G. (1981). *Bitkisel Dokular için Mikroteknik*. Elazığ: Fırat Üniversitesi Yayınları,
2. Al-Shehbaz, I.A., Beilstein, M.A. and Kellogg, E.A. (2006). Systematics and phylogeny of the Brassicaceae (Cruciferae): an overview. *Plant Systematics and Evolution*, 259, 89-120.
3. Barthlott, W. (1981). Epidermal and seed surface characters of plants: systematic applicability and some evolutionary aspects. *Nordic Journal of Botany*, 1, 345-355.
4. Barthlott, W. (1984). Microstructural features of seed surface. In: Heywood, V.H. and Moore, D.C. (eds.). *Current Concepts in Plant Taxonomy* (95-105 pp.). London: Academic Press.
5. Barton, A. (1967). *Bibliography of seeds*. New York & London: Columbia University Press.
6. Berggren, G. (1962). Reviews on the taxonomy of some species of the genus *Brassica* based on their seeds. *Svensk Botanisk Tidskrift*, 56, 135.
7. Bernard, C. (2000). Comparative seed micromorphology of *Brassica* L. and *Sinapsis* L. species growing in France. *Seed Science and Technology*, 3, 699-707.
8. Bona, M. (2013). Seed-coat microsculpturing of Turkish *Lepidium* (Brassicaceae) and its systematic application. *Turkish Journal of Botany*, 37, 662-668.
9. Bouman, F. (1975). Integument initiation and testa development in some Cruciferae. *Botanical Journal of the Linnean Society*, 70, 213-299.
10. Buth, G.M. and Ara, R. (1981). Seed coat anatomy of some cultivated *Brassica*. *Phytomorphology*, 31, 69-78.
11. Brisson, J.D. and Peterson, R.L. (1977). The scanning electron microscope and X-ray microanalysis in the study of seeds: a bibliography covering the period of 1967-1976. *Scanning Electron Microscopy*, 2, 697-712.
12. Corner, E.J. (1976). *The Seeds of Dicotyledons*. Cambridge: Cambridge University Press.
13. El-Naggar, S.M. (1996). Seed coat morphology of the Egyptian species of tribe Alyseae (Brassicaceae) and its taxonomic significance. *Bulletin of the Faculty of Science Assiut University*, 25, 51-7.
14. Franzke, A., Lysak, M.A., Al-Shehbaz, I.A., Koch, M.A. and Mummenhoff, K. (2011). Cabbage family affairs: The evolutionary history of Brassicaceae. *Trends in Plant Science*, 16, 108-116.
15. Ghaempanah, S., Ejtehadi, H., Vaezi, J. and Farsi, M. (2013). Seed-coat anatomy and microsculpturing of the genus *Erysimum* (Brassicaceae) in Northeast of Iran. *Phytotaxa*, 150, 41-53.
16. Heywood, V.H. (1971). *Scanning electron microscopy*. London: Systematic and evolutionary applications.
17. Iwanowska, A., Tykarska, T., Kuras, M. and Zobel, A. (1994). Localization of phenolic compounds in the covering tissues of the embryo of *Brassica napus* (L.) during different stages of embryogenesis and seed maturation. *Annals of Botany*, 74, 313-320.
18. Karaismailoğlu, M.C. (2015). Morphological and anatomical features of seeds of Turkish *Romulea* taxa (Iridaceae) and their taxonomic significance. *Acta Botanica Croatica*, 74, 31-41.
19. Karaismailoğlu, M.C. (2016). Addition to characters of endemic *Aubrieta canescens* subsp. *canescens* Bornm. (Brassicaceae) from Turkey. *Bangladesh Journal of Botany*, 45, 509-515.

20. Karaismailoğlu, M.C. (2017). Palynological features of eleven *Aethionema* taxa from Turkey and their systematic implications. *Bangladesh Journal of Plant Taxonomy*, 24, 197-204.
21. Karaismailoğlu, M.C. (2018). Systematic Investigations on Some Taxa of Genus *Thlaspi* L. (Brassicaceae); Sections *Nomisma* DC., *Thlaspi* L., *Pterotropis* DC., Doctoral Thesis, Istanbul University.
22. Karaismailoğlu, M.C. (2019). Notes on the taxonomical, morphological and mucilage features of *Capsella bursa-pastoris* Medik. and *Capsella rubella* Reuter taxa (Brassicaceae). *Artvin Coruh University Journal of Forestry Faculty*, 20(1), 1-7.
23. Karaismailoğlu, M.C. and Erol, O. (2018). Seed structure and its taxonomic implications for genus *Thlaspi* sensu lato sections *Nomisma*, *Thlaspi*, and *Pterotropis* (Brassicaceae). *Turkish Journal of Botany*, 42(5), 591-609.
24. Karaismailoğlu, M.C. and Erol, O. (2019). Pollen morphology of some taxa of *Thlaspi* L. sensu lato (Brassicaceae) from Turkey and its taxonomical importance. *Palynology*, 42(2), 244-254.
25. Karcz, J., Książczyk, T. and Maluszynska, J. (2005). Seed coat patterns in rapid-cycling *Brassica* forms. *Acta Biologica Cracoviensia Series Botanica*, 47, 159-165.
26. Kasem, W.T., Ghareeb, A. and Marwa, E. (2011). Seed Morphology and Seed Coat Sculpturing of 32 Taxa of Family Brassicaceae. *Journal of American Science*, 7, 166-178.
27. Kaya, A., Ünal, M., Özgökçe, F., Doğan, B. and Martin, E. (2011). Fruit and seed morphology of six species previously placed in *Malcolmia* (Brassicaceae) in Turkey and their taxonomic value. *Turkish Journal of Botany*, 35, 653-662.
28. Khalik, K. and Maesen, L.J.G. (2002). Seed morphology of some tribes of Brassicaceae (Implication for taxonomy and species identification for the flora of Egypt). *Blumea*, 47, 363-83.
29. Khosravi, A.R., Mohsenzadeh, S. and Mummenhoff, K. (2009). Phylogenetic relationships of Old World Brassicaceae from Iran based on nuclear ribosomal DNA sequences. *Biochemical Systematics and Ecology*, 37, 106-115.
30. Koul, K.K., Ranjna, N. and Raina, S.N. (2000). Seed coat microsculpturing in *Brassica* and allied genera (subtribes Brassicinae, Raphaninae, Moricandiinae). *Annals of Botany*, 86, 385-97.
31. Meyer, F.K. (1973). *Conspectus der "Thlaspi"-Arten Europas, Afrikas und Vorderasiens. Feddes Repertorium*, 84, 449-470.
32. Meyer, F.K. (1979). Kritische Revision der "Thlaspi"-Arten Europas, Afrikas und Vorderasiens I. Geschichte, Morphologie und Chorologie. *Feddes Repertorium*, 90, 129-154.
33. Meyer, F.K. (1991). Seed-coat anatomy as a character for a new classification of *Thlaspi*. *Flora et Vegetation Mundi*, 9, 9-15.
34. Meyer, F.K. (2001). Kritische Revision der "Thlaspi"-Arten Europas, Afrikas und Vorderasiens, Spezieller Teil, II. *Thlaspi* L. *Hausknechtia*, 8, 3-42.
35. Meyer, F.K. (2006). Kritische Revision der "Thlaspi"-Arten Europas, Afrikas und Vorderasiens. Spezieller Teil. IX. *Noccaea* Moench. *Hausknechtia*, 12, 1-343.
36. Moazzeni, H., Zarre, S., Al-Shehbaz, I.A. and Mummenhoff, K. (2007). Seed-coat microsculpturing and its systematic application in *Isatis* (Brassicaceae) and allied genera in Iran. *Flora*, 202, 447-454.
37. Mulligan, G.A. and Bailey, L.G. (1976). Seed coat of some *Brassica* and *Sinapis* weeds and cultivated in Canada. *Economic Botany*, 30, 143-148.
38. Murley, M.R. (1951). Seeds of the Cruciferae of North Eastern America. *American Middle Naturalichen*, 46, 1-81.

39. Özüdođru, B., Akaydın, G., Erik, S. and Mummenhoff, K. (2016). Seed Morphology of *Ricotia* and its phylogenetic and systematic implication. *Flora*, 222, 60-67.
40. Pınar, N.M., Duran, A., Ceter, T. and Tuđ, G.N. (2009). Pollen and seed morphology of the genus *Hesperis* L. (Brassicaceae) in Turkey. *Turkish Journal of Botany*, 33, 83-96.
41. Simpson, M.G. (2006). *Plant Systematics*. London: Elsevier Academic Press.
42. Stearn, W.T. (1985). *Botanical Latin: history, grammar syntax, terminology, and vocabulary*. London: David & Charles.
43. Tantawy, M.E., Khalifa, S.F., Hassan, S.A. and Al-Rabiai, G.T. (2004). Seed exomorphic characters of some Brassicaceae (LM and SEM Study). *International Journal of Agriculture and Biology*, 6, 821-830.
44. Tekin, M., Yılmaz, G. and Martin, E. (2013). Morphological, Anatomical and Palynological Studies on Endemic *Matthiola anchoniifolia* Hub.-Mor. (Brassicaceae). *Notulae Scientia Biologicae*, 5(2), 163-168.
45. Vaughan, J.G. and Whitehouse, J.M. (1971). Seed structure and the taxonomy of the Cruciferae. *Botanical Journal of the Linnean Society*, 64, 383-409.
46. Vaughan, J.G., Phelan, J.R. and Denford, K.E. (1976). Seed studies in the Cruciferae. In: Vaughan, J.G., Macleod, A.J. and Jones, B.M.G. (eds.). *The biology and chemistry of the Cruciferae* (119-144 pp.). London: Academic Press.
47. Zeng, C.H.L., Wang, J.B., Liu, A.H., Wu, X.M., 2004: Seed coat microsculpturing changes during seed development in diploid and amphidiploid *Brassica* species. *Annals of Botany*, 93, 555-566.

# COMPARISON OF ANTIOXIDANT CAPACITY OF OXIDANT IN BEE POLLEN IN TERMS OF REGION AND STORAGE CONDITIONS

Naci Ömer ALAYUNT<sup>1</sup>



---

<sup>1</sup> Uşak University, Banaz Vocational School Department of Chemical and Chemical Processing Technology, Laboratory Technology Program, Uşak.



## 1. Introduction

Bee pollen is a highly complex and nutritious chemical product used in supplements and alternative diets, especially because of its nutritional properties and health benefits. Phenolic and flavonoid compounds which can act as a potent antioxidant, are a mixture of many bioactive substances such as terpenes and tocopherol. Antimicrobial, antifungal, antioxidant, antiinflammatory and liver preservation properties have been demonstrated in various studies using bee pollen collected in different geographical and botanical environments.

Pollen obtained from *Apis Mellifera Caucasicus* bee species In order to determine the antioxidant and oxidant properties of three different geographical regions in two different seasons, B1, B2 vitamins and MDA analyzes as well as DPPH radical scavenging method were measured in HPLC. Regional data on climatic conditions, vegetation-based and storage conditions that we think that different data was obtained. We have observed that bee pollen has an effect on the region and climate conditions by minimizing the effect of oxidizing agents in the organism.

### 1.1. Pollen

Honey bees collect the pollen grains that are released from various plants in the land they spread, carry them to the hives, store them in the cells and use it to feed larvae when the time comes. Pollen grains are a good indicator of the botanical and geographical origin of bee products (1, 2, 3). Our country has the potential to be one of the highest quality pollen producers in the world because of the resistance of *Apis mellifera* bee species which is known to be the indispensable Caucasian race of especially beekeepers.

This biodiversity may provide useful nutritional supplements with antimicrobial, antifungal, antioxidant, anti-inflammatory and liver protection properties, as well as phenolic and flavonoid compounds, terpenes and tocopherol, as well as many other bioactive substances, such as phenolic and flavonoid compounds collected throughout the year (4, 5).

In addition, this bee product is considered to be a healthy food with a wide variety of beneficial effects, including human health, protection against depression and anxiolytic characteristics, memory improvement and antiepileptic effect, as well as decreased bone loss due to osteoporosis in mice (6, 7).

## 2. Material and Method

### 2.1. Experimental Design

In our study, we aimed to investigate the effect of region differences and storage conditions in terms of oxidant-antioxidant capacity in bee pollen and to draw attention to plant origin, geographical location and seasonality. In June 2018 *Apis Mellifera Caucasicus* honey bee colonies were collected from

three different geographical regions. Samples of section 1 were studied freshly and section 2 samples were separated in February for proper storage (Table 1).

4 samples from 6 hives were taken from each region. The samples were divided into two parts. To be studied in June and February, each region was divided into 4 groups. No special permission was required on the site. Sample collection was done on private land and with the permission of hive owners. There were no endangered or protected species in beehives. Region names and altitudes are given in Table 1.

## 2.2. Location of hives

- Kahta District of Adıyaman Province (KH).
- Sivrice District of Elazığ Province (SV).
- Ovacık District of Tunceli Province (OV).

**Tablo 1.** Bölge ve rakımlar

| Sample taken | Altitude (meters) |
|--------------|-------------------|
| Ovacık (OV)  | 1300              |
| Sivrice (SV) | 1271              |
| Kahta (KH)   | 832               |

## 2.3. Receiving Pollen Samples

Pollen taken from beehives to sterile glass jars were brought to the laboratory and kept in a cool and dry place (1-2 ° C, 25% relative humidity) until extraction (13). Pollen samples were stored until the working day and the working day was prepared according to the appropriate procedure for B1, B2 vitamins and MDA, DPPH analyzes. First, the fresh pollen of the June group was analyzed and the results were recorded. Then, in February 2019, the group of pollen which were kept in a cool and dark place in room runs were analyzed in February. All of the results were gathered and statistical analyzes were given in tables and graphs.

## 2.4. Preparation of Pollen Ethanol Extract

Ethanol extracts of pollen were prepared in 4.5 mL of 80% ethanol per g of pollen. It was kept in a water bath at 70 ° C until completely dissolved. The solution was filtered (80 g / m<sup>2</sup>) on filter paper (14). Samples were prepared for analysis.

## 2.5. B1 and B2 Vitamin Analysis

The 1 ml pollen-containing ethanol extract was removed and the mixture was vortexed after treatment with 0.5 ml of 0.5 M HClO<sub>4</sub>. 2 ml of distilled water was added to the mixture, and after standing for 10 minutes in an ultrasonic water bath, 4500 rpm was centrifuged for 5 minutes. 20 µl of the

supernatant from the clear portion on the solution was analyzed by HPLC. The mobile phase of 5 mM heptano sulfonic acid was dissolved in methanol followed by a 750 ml solution containing 0.1% triethylamine and a volume ratio of 25: 75 with phosphoric acid to be pH 2.8 (15).

## 2.6. Malondialdehyde (MDA) Analysis

The 1ml pollen-containing ethanol extract was taken up and mixed with water at a one-to-one ratio and the dissolved fraction was analyzed by HPLC apparatus. 1 ml of the new solution extract was removed and 0.5 ml of 0.5 M HClO<sub>4</sub> was added. With the addition of 4.5 ml of distilled water, the mixture was centrifuged at 4500 rpm for 5 minutes. 20 µl of the supernatant was analyzed in HPLC and MDA was analyzed by HPLC (16). The flow rate was analyzed as 1 ml / min using inertsil 5 µ C-18 (15 cm x 4.6 mm) column at 250 nm in a mixture of KH<sub>2</sub>PO<sub>4</sub> - methanol (82.5 - 17.5; pH: 4) as mobile phase.

## 2.7. Free Radical Cleaning Activity

To a solution of 0.1 ml of pollen was added 1 ml of 250 -mol.l-1 DPPH methanol solution. After 30 minutes of incubation, the reduction of free radical DPPH was calculated by using a Spectrophotometer (517 nm absorbance against a blank (ethanol) and the percentage inhibition activity by using the formula  $\% I = \frac{(A_0 - A_1)}{A_0} \times 100$ : Control absorbance: A<sub>0</sub> and The absorbance of the extract / standard was calculated as A<sub>1</sub>. The concentration required to reduce DPPH absorption by 50% was expressed as DPPH (sweeping activity) (IC<sub>50</sub>). Low IC<sub>50</sub> values indicate higher radical scavenging activity.

## 2.8. Statistical analysis

The statistical differences with SPSS 15.0 statistical program were found by using mean and standard deviation. The Mann Whitney-U test was used to compare the means of different groups. Results were shown as mean ± standard deviation and p <0.05 was accepted as significant level.

### 3. Results

**Table 2.** DPPH, MDA, B and B2 Vitamin Levels.

| Samples     | DPPH (IC <sub>50</sub> )    | MDA(nmol/ml)              | B1 (µg.g <sup>-1</sup> ) | B2 (µg.g <sup>-1</sup> ) |
|-------------|-----------------------------|---------------------------|--------------------------|--------------------------|
| OV June     | 85.12 ± 2.22 <sup>a</sup>   | 0.282±0.025 <sup>a</sup>  | 59.44±3.12 <sup>a</sup>  | 95.31±4.25 <sup>a</sup>  |
| OV February | 139.51 ± 2.89 <sup>b</sup>  | 0.461±0.041 <sup>b</sup>  | 48.11±2.84 <sup>b</sup>  | 92.55±3.41 <sup>a</sup>  |
| SV June     | 125.82 ± 3.08 <sup>bc</sup> | 0.518±0.055 <sup>bc</sup> | 57.22±4.14 <sup>a</sup>  | 91.54±3.12 <sup>a</sup>  |
| SV February | 229.42 ± 2.48 <sup>d</sup>  | 0.823±0.044 <sup>d</sup>  | 48.48±3.52 <sup>b</sup>  | 78.88±3.17 <sup>b</sup>  |
| KH June     | 158,17 ± 2.43 <sup>e</sup>  | 1.061±0.085 <sup>e</sup>  | 39.84±4.02 <sup>c</sup>  | 77.63±3.41 <sup>b</sup>  |
| KH February | 353.22 ± 5.31 <sup>f</sup>  | 1.299±0.059 <sup>f</sup>  | 32.76±3.03 <sup>d</sup>  | 57.11±3.44 <sup>c</sup>  |

Low IC<sub>50</sub> values indicate higher radical scavenging activity.

a-e: The difference between the groups with different letters on the same line is significant. (P <0.05) The statistical difference was determined by Mann Whitney -U test.

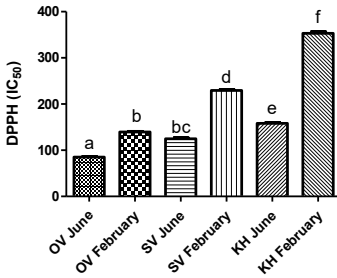


**Figure 1.** DPPH graphics

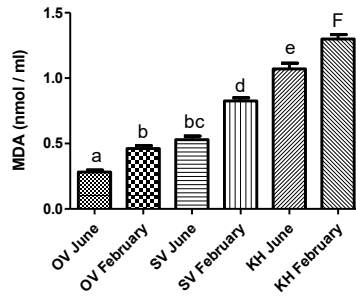


**Figure 2.** MDA graphics

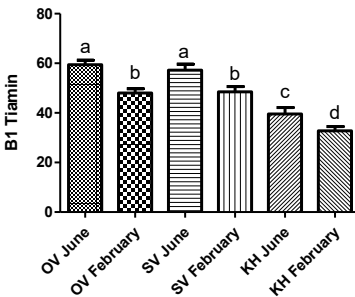


**Figure 3.** Vitamin B1graphics

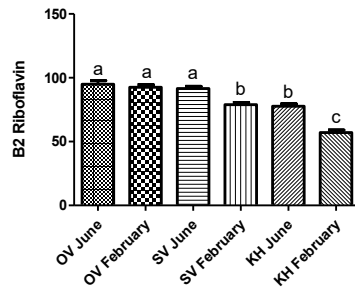


**Figure 4.** Vitamin B2 graphics

When DPPH levels were evaluated, it was observed that Ovacık pollen was the lowest IC50 level in June and Kahta pollen was the highest IC50 value in February (Figure 1). When compared between the months of June and February, statistically different results were observed. Analysis data in February were higher than in June ( $p < 0.05$ ).

When MDA levels were evaluated, it was observed that Ovacık pollen was at the lowest MDA level in June and Kahta pollen was the highest MDA value in February (Figure 2). When compared between the months of June and February, statistically different results were observed. Analysis data in February were higher than in June ( $p < 0.05$ ).

When B1 and B2 vitamin levels were evaluated, it was found that Ovacık pollen was the highest in B1 and B2 levels in June. The lowest B1 and B2 levels were observed in the Kahta region in February (Figure 3.4). When compared between the months of June and February, statistically different results were observed ( $p < 0.05$ ). Analysis data in February were lower than in June ( $p < 0.05$ ). The data presented in the table were calculated statistically and p value was given as  $p < 0.05$  significance level (Table 2).

#### 4. Discussion

Lipid peroxidation product MDA levels were found to be the lowest in fresh form of Ovacık pollen. In addition, MDA levels of other regional crops were low when they were fresh but increased as they were kept. As antioxidant properties, it is possible to find many studies that pollens are the subject of research. In studies on oxidative stress markers, pollen is an antioxidant product. In a study, oxidative stress levels in rats were measured and pollen supplementation and total antioxidant vitamin status levels were reported to be significantly increased (17). In another study on oxidative stress quail quails, increased plasma MDA levels after stress were significantly reduced in the pollen supplemented group (18).

In our study, it was found that the three different pollen regions had different results both in free radical scavenging activity (Low DPPH) and in the ability to prevent lipid peroxidation. The results indicated that the elevation level increased radically increasing activity of the different regions. MDA levels were decreased with the increase in altitude. Vitamin B1 and B2 levels, also known as water-soluble vitamins, increased at higher altitudes.

Studies show that the use of bee pollen is preventive and protective against oxidative stress at the basis of many diseases. However, detailed and comprehensive studies are needed. It is possible to change the therapeutic properties of the compounds qualitatively and quantitatively (19). Even the pollen produced by the bee species living in the colony of the same region may show different biological activities.

It has been reported in various studies that bee pollens vary in terms of polyphenolic contents resulting from differences in regional climatic conditions. In our study, we have obtained different results that we believe

are due to environmental factors such as altitude difference, plant diversity, climatic conditions and drought.

Due to the effects of chemical variability in pollen structure, consistent dose determination studies are needed in phytotherapy. As a result of this approach, different therapeutic effects can be expected according to bee pollen characteristics and biological activities. As far as we understand in our data, it is possible to say that pollen, which is a bee product, has antioxidant capacity and is a product that can be recommended as a nutritional supplement. However, the decrease in the antioxidant properties of the samples waiting for about 8 months in closed, dark and dehumidified places, as well as the increase of MDA values known as lipid peroxidation product gave us an idea about the fresh consumption of pollen.

## References

1. Borges R.L.B., Lima L.C.L., Oliveira P.P., Silva F.H.M., Novais J.S., Dórea M.C., Santos F.A.R. O pólen no mel do Semi-Árido brasileiro. In: Santos F.A.R., editor. *Apium Plantae*. IMSEAR; Recife, Brasil: 2006. pp. 103–118.
2. Morais M., Moreira L., Feás X., Estevinho L.M. Honeybee-collected pollen from five Portuguese natural parks: Palynological origin, phenolic content, antioxidant properties and antimicrobial activity. *Food Chem. Toxicol.* 2011;49:1096–1101.
3. Estevinho L.M., Rodrigues S., Dias T., Da Silva J.P., Feás X. Botanical, nutritional and microbiological characterisation of honeybee-collected pollen from Portugal. *Food Chem. Toxicol.* 2012 in press.
4. Morais M., Moreira L., Feás X., Estevinho LM Five pollen collected from the honeybee from the Portuguese Nature Park: Palynological origin, phenolic content, antioxidant properties and antimicrobial activity. *Food Chemistry Toxicol.* , 2011; 49: 1096-1101.
5. Tohamy AA, Abdella EM, Ahmed RR, Ahmed YK Evaluation of anti-mutagenic, anti-histopathological and antioxidant capacity of corn bee pollen and propolis extracts. *Cytotechnology.* 2014; 66 : 283-297.
6. Karampour NS, Hemmati AA, Malmir A. Anxiolytic effect of bee pollen hydroalcoholic extract in mice. *Natl. J. Physiol. Pharm. Pharmacol.* 2017: 7.
7. Yıldız O., Karahalil F., Can Z., Şahin H., Kolaylı S. Kesin inhibition of total monoamine oxidase (MAO) with honey, pollen and própolis. *J. Enzyme Inhib. Med. Chem.* 2014; 29 : 690-694.
8. Melo AAM, Estevinho MLMF, Sattler JAG, Souza BR, Freitas AS, Barth OM, Almeida-Muradian LB İşleme koşullarının susuz arı poleni özellikleri ve kalite parametreleri arasındaki korelasyona etkisi. *Besin Bilgisi Technol.* 2016; 65 : 808–815.
9. Rebiai A., Lanez T. Chemical composition and antioxidant activity of *Apis mellifera* bee pollen from northwest Algeria. *J. Fundam. Bas. Sci.* 2012; 4 :155-163.
10. Almaraz-Abarca N., Campos MG, Ávila-Reyes JA, Naranjo-Jiménez N., Herrera-Corral J., González-Valdez LS Variability of antioxidant activity among pollen collected from honey bee of different vegetable origin. *Interciencia.* 2004; 29 : 574-578.
11. Kral A., Genç G. Fenolik fitokimyasalların özellikleri ve oluşumu. *J. Am. Diyet. Doç.* 1999; 99 : 213-218.
12. Rzepecka-Stojko A., Stojko J., Kurek-Górecka A., Górecki M., Kabała-Dzik A., Kubina R., Moździerz A., Buszman E. Polyphenols from bee pollen: structure, absorption, metabolism and biological activity. *Molecules.*2015; 20 : 21732-21749.
13. Bankova, V. (2005). Chemical diversity of propolis and the problem of standardization. *Journal of Ethnopharmacology*, 100: 114–117.
14. Alencar, S.M., Oldoni, T.L.C., Castro, M.L., Cabral, I.S.R., Costa-Neto, C.M., Cury, J.A. (2007). Chemical composition and biological activity of a new type of Brazilian propolis: red propolis. *Journal of Ethnopharmacology*, 113: 278–283.
15. Amidzic, R., Brboric, J., Cudina, O., Vladimirov, S. (2005). RP-HPLC Determination of vitamins B1, B3, B6, folic acid and B12 in multivitamin tablets, *J. Serb. Chem. Soc.*70(10), 1229–1235.
16. Karatas, F., Karatepe, M., Baysar, A. (2002). Determination of free malondialdehyde in human serum by high performance liquid chromatography. *Anal Biochem*, 311: 76-79.

17. Capcarova, M., Kolesarova, A., Kalafova, A., Branislav, Galik, Simko, M., Juracek, M., Toman, R. (2013). The role of dietary bee pollen in antioxidant potential in rats. *Eurasian Journal of Veterinary Sciences*, 29(3):133- 137.
18. Tatlı Seven, P., Sur Arslan, A., Seven, I., Gökçe, Z. (2016b). The effects of dietary bee pollen on lipid peroxidation and fatty acids composition of Japanese quails (*Coturnix coturnix japonica*) meat under different stocking densities. *Journal of Applied Animal Research* 44 (1): 487-491.
19. Huang, S., Zhang, C.P., Wang, K., Li, G.L., Hu, F.L. (2014). Recent Advances in the Chemical Composition of Propolis. *Molecules*, 19: 19610–19632.

# PRODUCTS OF FOUR HOMOGENEOUS COMPONENTS IN FREE LIE ALGEBRAS

Nil MANSUROĞLU<sup>1</sup>

Derya KARATAŞ<sup>2</sup>



---

<sup>1</sup> Asst. Prof. Dr., Department of Mathematics, Kirşehir Ahi Evran University, Bağbaşı Yerleşkesi, Merkez, Kirşehir, Turkey.

<sup>2</sup> Department of Mathematics, Kirşehir Ahi Evran University, Bağbaşı Yerleşkesi, Merkez, Kirşehir, Turkey.



## 1. INTRODUCTION

Let  $L$  be a free Lie algebra of finite rank  $r$  over a field  $F$  and let  $L_n$  denote the degree  $n$  homogeneous component of  $L$ . The algebra  $L$  has a natural graded as

$$L = L_1 \oplus L_2 \oplus \dots \oplus L_n \oplus \dots$$

In this note, we use the left normed convention for Lie brackets, namely, for  $a_1, a_2, \dots, a_s \in L$  we write  $[a_1, a_2, \dots, a_s] = [[a_1, a_2, \dots, a_{s-1}], a_s]$ . We calculate the dimension of  $L_n$  by Witt's formula

$$\dim L_n = f(n, r) = \frac{1}{n} \sum_{d|n} \mu(d) r^{\frac{n}{d}},$$

where  $\mu$  is the Mobius function (see [8], [1, Theorem 5.11]). In [7], R. Stöhr and M. Vaughan-Lee proved formulae for the dimension of the subspaces  $[L_m, L_n] \leq L_{m+n}$  for all  $m, n \geq 1$  as follows: If  $m > n$  and  $n \nmid m$ , then

$$(1.1) \quad \dim[L_m, L_n] = \dim L_m \dim L_n,$$

and if  $m = sn$  with  $s \geq 1$ , then

$$(1.2) \quad \dim[L_m, L_n] = (\dim L_m - f(s, \dim L_n)) \dim L_n + f(s + 1, \dim L_n).$$

Given a subset  $Y$  of  $L$ , let  $L(Y)$  be the Lie subalgebra generated by  $Y$  in  $L$  and we denote the degree  $n$  homogeneous component of  $L(Y)$  by  $L_n(Y)$ . We say that a set  $Y$  of homogeneous elements in  $L$  is a reduced set if none of its elements is contained in the subalgebra of  $L$  generated by the remaining elements of  $Y$ . The following lemma is referred to as Shirshov's Lemma which is played an important role in the proof of the Shirshov-Witt Theorem (see [5, 6]).

**Lemma 1.1 ([5, Proof of Theorem 2]).** If  $L$  is a free Lie algebra and  $Y$  is a reduced set of homogeneous elements in  $L$ , then  $Y$  is a set of free generators for the subalgebra  $L(Y)$ . Let  $U$  be any homogeneous subspace in  $L_n$ . The Lie subalgebra  $L(U)$  is free of rank  $\dim U$  and any  $F$ -basis of  $U$  is a free generating set for the Lie subalgebra  $L(U)$ . In [4], the second author and R. Stöhr investigated the dimension of product of two homogeneous subspaces and derived formulae for dimension of products of three homogeneous components. They proved the following lemma which will be the key step in the proof of our main results.

**Lemma 1.2 ([4, Lemma 2.2]).** Let  $U$  and  $V$  be subspaces of  $L$  such that  $U \subseteq L_m$ ,  $V \subseteq L_n$  with

$m \geq n \geq 1$ . Then

$$(1.3) \quad \dim[U, V] = \dim[U \setminus L(V), V] + (\dim U - \dim(U \setminus L(V))) \dim V.$$

### 2. MAIN RESULTS

In this paper, our aim is to investigate the dimension of the subspaces in the forms  $[L_m, L_n, L_k, L_p]$  and  $[[L_m, L_n], [L_k, L_p]]$ . Firstly, we give two technical lemmas for the proof of main results.

**Lemma 2.3.** Let  $m, n, k, p$  be positive integers.

(i) If  $m = s_1p, n = s_2p$  and  $k = s_3p$  for some positive integers  $s_1, s_2$  and  $s_3$ , then

$$[L_m, L_n, L_k] \setminus L(L_p) = [L_{s_1}(L_p), L_{s_2}(L_p), L_{s_3}(L_p)].$$

(ii) If  $p \nmid m$  or  $p \nmid n$  or  $p \nmid k$ , then

$$[L_m, L_n, L_k] \setminus L(L_p) = 0.$$

Proof. (i) Absolutely, we have

$$[L_{s_1}(L_p), L_{s_2}(L_p), L_{s_3}(L_p)] \subseteq [L_m, L_n, L_k] \setminus L(L_p).$$

It is sufficient to show that

$$[L_m, L_n, L_k] \setminus L(L_p) \subseteq [L_{s_1}(L_p), L_{s_2}(L_p), L_{s_3}(L_p)].$$

Now, we take the subalgebra  $L^p = L_p \oplus L_{p+1} \oplus L_{p+2} \oplus \dots$ , this is the  $p$ -th term of the lower central series of  $L$ . This subalgebra has a homogeneous free generating set of the form  $M = M_p \cup M_{p+1} \cup M_{p+2} \cup \dots$ , where  $M_i \subset L_i$  ( $i = p, p + 1, \dots$ ). It is easy to obtain a free generating set for  $L^p$ . First, we consider an  $F$ -basis of  $L_p$  for  $M_p$ , then for  $i > p$  we proceed inductively by taking a basis of a vector space complement of  $L_i \setminus L(M_i \cup \dots \cup M_{i-1})$  as the set  $M_i$ . By Lemma 1.1, it is clear to verify that the set is a generating set for  $L_p$  and also it is a free generating set. Hence,  $L_p = \langle M_p \rangle$  and  $M_p$  is a free generating set for  $L(L_p)$ . We now consider a projection map  $\pi: L^p \rightarrow L(L_p)$  defined by  $\pi(a) = a$  for  $a \in M_p$  and  $\pi(a) = 0$  for  $a \in M \setminus M_p$ . This map is also a Lie algebra homomorphism. Arbitrary chosen an element  $B$  in  $[L_m, L_n, L_k]$  can be expressed as a linear combination of the Lie products  $[u_j, v_j, w_j]$  for  $u_j \in L_m, v_j \in L_n, w_j \in L_k$ , that is,

$$B = \sum_j \alpha_j [u_j, v_j, w_j]$$

for some scalars  $\alpha_j \in F$ . Here,  $\pi(u_j) \in L_{s_1}(L_p), \pi(v_j) \in L_{s_2}(L_p)$  and  $\pi(w_j) \in L_{s_3}(L_p)$ . Suppose that  $B \in L(L_p)$ . Since  $\pi$  is a Lie algebra homomorphism, we have

$$\begin{aligned} B &= \pi(B) = \pi\left(\sum_j \alpha_j [u_j, v_j, w_j]\right) \\ &= \sum_j \alpha_j [\pi(u_j), \pi(v_j), \pi(w_j)] \in [L_{s_1}(L_p), L_{s_2}(L_p), L_{s_3}(L_p)]. \end{aligned}$$

Therefore, we proved the inverse inclusion

$$L(L_p) \setminus [L_m, L_n, L_k] \subseteq [L_{s_1}(L_p), L_{s_2}(L_p), L_{s_3}(L_p)].$$

(ii) We have  $p \nmid m$  or  $p \nmid n$  or  $p \nmid k$ . Here in order to prove this part of lemma, we use the

projection  $\pi$  as in (i) and we choose arbitrary element in  $L(L_p)$ , say  $B = \sum \alpha_j [u_j, v_j, w_j]$

with  $u_j \in L_m$ ,  $v_j \in L_n$  and  $w_j \in L_k$ . Since any element in  $L(L_p)$  is written as a linear

combination of elements of degree  $\lambda p$  with  $\lambda = 1, 2, \dots$ , all homogeneous components  $L_s$

with  $s \geq p$  and  $p \nmid s$  are in the kernel of  $\pi$ . As  $p \nmid m$  or  $p \nmid n$  or  $p \nmid k$ , at least one of  $\pi(u_j)$ ,  $\pi(v_j)$  and  $\pi(w_j)$  is zero. Thus,

$$\pi([u_j, v_j, w_j]) = [\pi(u_j), \pi(v_j), \pi(w_j)] = 0$$

for all  $j$ . Therefore, we conclude that

$$[L_m, L_n, L_k] \setminus L(L_p) = 0.$$

**Lemma 2.4.** Let  $m, n, k, p$  be positive integers.

(i) If  $m = s_1(k + p)$  and  $n = s_2(k + p)$  for some positive integers  $s_1$  and  $s_2$ , then

$$[L_m, L_n] \setminus L([L_k, L_p]) = [L_{s_1}([L_k, L_p]), L_{s_2}([L_k, L_p])].$$

(ii) If  $k + p \nmid m$  or  $k + p \nmid n$ , then

$$[L_m, L_n] \setminus L([L_k, L_p]) = 0.$$

Proof. (i) Since  $[L_k, L_p] \leq L_{k+p}$ , we have  $[[L_m, L_n], [L_k, L_p]] \leq [[L_m, L_n], L_{k+p}]$ . According

to Lemma 3.1 in [4], if  $m = s_1(k + p)$  and  $n = s_2(k + p)$ , then

$$[L_m, L_n] \setminus L(L_{k+p}) = [L_{s_1}(L_{k+p}), L_{s_2}(L_{k+p})].$$

Hence,  $[L_m, L_n] \setminus L([L_k, L_p]) = [L_{s_1}([L_k, L_p]), L_{s_2}([L_k, L_p])]$ .

(ii) Now suppose that  $k + p \nmid m$  or  $k + p \nmid n$ . As in (i), following Lemma 3.1 in [4], we say

that  $[L_m, L_n] \setminus L(L_{k+p}) = 0$ . Consequently, we have  $[L_m, L_n] \setminus L([L_k, L_p]) = 0$  and this result follows since  $[L_k, L_p] \leq L_{k+p}$ .

We are now in the position to give our theorems and their proofs.

**Theorem 2.1.** Let  $m, n, k$  and  $p$  be positive integers with  $m \geq n$ .

(i) If  $m + n + k > p$  and  $p \nmid m$  or  $p \nmid n$  or  $p \nmid k$ , then

$$\dim[L_m, L_n, L_k, L_p] = \dim[L_m, L_n, L_k] \dim L_p,$$

(ii) if  $m + n + k > p$  and  $m = s_1 p, n = s_2 p$  and  $k = s_3 p$  with  $s_1, s_2, s_3 \geq 1$ , then

$$\begin{aligned} \dim[L_m, L_n, L_k, L_p] &= \dim[L_{s_1}(L_p), L_{s_2}(L_p), L_{s_3}(L_p), L_p] + (\dim[L_m, L_n, L_k] \\ &\quad - \dim[L_{s_1}(L_p), L_{s_2}(L_p), L_{s_3}(L_p)]) \dim L_p, \end{aligned}$$

(iii) if  $p \geq m + n + k$  and  $(m + n + k) \nmid p$ , then

$$\dim[L_m, L_n, L_k, L_p] = \dim[L_m, L_n, L_k] \dim L_p,$$

(iv) and if  $p \geq m + n + k$  and  $p = s(m + n + k)$  with  $s \geq 1$ , then

$$\begin{aligned} \dim[L_m, L_n, L_k, L_p] &= \dim L_{s+1}([L_m, L_n, L_k]) + (\dim L_p \\ &\quad - \dim L_s([L_m, L_n, L_k])) \dim[L_m, L_n, L_k]. \end{aligned}$$

Proof. (i) We apply Lemma 1.2 with  $U = [L_m, L_n, L_k]$  and  $V = L_p$ . Thus we get

$$\begin{aligned} \dim[L_m, L_n, L_k, L_p] &= \dim([L_m, L_n, L_k], L_p) \\ &= \dim([L_m, L_n, L_k] \setminus L(L_p), L_p) + (\dim[L_m, L_n, L_k] \\ &\quad - \dim([L_m, L_n, L_k] \setminus L(L_p))) \dim L_p. \end{aligned}$$

By Lemma 2.3 (ii), we have  $[L_m, L_n, L_k] \setminus L(L_p) = 0$ . This gives

$$\dim[L_m, L_n, L_k, L_p] = \dim[L_m, L_n, L_k] \dim L_p.$$

(ii) By applying Lemma 1.2 with  $U = [L_m, L_n, L_k]$  and  $V = L_p$ , we get

$$\begin{aligned} \dim[L_m, L_n, L_k, L_p] &= \dim([L_{s_1 p}, L_{s_2 p}, L_{s_3 p}] \setminus L(L_p), L_p) \\ &\quad + (\dim[L_m, L_n, L_k] \\ &\quad - \dim([L_{s_1 p}, L_{s_2 p}, L_{s_3 p}] \setminus L(L_p))) \dim L_p. \end{aligned}$$

By Lemma 2.3 (i), we have

$$[L_{s_1 p}, L_{s_2 p}, L_{s_3 p}] \setminus L(L_p) = [L_{s_1}(L_p), L_{s_2}(L_p), L_{s_3}(L_p)]. \text{ Hence}$$

$$\begin{aligned} \dim[L_m, L_n, L_k, L_p] &= \dim[L_{s_1}(L_p), L_{s_2}(L_p), L_{s_3}(L_p), L_p] + (\dim[L_m, L_n, L_k] \\ &\quad - \dim[L_{s_1}(L_p), L_{s_2}(L_p), L_{s_3}(L_p)]) \dim L_p. \end{aligned}$$

(iii) Clearly,  $[L_m, L_n, L_k, L_p] = [L_p, [L_m, L_n, L_k]]$ . Then by applying Lemma 1.2 with  $U = L_p$  and  $V = [L_m, L_n, L_k]$ , we obtain

$$\begin{aligned}
\dim[L_m, L_n, L_k, L_p] &= \dim[L_p, [L_m, L_n, L_k]] \\
&= \dim[L_p \setminus L([L_m, L_n, L_k]), [L_m, L_n, L_k]] \\
&\quad + (\dim L_p \\
&\quad - \dim(L_p \setminus L([L_m, L_n, L_k]))) \dim[L_m, L_n, L_k].
\end{aligned} \tag{2.4}$$

By our assumption  $m + n + k \nmid p$ , we have  $L_p \setminus L([L_m, L_n, L_k]) = 0$ . Therefore, (2.4) turns into the formula

$$\dim[L_m, L_n, L_k, L_p] = \dim L_p \dim[L_m, L_n, L_k].$$

(iv) We use the same method as in (iii). We apply Lemma 1.2 with  $U = L_p$  and  $V = [L_m, L_n, L_k]$ , and since  $p = s(m + n + k)$ , we have  $L_p \setminus L([L_m, L_n, L_k]) = L_s([L_m, L_n, L_k])$ .

This implies that (2.4) turns into

$$\begin{aligned}
\dim[L_m, L_n, L_k, L_p] &= \dim[L_s([L_m, L_n, L_k]), [L_m, L_n, L_k]] \\
&\quad + (\dim L_p - \dim L_s([L_m, L_n, L_k])) \dim[L_m, L_n, L_k].
\end{aligned}$$

Since  $[L_s([L_m, L_n, L_k]), [L_m, L_n, L_k]] = L_{s+1}([L_m, L_n, L_k])$ , we have the required result.

This main result gives formulae for the dimension of subspaces  $[L_m, L_n, L_k, L_p]$  under certain conditions on  $m, n, k$  and  $p$ . Since there exist the dimensions of subspaces in the form  $[L_m, L_n, L_k]$  on the right hand sides of the four formulae in Theorem 2.1, we can use formulae in [4] for calculating of  $\dim[L_m, L_n, L_k]$ . Unfortunately, the obstacle are the products in the forms  $[L_s(L_k), L_t(L_k), L_k]$  and  $[L_{s_1}(L_p), L_{s_2}(L_p), L_{s_3}(L_p), L_p]$ . However, if formulae in Theorem 2.1 contain  $\dim[L_2, L_2, L_1]$ , then by [3], it is possible to say that the dimension of the product  $[L_m, L_n, L_k, L_p]$  depends on the characteristic of the ground field.

**Theorem 2.2.** Let  $m, n, k$  and  $p$  be positive integers with  $m \geq n$  and  $k \geq p$ .

(i) If  $m + n > k + p$  and  $k + p \nmid m$  or  $k + p \nmid n$ , then

$$\dim[L_m, L_n, [L_k, L_p]] = \dim[L_m, L_n] \dim[L_k, L_p],$$

(ii) if  $m + n > k + p$  and  $m = s_1(k + p)$  and  $n = s_2(k + p)$  with  $s_1, s_2 \geq 1$ , then

$$\begin{aligned}
\dim[L_m, L_n, [L_k, L_p]] &= \dim[L_{s_1}([L_k, L_p]), L_{s_2}([L_k, L_p])] \\
&\quad + (\dim[L_m, L_n]) \\
&\quad - \dim[L_{s_1}([L_k, L_p]), L_{s_2}([L_k, L_p])] \dim[L_k, L_p],
\end{aligned}$$

(iii) if  $k + p \geq m + n$  and  $(m + n) \nmid k$  or  $(m + n) \nmid p$ , then

$$\dim [ [L_m, L_n], [L_k, L_p] ] = \dim [L_k, L_p] \dim [L_m, L_n],$$

(iv) and if  $k + p \geq m + n$  and  $k = s_1(m + n)$  and  $p = s_2(m + n)$  with  $s_1, s_2 \geq 1$ , then

$$\begin{aligned} \dim [ [L_m, L_n], [L_k, L_p] ] &= \dim [L_{s_1}([L_m, L_n]), L_{s_2}([L_m, L_n]), [L_m, L_n]] \\ &+ (\dim [L_k, L_p] \\ &- \dim [L_{s_1}([L_m, L_n]), L_{s_2}([L_m, L_n])]) \dim [L_m, L_n]. \end{aligned}$$

Proof. (i) We apply Lemma 1.2 with  $U = [L_m, L_n]$  and  $V = [L_k, L_p]$ . This gives

$$\begin{aligned} \dim [ [L_m, L_n], [L_k, L_p] ] &= \dim [ [L_m, L_n] \setminus L([L_k, L_p]), [L_k, L_p] ] \\ &+ (\dim [L_m, L_n] - \dim ([L_m, L_n] \setminus L([L_k, L_p]))) \dim [L_k, L_p]. \end{aligned}$$

By Lemma 2.4 (ii), we have  $[L_m, L_n] \setminus L([L_k, L_p]) = 0$ . Hence,

$$\dim [ [L_m, L_n], [L_k, L_p] ] = \dim [L_m, L_n] \dim [L_k, L_p].$$

(ii) Again, by applying Lemma 1.2 with  $U = [L_m, L_n]$  and  $V = [L_k, L_p]$ , we obtain

$$\begin{aligned} \dim [ [L_m, L_n], [L_k, L_p] ] &= \dim [ [L_m, L_n] \setminus L([L_k, L_p]), [L_k, L_p] ] + (\dim [L_m, L_n] \\ &- \dim ([L_m, L_n] \setminus [L_k, L_p])) \dim [L_k, L_p]. \end{aligned}$$

Following from Lemma 2.4 (i), we have

$$\begin{aligned} \dim [ [L_m, L_n], [L_k, L_p] ] &= \dim [ [L_{s_1}([L_k, L_p]), L_{s_2}([L_k, L_p])], [L_k, L_p] ] + (\dim [L_m, L_n] \\ &- \dim [L_{s_1}([L_k, L_p]), L_{s_2}([L_k, L_p])]) \dim [L_k, L_p]. \end{aligned}$$

(iii) Clearly,  $[ [L_m, L_n], [L_k, L_p] ] = [ [L_k, L_p], [L_m, L_n] ]$ . Then we apply Lemma 1.2 with  $U = [L_k, L_p]$  and  $V = [L_m, L_n]$ . This gives

$$\begin{aligned} \dim [ [L_m, L_n], [L_k, L_p] ] &= \dim [ [L_k, L_p], [L_m, L_n] ] \\ &= \dim [ [L_k, L_p] \setminus L([L_m, L_n]), [L_m, L_n] ] \\ &+ (\dim [L_k, L_p] \\ &- \dim ([L_k, L_p] \\ &\setminus L([L_m, L_n]))) \dim [L_m, L_n]. \end{aligned} \tag{2.5}$$

By Lemma 2.4 (ii), we have  $[L_k, L_p] \setminus L([L_m, L_n]) = 0$ . Hence,

$$\dim[[L_k, L_p], [L_m, L_n]] = \dim[L_k, L_p] \dim[L_m, L_n].$$

(iv) By similar way in (iii), we apply Lemma 1.2 with  $U = [L_k, L_p]$  and  $V = [L_m, L_n]$ . Because of our assumption, we have

$$[L_k, L_p] \setminus L([L_m, L_n]) = [L_{s_1}([L_m, L_n]), L_{s_2}([L_m, L_n])].$$

Therefore, the formula (2.5) turns into the formula

$$\begin{aligned} \dim[[L_m, L_n], [L_k, L_p]] &= \dim[[L_{s_1}([L_m, L_n]), L_{s_2}([L_m, L_n]), [L_m, L_n]] \\ &+ (\dim[L_k, L_p] \\ &- \dim[L_{s_1}([L_m, L_n]), L_{s_2}([L_m, L_n])]) \dim[L_m, L_n]. \end{aligned}$$

In Theorem 2.2, unfortunately we do not have explicit formulae for the dimension of products in the form  $[L_{s_1}([L_k, L_p]), L_{s_2}([L_k, L_p]), [L_k, L_p]]$ . However, we use the formulae (1.1) and (1.2) for calculating the dimensions of the remaining products on the right hand side of four formulae.

**REFERENCES**

1. W. Magnus, A. Karrass and D. Solitar, *Combinatorial Group Theory, Presentations of Groups in terms of Generators and Relations*, Dover Publications, New York, NY, USA: 2nd revised ed., (1976).
2. N. Mansuroğlu, *Products of homogeneous subspaces in free Lie algebras*, MSc The University of Manchester, Manchester, UK, (2010).
3. N. Mansuroğlu, On the dimension of the product  $[L_2; L_2; L_1]$  in free Lie algebras, *International Journal of Group Theory* doi: 10.22108/IJGT.2017.21481, Volume 7, Issue 2, June 2018, page 45-50.
4. N. Mansuroglu and R. Stöhr, On the dimension of products of homogeneous subspaces in free Lie algebras, *Internat. J. Algebra Comput.* 23 (2013), no.1, 205-213.
5. A.I. Shirshov, Subalgebras of free Lie algebras, *Mat. Sb.* 33 (1953), 441-452 (in Russian).
6. A.I. Shirshov, *Selected works of A. I. Shirshov*, Translated from the Russian by Murray Bremner and Mikhail V. Kotchotov, Edited by Leonid A. Bokut, Victor Latyshev, Ivan Shestakov and Efim Zelmanov, *Contemporary Mathematicians*, Birkhuser Verlag, Basel (2009), viii+242 pp.
7. R. Stöhr and M. Vaughan-Lee, Products of homogeneous subspaces in free Lie algebras, *Internat. J. Algebra Comput.* 5 (2009), 19, 699-703.
8. E. Witt, *Treue Darstellungen Liescher Ringe*, *J. Reine Angew. Math.* (1937), 177, 152-160.
9. E. Witt, *Die Unterringe der freien Lieschen Ringe*, *Math. Z.* 64 (1956), 195-216.